Relativistic Fermion-Fermion Two-Vector-Exchange Potentials.

Th.A. Rijken
Institute for Mathematics, Astrophysics and Particle Physics,
Radboud University, Nijmegen, the Netherlands
(Dated: version of: October 22, 2020)

Background: It appeared that the extended-soft-core (ESC) model BBM-couplings can be understood in the constituent quark-model (CQM) by the application of the quark-pair creation (QPC) mechanism. Recently a connection was derived between the one-boson-exchange (OBE) baryon-baryon-meson (BBM) and quark-quark-meson (QQM) interactions using the CQM by adding at the quark-level only a few restricted interaction terms.

Purpose: The derivation of the two-meson-exchange (TME) potentials for the application of meson-exchange between quarks a relativistic formulation in the framework of QCD of meson-exchange is desirable as well as for two-gluon-exchange. As for the latter the focus is on Soft Two-vector-exchange (TVE) fermion-fermion potentials.

Method: This derivation is based on the formulation of Relativistic Quantum Field Theory as developed by Kadyshevsky. Here, in contrast to the usual with Feynman graphs, the particles in the Kadyshevsky-graphs remain on-mass-shell. This implies that Gaussian form factors, a characteristics of the soft-core models, can be handled easily in the Kadyshevsky-formalism, in contrast to the standard formulation using Feynman graphs.
The framework of this application to low momentum transfer physics is the constituent quark model (CQM) in the context of the liquid-instanton structure of the QCD-vacuum.

Results: Explicit momentum-space expressions for two-fermion-exchange potentials are derived. This can be used in momemtum-space calculations using the Kadyshevsky quasi-potential two-body integral equations. Given are also the adiabatic and first-order non-adiabatic expressions, useful for configuration-space calculations. Finally, we apply these potentials to the derivation of the Pomeron potential in Quark-quark and Nucleon-nucleon scattering, leading to a connection between the QCD- and the phenomenological Pomeron-parameters used in the ESC-potentials.

PACS numbers: 13.75.Cs, 12.39.Pn, 21.30.+y

I. INTRODUCTION

The general aim of this work is to give a relativistic formulation of the two-meson-exchange (TME) interactions for fermion-fermion (spin 1/2-1/2) in the Extended-soft-core (ESC) model [1, 2]. For this purpose the formulation of relativistic quantum field theory (RQFT) as given by Kadyshevsky [3–6] is used. In this first paper we derive the Two-vector-Exchange (TVE) using the formulation of relativistic quantum field theory (RQFT) as given by Kadyshevsky [3–6].

In the Kadyshevsky formulation of field theory, in contrast to the usual one using Feynman propagators, the particles stay always on the mass-shell. The consequence of this is that there is no four-momentum conservation at the vertices. Besides non-conservation of energy, as happens in the Lippmann-Schwinger equation for the intermediate states, there is in principle also non-conservation of three-momentum, in general. The motive for taking this formulation RQFT as the starting point is that for nucleon-nucleon we have composite particles and not elementary ones. Therefore, a relativistic formulation of a theory using phenomenological form factors which possibly suppress the transition between positive and negative energy states is desirable. Below we will give an example of such form factors, the consequences of which can be proved easily in the on-mass-shell formulation.
The derivation of the TVEP starts from the relativistic two-body equation [7–9], where the interaction kernel is given by the two-nucleon-irreducible Feynman diagrams. The relativistic Kadyshevsky two-body equation is analogous to the Bethe-Salpeter equation (BSE) [9], and leads in the center-of-mass system to the Kadyshevsky quasi-potential equation. This is an three-dimensional integral equation similar to the Lippmann-Schwinger and Thompson [10] equation. This is reviewed for spinless nucleons, and we refer to Ref. [1] for spin 1/2-1/2. The latter system is treated furtheron in this paper.

The diagrams which we calculate are the parallel and crossed TVE-diagrams. In carrying through the analytic derivation of our formulas, we generalize the techniques used in Ref's. [11–13] deriving formulas for the amplitudes where the three-momenta of the two mesons are separated using integral representations. The procedures, indicated above, are first carried out for pointlike vertices. Then, we generalize the results for the presence of the Gaussian form factors.

We apply the results ontained in this paper for the TVE-potential to two-gluon-exchange (TGE) in the two-quark systems at low energy. This in the constituent quark model (CQM) in the context of the liquid-instanton picture of the QCD-vacuum. We indentify the TVE-potentials with the Pomeron, analogously to the Low-Nussinov [14, 15] two-vector picture.

The content of this paper is arranged into eight sections and six appendices. Section II reviews the CQM from the instanton point of view. In sections III, IV, and V the general approach within the framework of relativistic quantum mechanics is presented. Especially the connection between the relativistic two-body equation description and that of the three-dimensional formalism is reviewed. In section VI and Appendix F the vector interactions and vertices are given. In section VII the CM-momenta are defined. In section VIII $\rho-\omega$-exchange kernels are derived for point-interactions. This for fermion-fermion and fermion-antifermion intermediate states. Section IX contains the application to two-gluon-exchange between constituent quarks. In section IX A using folding the two-gluon-exchange is applied to derive Pomeron-exchange between baryons. A discussion and conclusions are given in section X. Appendix A contains a review of the Kadyshevsky rules in momentum space. In Appendix B the orientation of the momenta in the Kadyshevsky graphs for positive and negative energy are given. In appendices C, D, and E the fourth-order Kadyshevsky graphs are given for respectively positive-positive, positive-negative, and negative-negative energy intermediate states. Appendix G the folding of the quark-quark matrix elements with the baryon constituent quark wave-functions is described.

II. CONSTITUENT QUARKS AND INSTANTONS

According to the two-scale picture of Manohar and Georgi [16] the effective degrees for the 3-flavor QCD at distances beyond that of SCSB ($\Lambda_{\chi SB}^{-1} \approx 0.2-0.3$ fm), should be the constituent quarks and mesons. The two non-perturbative effects in QCD are confinement and chiral symmetry breaking. The $SU(3)_L \otimes SU(3)_R$ chiral symmetry is sponteneously broken to an $SU(3)_v$ symmetry at a scale $\Lambda_{\chi SB} \approx 1$ GeV. The confinement scale is $\Lambda_{QCD} \approx 100-300$ MeV, which roughly corresponds to the baryon radius ≈ 1 fm. The pseudoscalar octet are the Goldstone bosons associated with the hidden (approximate) chiral symmetry of QCD. The SU(3) singlet pseudoscalar η' decouples from the original nonet because of the U(1) anomaly [17, 18].

Due to the complex structure of the QCD vacuum, which can be understood as a liquid of BPST [19] instantons and anti-instantons [20–22], the valence quarks, and also the gluon, acquire a dynamical or constituent mass [16, 17, 21–23]. The interaction between the instanton and the anti-instanton is a dipole-interaction [24], similar to ordinary molecules: weak attraction at large distances and strong repulsion at small ones. With the empirical value of the gluon condensate [25] as input the instanton density and radius become [24] $n_c = 8 \cdot 10^{-4}$ GeV^4, $\rho_c \approx 0.3$ fm. Also, with these parameters the non-perturbative vacuum expectation value for the quark fields is $\langle vac|\psi\psi|vac\rangle \approx -10^{-2}$ GeV^3 and the quark effective mass ≈ 200 MeV. In the calculation of light quarks in the instanton vacuum [22, 26] the effective quark mass $m_Q(p=0) = 345$ MeV was calculated, which is remarkably close to the constituent mass $M_N/3$ [1]. Furthermore, the gluon mass in this non-perturbative = "physical vacuum" is $m_G(p=0) \approx 420$ MeV [26].
These masses are used in this paper in the evaluation of the TGE-diagrams within the Kadyshevsky formalism, which according to the Low-Nussinov [14, 15] can serve as a description of the Pomeron.

III. RELATIVISTIC TWO-BODY EQUATION

We consider the nucleon-nucleon reaction

$$N_a(p_a, s_a) + N_b(p_b, s_b) \to N'_a(p'_a, s'_a) + N'_b(p'_b, s'_b) \ . \tag{3.1}$$

Introducing, as usual, the total and relative four-momentum for the initial and final state

$$\begin{array}{lll} P = p_a + p_b & , & P' = p'_a + p'_b \ , \\ p = \frac{1}{2}(p_a - p_b) & , & p' = \frac{1}{2}(p'_a - p'_b) \ , \end{array} \tag{3.2}$$

We use in the following the notation $P_0 \equiv W$ and $P'_0 \equiv W'$. In the Kadyshevsky formulation one introduces four-momenta spurions, making formally four-momentum conservation at the vertices. These are described by quasi-particle states $|\kappa\rangle$, normalized by $\langle\kappa'|\kappa\rangle = \delta(\kappa'-\kappa)$. Then the four-momentum of such a state is κn^μ, where n^μ is

[1] Note that for $m_Q = M_N/3$ a relation between the OBE-couplings of the ESC-models and the meson-couplings at the quark level can be derived such that the 1/M-expansion is reproduced in detail (M=baryon mass) [27]. To achieve this a few extra terms in the quark-quark-meson interactions have to be added for the vector-, scalar-, and axial-vector-mesons. For example, in order to get the spin-orbit correct an interesting new term in the quark-quark-axial-vector coupling has to be added.

time-like with $n^0 > 0$ and $n^2 = 1$. So, we consider the process in (3.1) with non-conservation of the four-momentum, i.e. off-momentum-shell. This off-shellness is given by

$$p_a + p_b + \kappa n = p'_a + p'_b + \kappa' n \tag{3.3}$$

In the following, the on-mass-shell momenta for the initial and final states are denoted respectively by p_i and p_f. So, $p_{i0} = E(\mathbf{p}_i) = \sqrt{\mathbf{p}_i^2 + M^2}$ and $p_{f0} = E(\mathbf{p}_f) = \sqrt{\mathbf{p}_f^2 + M^2}$.

In the Kadyshevsky-formulation the particles are on-mass-shell in the Green-functions. The on-mass-shell propagator $S^{(\pm)}(p)$ of a spin-0 particle can be written as

$$S^{(\pm)}(p) = \delta_\pm(p^2 - M^2) = \frac{1}{2E(\mathbf{p})}\delta\left(p_0 \mp E(\mathbf{p})\right) \ , \tag{3.4}$$

with $\delta_\pm(p^2 - M^2) \equiv \theta(\pm p^0)\delta(p^2 - M^2)$. The propagator $G_0(\kappa)$ for the quasi-particles is given by [4]

$$G_0(\kappa) = (1/2\pi)\left[1/(\kappa - i\delta)\right] \ . \tag{3.5}$$

In the Kadyshevsky-formalism the rules for the computation of the off-shell S-matrix, denoted by R, corresponding to the analogs of the Feynman graphs are given [4, 5]. We introduce the usual M-matrix by

$$\begin{aligned} R_{\kappa',\kappa}(p'_a, p'_b; p_a, p_b) \ &= \ \delta(\kappa' - \kappa)\delta(p'_a - p_a)\delta(p'_b - p_b) - (2\pi)^4 i\delta^4(\kappa' n + p'_a + p'_b - p_a - p_b - \kappa n)\cdot \\ &\quad \times M_{\kappa',\kappa}(p'_a, p'_b; p_a, p_b) \ . \end{aligned} \tag{3.6}$$

Notice that the S-matrix is given by $R_{0,0}$ [4]. We also observ that

$$\delta(\kappa' - \kappa)\delta(p'_a - p_a)\delta(p'_b - p_b) = \delta(P' + \kappa' n - P - \kappa n)\delta(p'_a - p_a)\delta(p'_b - p_b) \ , \tag{3.7}$$

showing the overall 4-momentum conservation for the R-matrix, including the momentum spurions.
The M-amplitude satisfy the equation

$$\begin{aligned} M_{\kappa',\kappa}(p'_a, p'_b; p_a, p_b) \ &= \ I_{\kappa',\kappa}(p'_a, p'_b; p_a, p_b) + \int d^4p''_a \int d^4p''_b \int d\kappa'' I_{\kappa'\kappa''}(p'_a, p'_b; p''_a, p''_b)\cdot \\ &\quad \times G_{\kappa''}(p''_a, p''_b) M_{\kappa'',\kappa}(p''_a, p''_b; p_a, p_b)\cdot\delta(p''_a + p''_b + \kappa'' n - p_a - p_b - \kappa n) \ . \end{aligned} \tag{3.8}$$

Here the propagation of the two nucleons and of the quasi-particle is described by

$$G_\kappa(p_a, p_b)_{\alpha',\beta';\alpha,\beta} \ = \ \frac{-1}{(2\pi)^2}\delta(p_a^2 - M_a^2)\delta(p_b^2 - M_b^2)\cdot G_0(\kappa) \ . \tag{3.9}$$

IV. QUASI-POTENTIAL EQUATION

The Kadyshevsky analog (3.8) of the Bethe-Salpeter equation we write in the form

$$\begin{aligned} &M_{\kappa',\kappa}(p'_a, p'_b; p_a, p_b) = I_{\kappa',\kappa}(p'_a, p'_b; p_a, p_b) + \int d^4p''_a \int d^4p''_b \int d\kappa''\cdot \\ &\times I_{\kappa',\kappa''}(p'_a, p'_b; p''_a, p''_b) G_{\kappa''}(p''_a, p''_b) M_{\kappa'',\kappa}(p''_a, p''_b; p_a, p_b)\cdot \\ &\times\delta(p''_a + p''_b + \kappa'' n - p_a - p_b - \kappa n) \ . \end{aligned} \tag{4.1}$$

In the CM-frame we have

$$P = (W, \mathbf{0}) \ , \ \ p = (0, \mathbf{p}) \ ; P' = (W', \mathbf{0}) \ , \ \ p' = (0, \mathbf{p}') \ . \tag{4.2}$$

Following [4, 6] we assume that the unit vector n^μ, which defines the time axis, is collinear to $P = p_a + p_b$ and hence also to $P' = p'_a + p'_b$. Then [2]

$$n^\mu = \frac{p_a^\mu + p_b^\mu}{\sqrt{(p_a + p_b)^2}} = \frac{p_a'^\mu + p_b'^\mu}{\sqrt{(p'_a + p'_b)^2}} \xrightarrow{CM} (1, \mathbf{0}) \ . \tag{4.3}$$

---

[2] Notice that with this choice for n^μ, the four-velocity of the system is conserved even off the energy-shell.

In the CM-variables, equation (4.1), for the $(+,+)$-components only, reads

$$M_{\kappa',\kappa}(p',W';p,W) = I_{\kappa',\kappa}(p',W';p,W) + \int dW'' \int d^4p'' \int d\kappa'' \cdot$$
$$\times I_{\kappa',\kappa''}(p',W';p'',W'')G_{\kappa''}(p'',W'')M_{\kappa''}(p'',W'';p,W) \cdot$$
$$\times \delta\left[W'' - W + (\kappa'' - \kappa)n_0\right] \ . \tag{4.4}$$

In the CM-frame, the two-nucleon propagator (3.9) becomes

$$G_\kappa(W'',p'') \ = \ \frac{-1}{(2\pi)^2}\delta\left(\frac{1}{2}W'' + p_0'' - E_a''\right)\delta\left(\frac{1}{2}W'' - p_0'' - E_b''\right)G_0(\kappa'') \ . \tag{4.5}$$

Now, the integrations over W'', p_0'', and κ'' can be carried through in (4.4) giving

$$M_{\kappa',\kappa}(\mathbf{p}',W';\mathbf{p},W) = I_{\kappa',\kappa}(\mathbf{p}',W';\mathbf{p},W) + \int \frac{d^3p''}{(2\pi)^3} \cdot$$
$$\times I_{\kappa',\kappa''}(\mathbf{p}',W';\mathbf{p}'',W'')\left(\frac{M_aM_b}{E_a''E_b''}\right)\frac{1}{\sqrt{s''} - (\sqrt{s}+\kappa) - i\epsilon}M_{\kappa'',\kappa}(\mathbf{p}'',W'';\mathbf{p},W) \ , \tag{4.6}$$

with the constraints

$$W \ = \ \sqrt{s} \ \ , \ \ W' = \sqrt{s'} = \sqrt{s} + \kappa - \kappa' \ , \ W'' = \sqrt{s''} = E_a'' + E_b'' \ . \tag{4.7}$$

We notice that the left-half-off-shell M-matrix satisfies an integral equation of the type

$$M_{\kappa',0} = I_{\kappa',0} + \int \ I_{\kappa',\kappa''} \ G_{\kappa''} \ M_{\kappa'',0}$$

where the κ's are all fixed in terms of the momenta of the particles, since

$$\kappa' = \sqrt{s} - \sqrt{s'} \ \ , \ \ \kappa'' = \sqrt{s} - \sqrt{s''} \ .$$

Defining the T-matrix etc. in terms of the left-half-off-shell M-matrix , and the quasi-potential K in terms of the both left and right off-shell interaction kernel I, by

$$T(\mathbf{p}',\mathbf{p}) \ = \ M_{\kappa',\kappa=0}(\mathbf{p}',W';\mathbf{p},W) \ , \ K(\mathbf{p}',\mathbf{p}) = I_{\kappa',\kappa=0}(\mathbf{p}',W';\mathbf{p},W) \ , \tag{4.8}$$

we will have, instead of (4.6),

$$T(\mathbf{p}',\mathbf{p}) \ = \ K(\mathbf{p}',\mathbf{p}) + \int \frac{d^3p''}{(2\pi)^3} \ K(\mathbf{p}',\mathbf{p}'') \ \left(\frac{M_aM_b}{E_a''E_b''}\right)\frac{1}{\sqrt{s''} - \sqrt{s}} \ T(\mathbf{p}'',\mathbf{p}) \ , \tag{4.9}$$

which is the so-called 'quasi-potential' equation. Compare this equation given in [28], equations (II.26) and (II.27). Notice, that for $\kappa = 0$, one has $\kappa' = \sqrt{s} - \sqrt{s'}$, and so κ' is fixed by $p = |\mathbf{p}|$ and $p' = |\mathbf{p}'|$.

For equal masses, i.e. $M_a = M_b = M$, we have

$$E_a'' \ = \ E_b'' = E(\mathbf{p}'') \ , s = 4E^2(\mathbf{p}) = 4(p^2 + M^2) \ , s'' = 4E^2(\mathbf{p}'') = 4(p''^2 + M^2). \tag{4.10}$$

Then, (4.9) goes over into the equation

$$T(\mathbf{p}',\mathbf{p}) \ = \ K(\mathbf{p}',\mathbf{p}) + \frac{1}{(2\pi)^3}\int \frac{d^3p''}{2E(\mathbf{p}'')} \ K(\mathbf{p}',\mathbf{p}'') \ \frac{M^2}{E(\mathbf{p}'')\,]E(\mathbf{p}'') - E(\mathbf{p}) - i\epsilon]} \ T(\mathbf{p}'',\mathbf{p}), \tag{4.11}$$

where is the quasi-potential equation of Kadyshevsky, see [5] equation (3.33).

V. RELATIVISTIC LIPPMANN-SCHWINGER AMPLITUDE AND EQUATION

The Lippmann-Schwinger amplitude is obtained from (4.11) by the transformation

$$\mathcal{T}(\mathbf{p}',\mathbf{p}) = N(\mathbf{p}')\ T(\mathbf{p}',\mathbf{p})\ N(\mathbf{p})\ ,\ \mathcal{V}(\mathbf{p}',\mathbf{p}) = N(\mathbf{p}')\ K(\mathbf{p}',\mathbf{p})\ N(\mathbf{p}), \tag{5.1}$$

with $N(\mathbf{p}) = M/(\sqrt{2}E(\mathbf{p}))$. The non-relativistic Lippmann-Schwinger equation is obtained by using in the Green-function and the potential the non-relativistic approximation $E(\mathbf{p}) \approx M + \mathbf{p}^2/2M$ giving

$$\mathcal{T}(\mathbf{p}',\mathbf{p}) \ = \ \mathcal{V}(\mathbf{p}',\mathbf{p}) + \frac{1}{(2\pi)^3}\int \frac{d^3p''}{2E(\mathbf{p}'')}\ \mathcal{V}(\mathbf{p}',\mathbf{p}'')\ \frac{M}{(\mathbf{p}''^2 - \mathbf{p}^2 - i\epsilon)}\ \mathcal{T}(\mathbf{p}'',\mathbf{p}). \tag{5.2}$$

For the details of the formalism of spin 1/2-1/2 scattering, using the expansion in Pauli-invariants, we refer to the papers of the ESC-model e.g. [1].

VI. THE VECTOR-EXCHANGE FERMION-FERMION INTERACTION

The fermion-fermion-vector ($J^{PC} = 1^{--}$) interaction Hamiltonian reads [29]

$$\mathcal{H}_V = g_V \bar{\psi}\gamma_\mu \psi \phi_V^\mu + \frac{f_V}{4\mathcal{M}}\bar{\psi}\sigma_{\mu\nu}\psi(\partial^\mu\phi_V^\nu - \partial^\nu\phi_V^\mu), \tag{6.1}$$

where $\sigma_{\mu\nu} = i[\gamma_\mu,\gamma_\nu]/2$, and the scaling mass $\mathcal{M}$, will be taken to be the proton mass. In Appendix F the reduction for all types of Dirac-vertices in Pauli-spinor operators is give.
When the fermion-fermion-vector form factor $F(\mathbf{x}'-\mathbf{x})$ is included, the interaction density becomes modified

$$H_I(\mathbf{x}) = \int d^3x'\, F(\mathbf{x}'-\mathbf{x})\mathcal{H}_I(\mathbf{x}'). \tag{6.2}$$

The form of the potentials in momentum space is the same as for point interactions, except that the coupling constants are multiplied by the Fourier transform $F(\mathbf{k}^2)$ of the form factor, where $\mathbf{k}$ is the momentum transfer at the NNV-vertex, where V= ρ, ϕ, ω or gluon. We use for space-like momentum transfers a Gaussian parameterization of the form factors in the one-vector-exchange amplitudes, *i.e.* $F(\mathbf{k}^2) \approx \exp(-\mathbf{k}^2/\Lambda^2)$. Until section VI we treat the point-coupling limit of the interactions, which makes the discussion less complicated. In section VI we implement the Gaussian form factors by employing a dispersion representation for the OPE-amplitude, valid for all momentum transfers.

VII. CM THREE-MOMENTUM SPACE FORMULAS

In the CM, choosing n^μ as in (4.3), we have $n^\mu = (1,\mathbf{0})$, and

$$\mathbf{p}_a \ = \ -\mathbf{p}_b = \mathbf{p}\ \ ,\ \ \mathbf{p}'_a = -\mathbf{p}'_b = \mathbf{p}'\ . \tag{7.1}$$

The integration over the zero-components can be done using the δ_+-functions, which means that

$$\begin{aligned} p_{a,0} = E_a(\mathbf{p})\ \ ,\ \ p_{b,0} = E_b(\mathbf{p}) \\ p'_{a,0} = E_a(\mathbf{p}')\ \ ,\ \ p'_{b,0} = E_b(\mathbf{p}')\ . \end{aligned} \tag{7.2}$$

Also, the three-momenta of the intermediate state are now fixed in terms of the external momenta and the two meson momenta $\mathbf{k}_{1,2}$. For example in graphs (a), (a'), (b), the relation is

$$\mathbf{q} \equiv \mathbf{q}_a = -\mathbf{q}_b = \mathbf{p} - \mathbf{k}_1 = \mathbf{p}' + \mathbf{k}_2, \tag{7.3}$$

and always $\mathbf{q}_a = -\mathbf{q}_b \equiv \mathbf{q}$. For the other graphs (b'), (c), and (c') it is a little different, because of the direction of the meson four-momenta is otherwise, see figures in Appendices C-E. The direction of the three-momenta can always be choosen the same.

For the planar and crossed fourth-order Kadyshevsky graphs the matrix elements can be written in the general form [3]

$$M^{(//,a)}_{\sigma;\kappa',\kappa}\,(p'_a,p'_b;p_a,p_b) = +(2\pi)^3 g^4 \int d^3q \int \frac{d^3k_1}{(2\pi)^3 2\omega_1} \int \frac{d^3k_2}{(2\pi)^3 2\omega_2}\; N^{(\sigma)}_{//}(\mathbf{p}',\mathbf{p};\mathbf{q})\cdot$$

$$\times\delta^{(3)}(\mathbf{k}_1-\mathbf{p}+\mathbf{q})\;\delta^{(3)}(\mathbf{k}_2+\mathbf{p}'-\mathbf{q})\;D^{(//,a)}_{\sigma;\kappa',\kappa}(\omega_1,\omega_2), \tag{7.4a}$$

$$M^{(X,\alpha)}_{\sigma;\kappa',\kappa}\,(p'_a,p'_b;p_a,p_b) = +(2\pi)^3 g^4 \int d^3q \int \frac{d^3k_1}{(2\pi)^3 2\omega_1} \int \frac{d^3k_2}{(2\pi)^3 2\omega_2}\; N^{(\sigma)}_{X}(\mathbf{p}',\mathbf{p};\mathbf{q})\cdot$$

$$\times\delta^{(3)}(\mathbf{k}_1-\mathbf{p}_a+\mathbf{q}_a)\;\delta^{(3)}(\mathbf{k}_2+\mathbf{p}'_a+\mathbf{q}_a)\;D^{(X,a)}_{\sigma;\kappa',\kappa}(\omega_1,\omega_2), \tag{7.4b}$$

where the numerators $N^{(\sigma)}_{//}(p',p;q)$ and $N^{(\sigma)}_{X}(p',p;q)$ contains the vertex factors and the fermion Dirac-operator. They depend on $\sigma = ++,+-,-+,--$ referring to a fermion (+) and antifermion (-) in the intermediate state.
The expressions for the fourth-order Kadyshevsky graphs are given in Appendices C-E, where the denominators $D^{//,X}_{\sigma;\kappa',\kappa}$ are given for $\sigma = ++,+-,--$.
Since the spinor-numerator factors for all parallel, respectively crossed, graphs can be made to be the same, the fourth-order kernels $K(\mathbf{p}',\mathbf{p})$ have the denominators

$$D^{(//)}_{\sigma;\kappa',\kappa}(\omega_1,\omega_2) \;=\; \sum_{\alpha=a,a',b,b',c,c'} D^{(//,\alpha)}_{\sigma;\kappa',\kappa}(\omega_1,\omega_2), \tag{7.5a}$$

$$D^{(X)}_{\sigma;\kappa',\kappa}(\omega_1,\omega_2) \;=\; \sum_{\alpha=a,a',b,b',c,c'} D^{(X,\alpha)}_{\sigma;\kappa',\kappa}(\omega_1,\omega_2), \tag{7.5b}$$

The application of two-meson-exchange $K^{(4)}$-kernel in this paper will be in configuration space. Henceforth we consider only the on-energy-shell matrix elements, i.e. $\kappa=\kappa'=0$.

---

[3] In (7.4) the arguments in the $\delta^{(3)}$-functions can have a different sign for the meson momenta. Since the rest of the integrand via the ω-variables depends on the squares of the three-momenta, by a simple sign change in the relevant meson momenta the arguments can be made as in (7.4). *Then, the performance of the d^3q-integral leads to identical expressions for the numerators $N_G(\mathbf{p}',\mathbf{p};\mathbf{q})$ for $G=//$ and $G=X$ i.e. the parallel and crossed graphs respectively.*

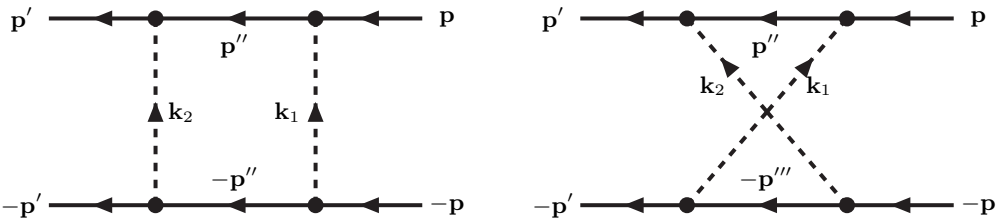

FIG. 1: *CM-three-momenta graphs $\sigma = ++$. The solid lines denote baryons. The dashed lines refers to the vector mesons, $\mathbf{k}_1 = \mathbf{k}_\rho$ and $\mathbf{k}_2 = \mathbf{k}_\omega$. The intermediate state momenta are $\mathbf{p}'' = \mathbf{p} + \mathbf{k}_1 = \mathbf{p}' - \mathbf{k}_2$ and $\mathbf{p}''' = \mathbf{p} + \mathbf{k}_2 = \mathbf{p}' - \mathbf{k}_1$.*

VIII. VECTOR-VECTOR-EXCHANGE POTENTIALS

A. Rho-Omega exchange

The formalism below is very similar to that used in [11–13]. This because for $\kappa' = \kappa = 0$, i.e. on-energy-shell potentials, the expressions of the energy denominators $D_{\sigma;0,0}$ are identical to those obtained in the Macke-Klein formalism. In Appendix C-E the two-meson exchange Kadyshevs graphs are evaluated. On-energy-shell the results are identical to those obtained of the old-fashioned perturbation theory (OPT) BW- and TMO-graphs graph's in e.g. Ref. [12] Fig's 1 and 2.

To be explicit we derive the $\rho\omega$-exchange potential. The other vector-vector exchange potentials can then be obtained by a simple transcription and change of the isospin structure. We will evaluate the potentials up to order $1/M^2$. Although the expansion of N-factors in Eq. (5.1) takes care of the normalization factors of the nucleon Dirac spinors of the initial and final nucleons, we still have to include the normalization factors of the nucleon Dirac spinors in the intermediate two-nucleon state, which also contribute a factor of order $1/M^2$.

In the following, $(\mathbf{k}_1, \omega_1)$ refers to the ρ meson and $(\mathbf{k}_2, \omega_2)$ refers to the ω meson. Using the vertex operators as given in Table VIII A, the planar (BW+TMO) graphs Fig. 1 give [4]

$$\begin{aligned} V^{(\sigma)}_{\rho\omega}(//) \;=\; & +C^{(//)}_{NN}(I) g^2_{NN\rho} g^2_{NN\omega} \int\!\!\int \frac{d^3k_1 d^3k_2}{(2\pi)^6}\, e^{i(\mathbf{k}_1+\mathbf{k}_2)\cdot\mathbf{r}}\; F_\rho(\mathbf{k}_1^2) F_\omega(\mathbf{k}_2^2)\; D^{(\sigma)}_{//}(\omega_1,\omega_2)\cdot \\ & \times \Big\{ A^0_\omega \phi^0_\omega + \mathbf{A}_\omega \cdot \boldsymbol{\phi}_\omega \Big\} \Big\{ A^0_\rho \phi^0_\rho + \mathbf{A}_\rho \cdot \boldsymbol{\phi}_\rho \Big\} \Big\{ B^0_\omega \phi^0_\omega + \mathbf{B}_\omega \cdot \boldsymbol{\phi}_\omega \Big\} \Big\{ B^0_\rho \phi^0_\rho + \mathbf{B}_\rho \cdot \boldsymbol{\phi}_\rho \Big\}. \end{aligned} \tag{8.1}$$

1. **Fermion-fermion in the intermediate states**: Here, with $\kappa_{\rho,\omega} = f_{NN\rho,\omega}/g_{NN\rho,\omega}$, the (a)-line factors $(A^0_V, \mathbf{A}_V)$ and (b)-line factors $(B^0_V, \mathbf{B}_V)$ are given in Table VIII A. We note that the factors in (8.1) can be commuted freely,

[4] For the sign compare with formulas in [12], and see footnote in Appendix A.

TABLE I: Planar graphs A- and B-operators fermion lines vector-vector exchange

$$
\begin{array}{|l|}
\hline
A^{(0)}_{\omega}(//,+) \;=\; 1+\big[\mathbf{p}'\cdot\mathbf{p}''+i\boldsymbol{\sigma}_1\cdot\mathbf{p}'\times\mathbf{p}''\big]/(4M^2)-\kappa_\omega\;\big[(\mathbf{p}'-\mathbf{p}'')^2-2i\boldsymbol{\sigma}_1\cdot\mathbf{p}'\times\mathbf{p}''\big]/(4M^2)\\
B^{(0)}_{\omega}(//,+) \;=\; 1+\big[\mathbf{p}'\cdot\mathbf{p}''+i\boldsymbol{\sigma}_2\cdot\mathbf{p}'\times\mathbf{p}''\big]/(4M^2)-\kappa_\omega\;\big[(\mathbf{p}'-\mathbf{p}'')^2-2i\boldsymbol{\sigma}_2\cdot\mathbf{p}'\times\mathbf{p}''\big]/(4M^2)\\
A^{(0)}_{\rho}(//,+) \;=\; 1+\big[\mathbf{p}\cdot\mathbf{p}''+i\boldsymbol{\sigma}_1\cdot\mathbf{p}\times\mathbf{p}''\big]/(4M^2)-\kappa_\rho\;\big[(\mathbf{p}-\mathbf{p}'')^2+2i\boldsymbol{\sigma}_1\cdot\mathbf{p}\times\mathbf{p}''\big]/(4M^2)\\
B^{(0)}_{\rho}(//,+) \;=\; 1+\big[\mathbf{p}\cdot\mathbf{p}''-i\boldsymbol{\sigma}_2\cdot\mathbf{p}\times\mathbf{p}''\big]/(4M^2)-\kappa_\rho\;\big[(\mathbf{p}-\mathbf{p}'')^2+2i\boldsymbol{\sigma}_2\cdot\mathbf{p}\times\mathbf{p}''\big]/(4M^2)\\
\hline
\mathbf{A}_{\omega}(//,+) \;=\; -\big[(\mathbf{p}'+\mathbf{p}'')+i(1+\kappa_\omega)\;\boldsymbol{\sigma}_1\times(\mathbf{p}'-\mathbf{p}'')\big]/(2M)\\
\mathbf{B}_{\omega}(//,+) \;=\; +\big[(\mathbf{p}'+\mathbf{p}'')+i(1+\kappa_\omega)\;\boldsymbol{\sigma}_2\times(\mathbf{p}'-\mathbf{p}'')\big]/(2M)\\
\mathbf{A}_{\rho}(//,+) \;=\; -\big[(\mathbf{p}''+\mathbf{p})+i(1+\kappa_\rho)\;\boldsymbol{\sigma}_1\times(\mathbf{p}''-\mathbf{p})\big]/(2M)\\
\mathbf{B}_{\rho}(//,+) \;=\; +\big[(\mathbf{p}''+\mathbf{p})+i(1+\kappa_\rho)\;\boldsymbol{\sigma}_2\times(\mathbf{p}''-\mathbf{p})\big]/(2M)\\
\hline
C^{(0)}_{\omega}(X,+) \;=\; 1+\big[\mathbf{p}\cdot\mathbf{p}'''+i\boldsymbol{\sigma}_2\cdot\mathbf{p}\times\mathbf{p}'''\big]/(4M^2)-\kappa_\omega\;\big[(\mathbf{p}-\mathbf{p}'')^2-2i\boldsymbol{\sigma}_2\cdot\mathbf{p}\times\mathbf{p}'''\big]/(4M^2)\\
C^{(0)}_{\rho}(X,+) \;=\; 1+\big[\mathbf{p}'\cdot\mathbf{p}'''-i\boldsymbol{\sigma}_2\cdot\mathbf{p}'\times\mathbf{p}'''\big]/(4M^2)-\kappa_\rho\;\big[(\mathbf{p}'-\mathbf{p}''')^2+2i\boldsymbol{\sigma}_2\cdot\mathbf{p}'\times\mathbf{p}'''\big]/(4M^2)\\
\hline
\mathbf{C}_{\omega}(X,+) \;=\; +\big[(\mathbf{p}+\mathbf{p}''')+i(1+\kappa_\omega)\;\boldsymbol{\sigma}_2\times(\mathbf{p}-\mathbf{p}''')\big]/(2M)\\
\mathbf{C}_{\rho}(X,+) \;=\; +\big[(\mathbf{p}'''+\mathbf{p}')+i(1+\kappa_\rho)\;\boldsymbol{\sigma}_2\times(\mathbf{p}'''-\mathbf{p}')\big]/(2M)\\
\hline
\end{array}
$$

because the corrections are of order $(1/M)^4$.
Neglecting terms with $\mathbf{k}_1\times\mathbf{k}_2$, which do not contribute much in the $d^3k_1d^3k_2$-integrals since $\Lambda_\rho\approx\Lambda_\omega$, we get

$$
\begin{aligned}
-A^0_\rho B^0_\rho+\mathbf{A}_\rho\cdot\mathbf{B}_\rho \;\approx\; & -1-\frac{1}{4M^2}\Big[6\mathbf{q}^2-6\mathbf{q}\cdot\mathbf{k}_2+\mathbf{k}_2^2-\frac{1}{2}(\mathbf{k}_1^2+\mathbf{k}_2^2)+2\mathbf{k}_2^2-2\kappa_\rho\mathbf{k}_1^2\\
& -i(3+4\kappa_\rho)(\boldsymbol{\sigma}_1+\boldsymbol{\sigma}_2)\cdot\mathbf{q}\times\mathbf{k}_1\\
& -(1+\kappa_\rho)^2\left\{(\boldsymbol{\sigma}_1\cdot\boldsymbol{\sigma}_2)\mathbf{k}_1^2-\boldsymbol{\sigma}_1\cdot\mathbf{k}_1\boldsymbol{\sigma}_2\cdot\mathbf{k}_1\right\}\Big],\\
-A^0_\omega B^0_\omega+\mathbf{A}_\omega\cdot\mathbf{B}_\omega \;\approx\; & -1-\frac{1}{4M^2}\Big[6\mathbf{q}^2+6\mathbf{q}\cdot\mathbf{k}_1-\frac{1}{2}(\mathbf{k}_1^2+\mathbf{k}_2^2)+2\mathbf{k}_1^2-2\kappa_\omega\mathbf{k}_2^2\\
& -i(3+4\kappa_\omega)(\boldsymbol{\sigma}_1+\boldsymbol{\sigma}_2)\cdot\mathbf{q}\times\mathbf{k}_2\\
& -(1+\kappa_\omega)^2\left\{(\boldsymbol{\sigma}_1\cdot\boldsymbol{\sigma}_2)\mathbf{k}_2^2-\boldsymbol{\sigma}_1\cdot\mathbf{k}_2\boldsymbol{\sigma}_2\cdot\mathbf{k}_2\right\}\Big].
\end{aligned}
$$

We have, using $\phi^0_V\cdot\phi^0_V=-1$, $\boldsymbol{\phi}_V\cdot\boldsymbol{\phi}=+1$ etc., in a concise form,

$$
\begin{aligned}
V^{(++)}_{\rho\omega}(//) \;\approx\; & +C^{(//)}_{NN}(I)g^2_{NN\rho}g^2_{NN\omega}\iint\frac{d^3k_1d^3k_2}{(2\pi)^6}\,e^{i(\mathbf{k}_1+\mathbf{k}_2)\cdot\mathbf{r}}\;F_\rho(\mathbf{k}_1^2)F_\omega(\mathbf{k}_2^2)\\
& \times\;\left\{-A^0_\omega B^0_\omega+\mathbf{A}_\omega\cdot\mathbf{B}_\omega\right\}\left\{-A^0_\rho B^0_\rho+\mathbf{A}_\rho\cdot\mathbf{B}_\rho\right\}D_{//}(\omega_1,\omega_2).
\end{aligned}
\tag{8.2}
$$

Multiplying these expressions and keeping terms up to order $(1/M)^2$ we obtain

$$
\begin{aligned}
V^{(++)}_{\rho\omega}(//) \;\approx\; & +C^{(//)}_{NN}(I)g^2_{NN\rho}g^2_{NN\omega}\iint\frac{d^3k_1d^3k_2}{(2\pi)^6}\,e^{i(\mathbf{k}_1+\mathbf{k}_2)\cdot\mathbf{r}}\;F_\rho(\mathbf{k}_1^2)F_\omega(\mathbf{k}_2^2)\;D_{//}(\omega_1,\omega_2)\cdot\\
& \times\;\Big\{1+\frac{1}{4M^2}\Big[12\mathbf{q}^2+(\mathbf{k}_1^2+\mathbf{k}_2^2)-2(\kappa_\rho\mathbf{k}_1^2+\kappa_\omega\mathbf{k}_2^2)\\
& -i(3+4\kappa_\rho)(\boldsymbol{\sigma}_1+\boldsymbol{\sigma}_2)\cdot\mathbf{q}\times\mathbf{k}_1-(1+\kappa_\rho)^2\left\{(\boldsymbol{\sigma}_1\cdot\boldsymbol{\sigma}_2)\mathbf{k}_1^2-\boldsymbol{\sigma}_1\cdot\mathbf{k}_1\boldsymbol{\sigma}_2\cdot\mathbf{k}_1\right\}\\
& -i(3+4\kappa_\omega)(\boldsymbol{\sigma}_1+\boldsymbol{\sigma}_2)\cdot\mathbf{q}\times\mathbf{k}_2-(1+\kappa_\omega)^2\left\{(\boldsymbol{\sigma}_1\cdot\boldsymbol{\sigma}_2)\mathbf{k}_2^2-\boldsymbol{\sigma}_1\cdot\mathbf{k}_2\boldsymbol{\sigma}_2\cdot\mathbf{k}_2\right\}\Big].
\end{aligned}
\tag{8.3}
$$

The crossed BW graphs of Figs. 1 (b) (and their "mirror" graphs) give

$$V_{\rho\omega}^{(++)}(X) \;=\; +C_{NN}^{(X)}(I) g_{NN\rho}^2 g_{NN\omega}^2 \iint \frac{d^3k_1 d^3k_2}{(2\pi)^6}\, e^{i(\mathbf{k}_1+\mathbf{k}_2)\cdot\mathbf{r}}\; F_\rho(\mathbf{k}_1^2) F_\omega(\mathbf{k}_2^2)\; D_X(\omega_1,\omega_2)\cdot$$
$$\times\; \Big\{ A_\omega^0\phi_\omega^0 + \mathbf{A}_\omega\cdot\boldsymbol{\phi}_\omega \Big\}\Big\{ A_\rho^0\phi_\rho^0 + \mathbf{A}_\rho\cdot\boldsymbol{\phi}_\rho \Big\}\Big\{ C_\rho^0\phi_\rho^0 + \mathbf{C}_\rho\cdot\boldsymbol{\phi}_\rho \Big\}\Big\{ C_\omega^0\phi_\omega^0 + \mathbf{C}_\omega\cdot\boldsymbol{\phi}_\omega \Big\}. \tag{8.4}$$

Here the (a)-line A-factors are the same as for the parallel graph, and the (b)-line C-factors are given in Table VIII A. Again, the factors in (8.4) can be commuted freely, because the corrections are of order $(1/M)^4$. Therefore

$$V_{\rho\omega}^{(++)}(X) \;\approx\; +C_{NN}^{(X)}(I) g_{NN\rho}^2 g_{NN\omega}^2 \iint \frac{d^3k_1 d^3k_2}{(2\pi)^6}\, e^{i(\mathbf{k}_1+\mathbf{k}_2)\cdot\mathbf{r}}\; F_\rho(\mathbf{k}_1^2) F_\omega(\mathbf{k}_2^2)$$
$$\times\; \Big\{ -A_\omega^0 C_\omega^0 + \mathbf{A}_\omega\cdot\mathbf{C}_\omega \Big\}\Big\{ -A_\rho^0 C_\rho^0 + \mathbf{A}_\rho\cdot\mathbf{C}_\rho \Big\} D_X(\omega_1,\omega_2). \tag{8.5}$$

The form factors are given by $F_{\rho,\omega}(\mathbf{k}_{1,2}^2) = F_{NN\rho,\omega}^2(\mathbf{k}_{1,2}^2)$. The Kadyshevsky energy denominators $D_i(\omega_1,\omega_2)$ can be found in Appendix C 1 equations (C2) and (C5).

Remark: In quark-quark scattering the iterated one-vector-exchange is included For the TMO graphs we have to subtract the Born iteration $K_{\rm Born}^{(4)}$ as described in Ref. [12]. This subtraction has already been accounted for in in $D_{//,X}^{(++)}$ in (9.5). This does not apply in the case of the application to the pomeron for baryon-baryon scattering.

Using the CM-momenta $\mathbf{p} = \mathbf{q} - (\mathbf{k}_1+\mathbf{k}_2)/2$, $\mathbf{p}' = \mathbf{q} + (\mathbf{k}_1+\mathbf{k}_2)/2$, the momenta for the intermediate nucleon lines $\mathbf{p}'', -\mathbf{p}'''$ are given by

$$\begin{aligned} \mathbf{p}'' &= \mathbf{p}+\mathbf{k}_1 = \mathbf{p}'-\mathbf{k}_2,\;\; \mathbf{p}''' = \mathbf{p}+\mathbf{k}_2 = \mathbf{p}'-\mathbf{k}_1, \\ \mathbf{p}'' &= \mathbf{q}+(\mathbf{k}_1-\mathbf{k}_2)/2,\;\; \mathbf{p}''' = \mathbf{q}-(\mathbf{k}_1-\mathbf{k}_2)/2. \end{aligned} \tag{8.6}$$

From these relations we get

$$\begin{aligned} &\mathbf{p}+\mathbf{p}'' = 2\mathbf{q}-\mathbf{k}_2, \quad \mathbf{p}+\mathbf{p}''' = 2\mathbf{q}-\mathbf{k}_1, \\ &\mathbf{p}'+\mathbf{p}'' = 2\mathbf{q}+\mathbf{k}_1, \quad \mathbf{p}'+\mathbf{p}''' = 2\mathbf{q}+\mathbf{k}_2, \\ &\mathbf{p}\cdot\mathbf{p}'' = \mathbf{q}^2 - \mathbf{q}\cdot\mathbf{k}_2 - \frac{1}{4}(\mathbf{k}_1^2-\mathbf{k}_2^2), \\ &\mathbf{p}\cdot\mathbf{p}''' = \mathbf{q}^2 - \mathbf{q}\cdot\mathbf{k}_1 + \frac{1}{4}(\mathbf{k}_1^2-\mathbf{k}_2^2), \\ &\mathbf{p}'\cdot\mathbf{p}'' = \mathbf{q}^2 + \mathbf{q}\cdot\mathbf{k}_1 + \frac{1}{4}(\mathbf{k}_1^2-\mathbf{k}_2^2), \\ &\mathbf{p}'\cdot\mathbf{p}''' = \mathbf{q}^2 + \mathbf{q}\cdot\mathbf{k}_2 - \frac{1}{4}(\mathbf{k}_1^2-\mathbf{k}_2^2), \\ &\mathbf{p}'\times\mathbf{p}'' = -\mathbf{q}\times\mathbf{k}_2 - \frac{1}{2}\mathbf{k}_1\times\mathbf{k}_2,\;\; \mathbf{p}'''\times\mathbf{p} = -\mathbf{p}'\times\mathbf{p}'', \\ &\mathbf{p}''\times\mathbf{p} = -\mathbf{q}\times\mathbf{k}_1 - \frac{1}{2}\mathbf{k}_1\times\mathbf{k}_2, \\ &\mathbf{p}'\times\mathbf{p}''' = -\mathbf{q}\times\mathbf{k}_1 + \frac{1}{2}\mathbf{k}_1\times\mathbf{k}_2. \end{aligned} \tag{8.7}$$

Neglecting terms with $\mathbf{k}_1\times\mathbf{k}_2$, which do not contribute much in the $d^3k_1 d^3k_2$-integrals since $\Lambda_\rho \approx \Lambda_\omega$, we get

$$\begin{aligned} -A_\rho^0 C_\rho^0 + \mathbf{A}_\rho\cdot\mathbf{C}_\rho \;\approx\; & -1 - \frac{1}{4M^2}\Big[6\mathbf{q}^2 - \frac{1}{2}(\mathbf{k}_1^2+\mathbf{k}_2^2) - 2\kappa_\rho\mathbf{k}_1^2 - i(3+4\kappa_\rho)(\boldsymbol{\sigma}_1+\boldsymbol{\sigma}_2)\cdot\mathbf{q}\times\mathbf{k}_1 \\ & -(1+\kappa_\rho)^2\left\{(\boldsymbol{\sigma}_1\cdot\boldsymbol{\sigma}_2)\mathbf{k}_1^2 - \boldsymbol{\sigma}_1\cdot\mathbf{k}_1\boldsymbol{\sigma}_2\cdot\mathbf{k}_1\right\}\Big], \\ -A_\omega^0 C_\omega^0 + \mathbf{A}_\omega\cdot\mathbf{C}_\omega \;\approx\; & -1 - \frac{1}{4M^2}\Big[6\mathbf{q}^2 - \frac{1}{2}(\mathbf{k}_1^2+\mathbf{k}_2^2) - 2\kappa_\omega\mathbf{k}_2^2 - i(3+4\kappa_\omega)(\boldsymbol{\sigma}_1+\boldsymbol{\sigma}_2)\cdot\mathbf{q}\times\mathbf{k}_2 \\ & -(1+\kappa_\omega)^2\left\{(\boldsymbol{\sigma}_1\cdot\boldsymbol{\sigma}_2)\mathbf{k}_2^2 - \boldsymbol{\sigma}_1\cdot\mathbf{k}_2\boldsymbol{\sigma}_2\cdot\mathbf{k}_2\right\}\Big]. \end{aligned}$$

TABLE II: Kinematic relations momenta planar and crossed diagrams.

$\mathbf{p}+\mathbf{p}''=2\mathbf{q}-\mathbf{k}_2$	, $\mathbf{p}+\mathbf{p}'''=2\mathbf{q}-\mathbf{k}_1$
$\mathbf{p}'+\mathbf{p}''=2\mathbf{q}+\mathbf{k}_1$	, $\mathbf{p}'+\mathbf{p}'''=2\mathbf{q}+\mathbf{k}_2$
$\mathbf{p}\cdot\mathbf{p}''=\mathbf{q}^2-\mathbf{q}\cdot\mathbf{k}_2-\frac{1}{4}(\mathbf{k}_1^2-\mathbf{k}_2^2)$	
$\mathbf{p}\cdot\mathbf{p}'''=\mathbf{q}^2-\mathbf{q}\cdot\mathbf{k}_1+\frac{1}{4}(\mathbf{k}_1^2-\mathbf{k}_2^2)$	
$\mathbf{p}'\cdot\mathbf{p}''=\mathbf{q}^2+\mathbf{q}\cdot\mathbf{k}_1+\frac{1}{4}(\mathbf{k}_1^2-\mathbf{k}_2^2)$	
$\mathbf{p}'\cdot\mathbf{p}'''=\mathbf{q}^2+\mathbf{q}\cdot\mathbf{k}_2-\frac{1}{4}(\mathbf{k}_1^2-\mathbf{k}_2^2)$	
$\mathbf{p}'\times\mathbf{p}''=-\mathbf{q}\times\mathbf{k}_2-\frac{1}{2}\mathbf{k}_1\times\mathbf{k}_2$	, $\mathbf{p}'''\times\mathbf{p}=-\mathbf{p}'\times\mathbf{p}''$
$\mathbf{p}''\times\mathbf{p}=-\mathbf{q}\times\mathbf{k}_1-\frac{1}{2}\mathbf{k}_1\times\mathbf{k}_2$	, $\mathbf{p}'\times\mathbf{p}'''=-\mathbf{q}\times\mathbf{k}_1+\frac{1}{2}\mathbf{k}_1\times\mathbf{k}_2$

Keeping terms up to order $(1/M)^2$ we obtain

$$
\begin{aligned}
V_{\rho\omega}^{(++)}(X) \;\approx\; & +C_{NN}^{(X)}(I)g_{NN\rho}^2 g_{NN\omega}^2 \int\!\!\int \frac{d^3k_1 d^3k_2}{(2\pi)^6}\, e^{i(\mathbf{k}_1+\mathbf{k}_2)\cdot\mathbf{r}}\; F_\rho(\mathbf{k}_1^2)F_\omega(\mathbf{k}_2^2) \\
& \times \left\{ 1+\frac{1}{4M^2}\Big[12\mathbf{q}^2-(\mathbf{k}_1^2+\mathbf{k}_2^2)-i(3+4\kappa_\rho)(\boldsymbol{\sigma}_1+\boldsymbol{\sigma}_2)\cdot\mathbf{q}\times\mathbf{k}_1 \right. \\
& -i(3+4\kappa_\omega)(\boldsymbol{\sigma}_1+\boldsymbol{\sigma}_2)\cdot\mathbf{q}\times\mathbf{k}_2-(1+\kappa_\rho)^2\left\{(\boldsymbol{\sigma}_1\cdot\boldsymbol{\sigma}_2)\mathbf{k}_1^2-\boldsymbol{\sigma}_1\cdot\mathbf{k}_1\boldsymbol{\sigma}_2\cdot\mathbf{k}_1\right\} \\
& \left.-(1+\kappa_\omega)^2\left\{(\boldsymbol{\sigma}_1\cdot\boldsymbol{\sigma}_2)\mathbf{k}_2^2-\boldsymbol{\sigma}_1\cdot\mathbf{k}_2\boldsymbol{\sigma}_2\cdot\mathbf{k}_2\right\}\Big]\right\}\cdot D_X(\omega_1,\omega_2). \qquad (8.8)
\end{aligned}
$$

To the expressions in Eqs. (8.1) and (8.4) we have to add the "time-reversed" diagrams, which are those of Figs. 1 and 2, but with the ρ line and ω line interchanged. The latter contributions cancel all terms in Eqs. (8.1) and (8.4) that are forbidden because of time-reversal invariance, and double the allowed terms.

It is convenient to write the final result of the $(1/4M^2)$ contributions as a sum of three terms proportional to 1, $(3+4\kappa_{\rho,\omega})$, and $(1+\kappa_{\rho,\omega})^2$, respectively. We refer to these as the electric-electric (e,e), the electric-magnetic (e,m), and the magnetic-magnetic (m,m) terms. We can then write the resulting potential as

$$
\begin{aligned}
V_{\rho\omega}^{(++)} \;=\; & \sum_{i=//,X} C_{NN}^{(i)}(I)g_{NN\rho}^2 g_{NN\omega}^2 \int\!\!\int \frac{d^3k_1 d^3k_2}{(2\pi)^6}\, e^{i(\mathbf{k}_1+\mathbf{k}_2)\cdot\mathbf{r}} F_\pi(\mathbf{k}_1^2)F_\rho(\mathbf{k}_2^2)\cdot \\
& \times \left[\left(1+\frac{3(\mathbf{q}^2+\mathbf{k}^2/4)}{M^2}\right)+\frac{1}{4M^2}\left\{O_{e,e}^{(i)}+O_{e,m}^{(i)}+O_{m,m}^{(i)}\right\}(\mathbf{k}_1,\mathbf{k}_2)\right]\; D_i(\omega_1,\omega_2), \qquad (8.9)
\end{aligned}
$$

where the operators $O^{(i)}(\mathbf{k}_1,\mathbf{k}_2)$ can be read off from Eqs. (8.3) and (8.8).

The full separation of the $\mathbf{k}_1$ and $\mathbf{k}_2$ dependence of the Fourier integrals can be achieved as shown in Ref. [11], and has been discussed above. Accordingly, we derive from Eq. (8.9) the form

$$
\begin{aligned}
V_{\rho\omega}^{(++)} \;=\; & \sum_{i=//,X} C_{NN}^{(i)}(I)g_{NN\rho}^2 g_{NN\omega}^2 \lim_{\mathbf{r}_1,\mathbf{r}_2\to\mathbf{r}}\left[1+\frac{3}{M^2}\left(\mathbf{q}^2-\frac{1}{4}\boldsymbol{\nabla}^2\right)\right. \\
& \left.+\frac{1}{4M^2}\left\{O_{e,e}^{(i)}+O_{e,m}^{(i)}+O_{m,m}^{(i)}\right\}(-i\boldsymbol{\nabla}_1,-i\boldsymbol{\nabla}_2)\right]B_{NN\rho\omega}^{(i)}(r_1,r_2), \qquad (8.10)
\end{aligned}
$$

where $\boldsymbol{\nabla}=\boldsymbol{\nabla}_1+\boldsymbol{\nabla}_2$. In [12], Appendix A a set of explicit formulas are given such that the result for $O^{(i)}(-i\boldsymbol{\nabla}_1,-i\boldsymbol{\nabla}_2)F(r_1)G(r_2)$ can be evaluated. The non-local term $\mathbf{q}^2+\mathbf{k}^2/4$ can be evaluated by operating on the function $B_{NN\rho\omega}^{(i)}(r,r)$, similar to the treatment of the non-local terms in the OBE-potentials.

2. **Fermion-antifermion in the intermediate states**: Taking the antifermion in the (b)-line we apply the rules for the momentum diagrams in Fig. 2 as given in Appendix A Table VII. Then for an antifermion in line (b) one gets

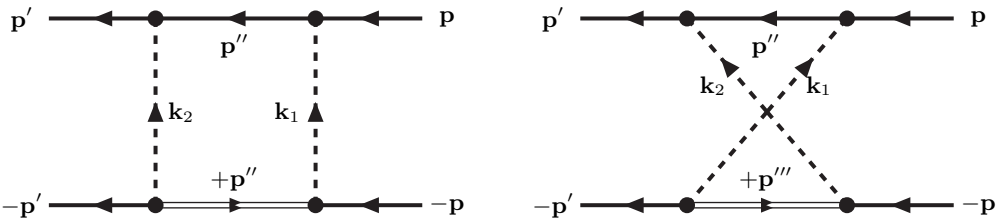

(a) (b)

FIG. 2: *CM-three-momenta graphs for $\sigma = +-$. The solid lines denote baryons. The dashed lines refers to the vector mesons, $\mathbf{k}_1 = \mathbf{k}_\rho$ and $\mathbf{k}_2 = \mathbf{k}_\omega$.*

the B-factors as given in Table VIII A. Keeping terms up to $1/M^2$ we get

$$\begin{aligned} -A^0_\rho B^0_\rho + \mathbf{A}_\rho \cdot \mathbf{B}_\rho \;&\approx\; -\frac{1}{2M}\Big\{\boldsymbol{\sigma}_2 \cdot \mathbf{p}'' - (1+2\kappa'_\rho)\;\boldsymbol{\sigma}_2 \cdot \mathbf{p})\Big\} - \frac{1}{4M^2}\big[(\mathbf{p}''+\mathbf{p}) + i(1+\kappa_\rho)\boldsymbol{\sigma}_1 \times (\mathbf{p}''-\mathbf{p})\big]\cdot \\ &\quad \times\big[(1+\kappa'_\rho)\boldsymbol{\sigma}_2 - \kappa'_\rho \boldsymbol{\sigma}_2 \cdot (\mathbf{p}''+\mathbf{p})\;(\mathbf{p}''-\mathbf{p})\big], \qquad (8.11a) \\ -A^0_\omega B^0_\omega + \mathbf{A}_\omega \cdot \mathbf{B}_\omega \;&\approx\; -\frac{1}{2M}\Big\{\boldsymbol{\sigma}_2 \cdot \mathbf{p}'' - (1+2\kappa'_\omega)\;\boldsymbol{\sigma}_2 \cdot \mathbf{p}')\Big\} - \frac{1}{4M^2}\big[(\mathbf{p}'+\mathbf{p}'') + i(1+\kappa_\omega)\boldsymbol{\sigma}_1 \times (\mathbf{p}'-\mathbf{p}'')\big]\cdot \\ &\quad \times\big[(1+\kappa'_\omega)\boldsymbol{\sigma}_2 - \kappa'_\omega \boldsymbol{\sigma}_2 \cdot (\mathbf{p}''+\mathbf{p}')\;(\mathbf{p}''-\mathbf{p}')\big]. \qquad (8.11b) \end{aligned}$$

This gives up to $1/M^2$ in a concise form,

$$\begin{aligned} V^{(+-)}_{\rho\omega}(//) \;&\approx\; +C^{(//)}_{NN}(I) g^2_{NN\rho} g^2_{NN\omega} \iint \frac{d^3k_1 d^3k_2}{(2\pi)^6}\, e^{i(\mathbf{k}_1+\mathbf{k}_2)\cdot\mathbf{r}}\; F_\rho(\mathbf{k}_1^2) F_\omega(\mathbf{k}_2^2) \\ &\quad \times\; \Big\{-A^0_\omega B^0_\omega + \mathbf{A}_\omega \cdot \mathbf{B}_\omega\Big\}\Big\{-A^0_\rho B^0_\rho + \mathbf{A}_\rho \cdot \mathbf{B}_\rho\Big\} D^{(+-)}_{//}(\omega_1,\omega_2), \qquad (8.12) \end{aligned}$$

and similar for $V^{(+-)}_{\rho\omega}(//)$.
For an antifermion in line (b) respectively in line (a) the products in (8.12), using Tables VIII A and VIII A, up to

TABLE III: Planar graphs A- and B-operators antifermion lines vector-vector exchange

$A^{(0)}_{\omega}(//,-)$	$= -(1+\kappa_\omega)\big[\boldsymbol{\sigma}_1\cdot(\mathbf{p}''-\mathbf{p}')/(2M)$
$B^{(0)}_{\omega}(//,-)$	$= +(1+\kappa_\omega)\big[\boldsymbol{\sigma}_2\cdot(\mathbf{p}''-\mathbf{p}')/(2M)$
$A^{(0)}_{\rho}(//,-)$	$= -(1+\kappa_\rho)\big[\boldsymbol{\sigma}_1\cdot(\mathbf{p}''-\mathbf{p})/(2M)$
$B^{(0)}_{\rho}(//,-)$	$= +(1+\kappa_\rho)\big[\boldsymbol{\sigma}_2\cdot(\mathbf{p}''-\mathbf{p})/(2M)$

$\mathbf{A}_{\omega}(//,-)$	$= +\big[(1+\kappa_\omega)\boldsymbol{\sigma}_1+\kappa_\omega\ \boldsymbol{\sigma}_1\cdot(\mathbf{p}''+\mathbf{p}')(\mathbf{p}''-\mathbf{p}')\big]/(2M)$
$\mathbf{B}_{\omega}(//,-)$	$= +\big[(1+\kappa'_\omega)\boldsymbol{\sigma}_2+\kappa'_\omega\ \boldsymbol{\sigma}_2\cdot(\mathbf{p}''-\mathbf{p}')(\mathbf{p}''+\mathbf{p}')\big]/(2M)$
$\mathbf{A}_{\rho}(//,-)$	$= +\big[(1+\kappa_\rho)\boldsymbol{\sigma}_1+\kappa_\rho\ \boldsymbol{\sigma}_1\cdot(\mathbf{p}''+\mathbf{p})(\mathbf{p}''-\mathbf{p})\big]/(2M)$
$\mathbf{B}_{\rho}(//,-)$	$= +\big[(1+\kappa_\rho)\boldsymbol{\sigma}_2+\kappa_\rho\ \boldsymbol{\sigma}_2\cdot(\mathbf{p}''-\mathbf{p})(\mathbf{p}''+\mathbf{p})\big]/(2M)$

$1/M^2$ become

$$
\begin{aligned}
V^{(+-)}_{\rho\omega}(//) \ &\approx\ +C^{(//)}_{NN}(I)g^2_{NN\rho}g^2_{NN\omega}\iint\frac{d^3k_1d^3k_2}{(2\pi)^6}\,e^{i(\mathbf{k}_1+\mathbf{k}_2)\cdot\mathbf{r}}\ F_\rho(\mathbf{k}_1^2)F_\omega(\mathbf{k}_2^2)\cdot\\
&\times\ \frac{1}{4M^2}\Big\{\mathbf{p}''^2-(1+2\kappa'_\omega)\ \boldsymbol{\sigma}_2\cdot\mathbf{p}'\ \boldsymbol{\sigma}_2\cdot\mathbf{p}''-(1+2\kappa'_\rho)\ \boldsymbol{\sigma}_2\cdot\mathbf{p}''\ \boldsymbol{\sigma}_2\cdot\mathbf{p}\\
&\quad+(1+2\kappa'_\rho)(1+2\kappa'_\omega)\ \boldsymbol{\sigma}_2\cdot\mathbf{p}'\ \boldsymbol{\sigma}_2\cdot\mathbf{p}\Big\}\cdot D^{(+-)}_{//}(\omega_1,\omega_2), \qquad (8.13a)\\
V^{(-+)}_{\rho\omega}(//) \ &\approx\ +C^{(//)}_{NN}(I)g^2_{NN\rho}g^2_{NN\omega}\iint\frac{d^3k_1d^3k_2}{(2\pi)^6}\,e^{i(\mathbf{k}_1+\mathbf{k}_2)\cdot\mathbf{r}}\ F_\rho(\mathbf{k}_1^2)F_\omega(\mathbf{k}_2^2)\cdot\\
&\times\ \frac{1}{4M^2}\Big\{\mathbf{p}''^2-(1+2\kappa'_\omega)\ \boldsymbol{\sigma}_1\cdot\mathbf{p}'\ \boldsymbol{\sigma}_1\cdot\mathbf{p}''-(1+2\kappa'_\rho)\ \boldsymbol{\sigma}_1\cdot\mathbf{p}''\ \boldsymbol{\sigma}_2\cdot\mathbf{p}\\
&\quad+(1+2\kappa'_\rho)(1+2\kappa'_\omega)\ \boldsymbol{\sigma}_1\cdot\mathbf{p}'\ \boldsymbol{\sigma}_1\cdot\mathbf{p}\Big\}\cdot D^{(-+)}_{//}(\omega_1,\omega_2), \qquad (8.13b)\\
& \qquad (8.13c)
\end{aligned}
$$

Working out the products in (8.13) with the momenta relations (8.6) and (8.7) gives

$$
\begin{aligned}
(+-)\ :\ \Big\{\ldots\Big\} &= 4\kappa'_\rho\kappa'_\omega\ \mathbf{q}^2-\frac{1}{4}(1+2\kappa'_\rho)(1+2\kappa'_\omega)\ \mathbf{k}^2-4i\kappa'_\rho\kappa'_\omega\ \boldsymbol{\sigma}_2\cdot\mathbf{q}\times\mathbf{k}+\frac{1}{2}(\kappa'_\rho-\kappa'_\omega)(\mathbf{k}_1^2-\mathbf{k}_2^2)-\frac{1}{2}\mathbf{k}_1\cdot\mathbf{k}_2\\
&-2\kappa'_\omega(\mathbf{q}\cdot\mathbf{k}_1)+2\kappa'_\rho(\mathbf{q}\cdot\mathbf{k}_2)-2i\kappa'_\omega\ \boldsymbol{\sigma}_2\cdot\mathbf{q}\times\mathbf{k}_1-2i\kappa'_\rho\ \boldsymbol{\sigma}_2\cdot\mathbf{q}\times\mathbf{k}_2,
\end{aligned}
$$

and with the substitution $\boldsymbol{\sigma}_2\to\boldsymbol{\sigma}_1$ the same expression for $(-+):\big\{\ldots\big\}$. Here we used the notation $\kappa'_V=\kappa_V\ (M/\mathcal{M})$ for $V=\omega,\rho$.
For an antifermion in line (a) the A-factors are given in Table VIII A. The crossed BW graph (b) of Figs. 2, and a similar one with the antifermion in line (a), give

$$
\begin{aligned}
V^{(+-)}_{\rho\omega}(X) \ &\approx\ +C^{(X)}_{NN}(I)g^2_{NN\rho}g^2_{NN\omega}\iint\frac{d^3k_1d^3k_2}{(2\pi)^6}\,e^{i(\mathbf{k}_1+\mathbf{k}_2)\cdot\mathbf{r}}\ F_\rho(\mathbf{k}_1^2)F_\omega(\mathbf{k}_2^2)\\
&\times\ \Big\{-A^0_\omega C^0_\omega(-)+\mathbf{A}_\omega\cdot\mathbf{C}_\omega\Big\}\Big\{-A^0_\rho C^0_\rho+\mathbf{A}_\rho\cdot\mathbf{C}_\rho\Big\}D_X(\omega_1,\omega_2), \qquad (8.14)
\end{aligned}
$$

and similar for $V^{(+-)}_{\rho\omega}(X)$. The form factors are given by $F_{\rho,\omega}(\mathbf{k}^2_{1,2})=F^2_{NN\rho,\omega}(\mathbf{k}^2_{1,2})$. The Kadyshevsky energy denominators $D_i(\omega_1,\omega_2)$ can be found in Appendix D, equations (D2) and (D4).
Notice that by reversing the b-line of the crossed graphs one can relate the spinor matrix elements to correspond to an incoming fermion with momentum $-\mathbf{p}'$ and outgoing fermion with momentum $-\mathbf{p}$. This can be seen as follows

$$
\big[\bar u(-p')\Gamma_\rho u(-p''')\ \bar u(-p''')\Gamma_\omega\ u(-p)\big]^*=\bar u(-p)\left(\gamma_0\Gamma^\dagger_\omega\gamma_0\right)\ u(-p''')\cdot\bar u(-p''')\left(\gamma_0\Gamma^\dagger_\rho\gamma_0\right)\ u(-p').
$$

TABLE IV: Crossed graphs C-operators for fermion and antifermion lines vector-vector exchange

$$
\begin{array}{|l|}
\hline
C_\omega^{(0)}(X,+) \;=\; 1+\big[\mathbf{p}\cdot\mathbf{p}'''+i\boldsymbol{\sigma}_2\cdot\mathbf{p}\times\mathbf{p}'''\big]/(4M^2)-\kappa_\omega\;\big[(\mathbf{p}-\mathbf{p}'')^2-2i\boldsymbol{\sigma}_2\cdot\mathbf{p}\times\mathbf{p}'''\big]/(4M^2)\\
C_\rho^{(0)}(X,+) \;=\; 1+\big[\mathbf{p}'\cdot\mathbf{p}'''-i\boldsymbol{\sigma}_2\cdot\mathbf{p}'\times\mathbf{p}'''\big]/(4M^2)-\kappa_\rho\;\big[(\mathbf{p}'-\mathbf{p}''')^2+2i\boldsymbol{\sigma}_2\cdot\mathbf{p}'\times\mathbf{p}'''\big]/(4M^2)\\
\hline
\mathbf{C}_\omega(X,+) \;=\; +\big[(\mathbf{p}+\mathbf{p}''')+i(1+\kappa_\omega)\;\boldsymbol{\sigma}_2\times(\mathbf{p}-\mathbf{p}''')\big]/(2M)\\
\mathbf{C}_\rho(X,+) \;=\; +\big[(\mathbf{p}'''+\mathbf{p}')+i(1+\kappa_\rho)\;\boldsymbol{\sigma}_2\times(\mathbf{p}'''-\mathbf{p}')\big]/(2M)\\
\hline
C_\omega^{(0)}(X,-) \;=\; +(1+\kappa_\omega)\big[\boldsymbol{\sigma}_2\cdot\mathbf{p}'''-\mathbf{p})\\
C_\rho^{(0)}(X,-) \;=\; +(1+\kappa_\rho)\big[\boldsymbol{\sigma}_2\cdot\mathbf{p}'''-\mathbf{p}')\\
\mathbf{C}_\omega(X,-) \;=\; +\big[(1+\kappa_\omega)\;\boldsymbol{\sigma}_2+\kappa_\omega\;\boldsymbol{\sigma}_2\cdot(\mathbf{p}'''-\mathbf{p})(\mathbf{p}'''+\mathbf{p}\big]/(2M)\\
\mathbf{C}_\rho(X,-) \;=\; +\big[(1+\kappa_\rho)\;\boldsymbol{\sigma}_2+\kappa_\rho\;\boldsymbol{\sigma}_2\cdot(\mathbf{p}'''-\mathbf{p}')(\mathbf{p}'''+\mathbf{p}'\big]/(2M)\\
\hline
\end{array}
$$

For an antifermion in line (b) respectively in line (a) the products in (8.14), using Tables VIII A and VIII A, up to $1/M^2$ become

$$
\begin{aligned}
V_{\rho\omega}^{(+-)}(X) \;&\approx\; +C_{NN}^{(X)}(I)g_{NN\rho}^2g_{NN\omega}^2\iint\frac{d^3k_1d^3k_2}{(2\pi)^6}\,e^{i(\mathbf{k}_1+\mathbf{k}_2)\cdot\mathbf{r}}\;F_\rho(\mathbf{k}_1^2)F_\omega(\mathbf{k}_2^2)\cdot\\
&\times\;\frac{1}{4M^2}\;\Big\{\mathbf{p}'''^2-(1+2\kappa'_\omega)\;\boldsymbol{\sigma}_2\cdot\mathbf{p}\;\boldsymbol{\sigma}_2\cdot\mathbf{p}'''-(1+2\kappa'_\rho)\;\boldsymbol{\sigma}_2\cdot\mathbf{p}'''\;\boldsymbol{\sigma}_2\cdot\mathbf{p}'\\
&\quad+(1+2\kappa'_\rho)(1+2\kappa'_\omega)\;\boldsymbol{\sigma}_2\cdot\mathbf{p}\;\boldsymbol{\sigma}_2\cdot\mathbf{p}'\Big\}\cdot D_X^{(+-)}(\omega_1,\omega_2),
\end{aligned}
\tag{8.15a}
$$

$$
\begin{aligned}
V_{\rho\omega}^{(-+)}(//) \;&\approx\; +C_{NN}^{(X)}(I)g_{NN\rho}^2g_{NN\omega}^2\iint\frac{d^3k_1d^3k_2}{(2\pi)^6}\,e^{i(\mathbf{k}_1+\mathbf{k}_2)\cdot\mathbf{r}}\;F_\rho(\mathbf{k}_1^2)F_\omega(\mathbf{k}_2^2)\cdot\\
&\times\;\frac{1}{4M^2}\;\Big\{\mathbf{p}''^2-(1+2\kappa'_\omega)\;\boldsymbol{\sigma}_1\cdot\mathbf{p}'\;\boldsymbol{\sigma}_1\cdot\mathbf{p}''-(1+2\kappa'_\rho)\;\boldsymbol{\sigma}_1\cdot\mathbf{p}''\;\boldsymbol{\sigma}_1\cdot\mathbf{p}\\
&\quad+(1+2\kappa'_\rho)(1+2\kappa'_\omega)\;\boldsymbol{\sigma}_1\cdot\mathbf{p}'\;\boldsymbol{\sigma}_1\cdot\mathbf{p}\Big\}\cdot D_X^{(-+)}(\omega_1,\omega_2).
\end{aligned}
\tag{8.15b}
$$

Working out the products in (8.15) with the momenta relations (8.6) and (8.7) gives

$$
\begin{aligned}
(+-)\;:\;\Big\{\ldots\Big\} &= 4\kappa'_\rho\kappa'_\omega\;\mathbf{q}^2-\frac{1}{4}(1+2\kappa'_\rho)(1+2\kappa'_\omega)\;\mathbf{k}^2+4i\kappa'_\rho\kappa'_\omega\;\boldsymbol{\sigma}_2\cdot\mathbf{q}\times\mathbf{k}+\frac{1}{4}(\mathbf{k}_1^2+\mathbf{k}_2^2)-\frac{1}{2}\mathbf{k}_1\cdot\mathbf{k}_2\\
&+\frac{1}{2}(\kappa'_\rho-\kappa'_\omega)(\mathbf{k}_1^2-\mathbf{k}_2^2)+2\kappa'_\omega(\mathbf{q}\cdot\mathbf{k}_1)-2\kappa'_\rho(\mathbf{q}\cdot\mathbf{k}_2)+2i\kappa'_\omega\;\boldsymbol{\sigma}_2\cdot\mathbf{q}\times\mathbf{k}_1+2i\kappa'_\rho\;\boldsymbol{\sigma}_2\cdot\mathbf{q}\times\mathbf{k}_2,\\
(-+)\;:\;\Big\{\ldots\Big\} &= 4\kappa'_\rho\kappa'_\omega\;\mathbf{q}^2-\frac{1}{4}(1+2\kappa'_\rho)(1+2\kappa'_\omega)\;\mathbf{k}^2+4i\kappa'_\rho\kappa'_\omega\;\boldsymbol{\sigma}_2\cdot\mathbf{q}\times\mathbf{k}+\frac{1}{4}(\mathbf{k}_1^2+\mathbf{k}_2^2)-\frac{1}{2}\mathbf{k}_1\cdot\mathbf{k}_2\\
&+\frac{1}{2}(\kappa'_\rho-\kappa'_\omega)(\mathbf{k}_1^2-\mathbf{k}_2^2)-2\kappa'_\omega(\mathbf{q}\cdot\mathbf{k}_1)+2\kappa'_\rho(\mathbf{q}\cdot\mathbf{k}_2)-2i\kappa'_\omega\;\boldsymbol{\sigma}_2\cdot\mathbf{q}\times\mathbf{k}_1-2i\kappa'_\rho\;\boldsymbol{\sigma}_2\cdot\mathbf{q}\times\mathbf{k}_2,
\end{aligned}
$$

3. **Addition $\rho-\omega$ interchange**: For the total potentials the contribution of the graphs with $\rho\leftrightarrow\omega$, i.e. $V_{\omega\rho}^{(\sigma)}(//,X)$. hier

IX. TWO-GLUON EXCHANGE

Application to two-gluon exchange between constituent quarks, with $\kappa_g = 0$, gives for the parallel graphs

$$V_{gg}^{(++)}(//) \approx g_s^4\, C_{//} \int\!\!\int \frac{d^3k_1 d^3k_2}{(2\pi)^6}\, e^{i(\mathbf{k}_1+\mathbf{k}_2)\cdot\mathbf{r}}\; F_g(\mathbf{k}_1^2)F_g(\mathbf{k}_2^2)\; D_{//}(\omega_1,\omega_2)\cdot$$
$$\times \left\{1+\frac{1}{4M^2}\left[12\mathbf{q}^2+(\mathbf{k}_1^2+\mathbf{k}_2^2)-3i(\boldsymbol{\sigma}_1+\boldsymbol{\sigma}_2)\cdot\mathbf{q}\times(\mathbf{k}_1+\mathbf{k}_2)\right.\right.$$
$$\left.\left.-\big\{(\boldsymbol{\sigma}_1\cdot\boldsymbol{\sigma}_2)\mathbf{k}_1^2-\boldsymbol{\sigma}_1\cdot\mathbf{k}_1\boldsymbol{\sigma}_2\cdot\mathbf{k}_1\big\}-\big\{(\boldsymbol{\sigma}_1\cdot\boldsymbol{\sigma}_2)\mathbf{k}_2^2-\boldsymbol{\sigma}_1\cdot\mathbf{k}_2\boldsymbol{\sigma}_2\cdot\mathbf{k}_2\big\}\right]\right\}. \tag{9.1}$$

For the crossed graphs

$$V_{gg}^{(++)}(X) \approx g_s^4\, C_X \int\!\!\int \frac{d^3k_1 d^3k_2}{(2\pi)^6}\, e^{i(\mathbf{k}_1+\mathbf{k}_2)\cdot\mathbf{r}}\; F_g(\mathbf{k}_1^2)F_g(\mathbf{k}_2^2)D_X(\omega_1,\omega_2)\cdot$$
$$\times \left\{1+\frac{1}{4M^2}\left[12\mathbf{q}^2-(\mathbf{k}_1^2+\mathbf{k}_2^2)-3i(\boldsymbol{\sigma}_1+\boldsymbol{\sigma}_2)\cdot\mathbf{q}\times(\mathbf{k}_1+\mathbf{k}_2)\right.\right.$$
$$\left.\left.-\big\{(\boldsymbol{\sigma}_1\cdot\boldsymbol{\sigma}_2)\mathbf{k}_1^2-\boldsymbol{\sigma}_1\cdot\mathbf{k}_1\boldsymbol{\sigma}_2\cdot\mathbf{k}_1\big\}-\big\{(\boldsymbol{\sigma}_1\cdot\boldsymbol{\sigma}_2)\mathbf{k}_2^2-\boldsymbol{\sigma}_1\cdot\mathbf{k}_2\boldsymbol{\sigma}_2\cdot\mathbf{k}_2\big\}\right]\right\} \tag{9.2}$$

For the different possibilities of the intermediate fermions ($\sigma = ++,+-,-+,--$)

$$V_{gg}^{(\sigma)} \approx +g_s^4 \int\!\!\int \frac{d^3k_1 d^3k_2}{(2\pi)^6}\, e^{i(\mathbf{k}_1+\mathbf{k}_2)\cdot\mathbf{r}}\; F_g(\mathbf{k}_1^2)F_g(\mathbf{k}_2^2)\cdot$$
$$\times\left[C_{//}\; D_{//}^{(\sigma)}(\omega_1,\omega_2)+C_X\; D_X^{(\sigma)}(\omega_1,\omega_2)\right], \tag{9.3}$$

where $\sigma = ++,+-,-+,--$. Labeling the incoming and outgoing fermions by (i) and (j), The color factors are [31]

$$C_{//} = \frac{2}{9}+\frac{1}{24}\sum_{a,c=1}^{8} d_{aac}\left(\lambda_c^{(i)}+\lambda_c^{(j)}\right)-\frac{1}{12}\left(\boldsymbol{\lambda}^{(i)}\cdot\boldsymbol{\lambda}^{(j)}\right), \tag{9.4a}$$

$$C_X = \frac{2}{9}+\frac{1}{24}\sum_{a,c=1}^{8} d_{aac}\left(\lambda_c^{(i)}+\lambda_c^{(j)}\right)+\frac{1}{12}\left(\boldsymbol{\lambda}^{(i)}\cdot\boldsymbol{\lambda}^{(j)}\right). \tag{9.4b}$$

Since only the first term is used in the following, which has the unit operator in color space, the color labels of the quarks are not altered and can be neglected henceforth.

The **adiabatic approximation** gives, putting $M = m_Q$, see Appendix C-D, the following denominators:

1a. **The planar-box diagram, with TMO:**

$$D_{//}^{(++)} = +\frac{1}{2\omega_1^2\omega_2^2}\left[\frac{1}{\omega_1}+\frac{1}{\omega_2}-\frac{1}{\omega_1+\omega_2}\right],$$
$$D_{//}^{(+-)} = \frac{1}{2\omega_1\omega_2}\left\{\frac{1}{\omega_1+\omega_2}\left[\frac{1}{\omega_1(\omega_1+2m_Q)}+\frac{1}{\omega_2(\omega_2+2m_Q)}\right]\right.$$
$$\left.+\;\frac{[\omega_1+\omega_2+2m_Q]}{\omega_1\omega_2(\omega_1+2m_Q)(\omega_2+2m_Q)}\right\}. \tag{9.5}$$

1b. **The planar-box diagram, no TMO:** Grouping the TMO-graphs in NN together with two-gluon-exchange between different quarks giving Van-der-Waals forces implies

$$D_{//}^{(++)} \to D_{//}^{(BW)} = -\frac{1}{2\omega_1^2\omega_2^2}\frac{1}{\omega_1+\omega_2}. \tag{9.6}$$

2. **The crossed-box diagram:** The **adiabatic approximation** gives the contributions

$$
\begin{aligned}
D_X^{(++)} &= -\frac{1}{2\omega_1^2\omega_2^2}\left[\frac{1}{\omega_1}+\frac{1}{\omega_2}-\frac{1}{\omega_1+\omega_2}\right], \\
D_X^{(+-)} &= \frac{1}{2\omega_1\omega_2}\Bigg\{\frac{1}{\omega_1+\omega_2}\left[\frac{1}{\omega_1(\omega_2+2m_Q)}+\frac{1}{\omega_2(\omega_1+2m_Q)}\right] \\
&+ \left[\frac{(\omega_1+m_Q)(\omega_2+m_Q)}{\omega_1\omega_2(\omega_1+2m_Q)(\omega_2+2m_Q)}\right]\frac{2}{m_Q}\Bigg\}. \qquad (9.7)
\end{aligned}
$$

A. Pomeron exchange in baryon-baryon: NN, YN, YY

The application to the Low-Nussinov [14, 15] two-vector-exchange pomeron model involves the folding of the two-gluon-exchange between quarks with the constituent quark model baryon(N,Y) wave functions. Since the baryons are color singlets one has $C_{//}=C_X \Rightarrow 2/9$. Then it follows that: **For $C_{//}=C_X$ the adiabatic potential $V_{gg}^{(++)}$ is of the order $(1/M^2)$ as is also the case for the adiabatic potential $V_{gg}^{(+-)}$. They both give repulsion**.

1. **Adiabatic Contributions** $\sigma=++$ The two-gluon exchange with two positive-energy quark in the intermediate state gives for the central potential

$$
\begin{aligned}
V_{gg}^{(++)} &\approx +\frac{g_s^4}{2m_Q^2}\int\!\!\int\frac{d^3k_1d^3k_2}{(2\pi)^6}\,e^{i(\mathbf{k}_1+\mathbf{k}_2)\cdot\mathbf{r}}\;F_g(\mathbf{k}_1^2)F_g(\mathbf{k}_2^2)\cdot \\
&\times\left[\mathbf{k}_1^2+\mathbf{k}_2^2\right]\;\left[C_{//}\;D_{//}^{(++)}(\omega_1,\omega_2)+C_X\;D_X^{(++)}(\omega_1,\omega_2)\right] \\
&\Rightarrow +\frac{8g_s^4}{3m_Q^2}\int\!\!\int\frac{d^3k_1d^3k_2}{(2\pi)^6}\,e^{i(\mathbf{k}_1+\mathbf{k}_2)\cdot\mathbf{r}}\;F_g(\mathbf{k}_1^2)F_g(\mathbf{k}_2^2)\;\left[\mathbf{k}_1^2+\mathbf{k}_2^2\right]\;\cdot \\
&\times\frac{1}{2\omega_1^2\omega_2^2}\left[\frac{1}{\omega_1}+\frac{1}{\omega_2}-\frac{1}{\omega_1+\omega_2}\right]. \qquad (9.8)
\end{aligned}
$$

Separation of ω_1 and ω_2 is achieved using the identities

$$
\begin{aligned}
\frac{1}{\omega^3} &= \frac{2}{\pi}\int_0^\infty\frac{d\lambda}{\lambda^2}\left[\frac{1}{\omega^2}-\frac{1}{\omega^2+\lambda^2}\right]\;,\;\frac{1}{\omega_1^2\omega_2^2}\frac{1}{\omega_1+\omega_2}= \\
&\frac{2}{\pi}\int_0^\infty\frac{d\lambda}{\lambda^2}\left[\frac{1}{\omega_1^2}-\frac{1}{\omega_1^2+\lambda^2}\right]\left[\frac{1}{\omega_2^2}-\frac{1}{\omega_2^2+\lambda^2}\right],
\end{aligned}
$$

one obtains

$$
D_{//}^{(++)} = \frac{1}{\pi}\int_0^\infty\frac{d\lambda}{\lambda^2}\left[\frac{1}{\omega_1^2\omega_2^2}-\frac{1}{(\omega_1^2+\lambda^2)(\omega_2^2+\lambda^2)}\right] \qquad (9.9)
$$

Then, the Fourier transform in (9.8) of (9.9 gives

$$
B_{gg}(r_1,r_2) = \frac{1}{\pi}\int_0^\infty\frac{d\lambda}{\lambda^2}\left[I_2(m_g,r_1)\;I_2(m_g,r_2)-F_g(\lambda,r_1)F_g(\lambda,r_2)\right],
$$

with $I_2(m,r)=(m/4\pi)\phi_C^0(m,r)$ the Fourier transform of $1/\omega^2$ [30], and $F_g(\lambda,r)=\exp[-\lambda^2/\Lambda_g]\;I_2(\sqrt{m_g^2+\lambda^2},r)$. This gives the potential

$$
V_{gg}^{(++)} \approx -\frac{8g_s^4}{3m_Q^2}\lim_{r_1,r_2\to r}\left[\boldsymbol{\nabla}_1^2+\boldsymbol{\nabla}_2^2\right]\;B_{gg}(r_1,r_2). \qquad (9.10)
$$

In the case of no TMO-graphs we get

$$
\begin{aligned}
V_{gg}^{(++)'} &\approx +\frac{g_s^4}{2m_Q^2}\int\!\!\int \frac{d^3k_1 d^3k_2}{(2\pi)^6}\, e^{i(\mathbf{k}_1+\mathbf{k}_2)\cdot\mathbf{r}}\; F_g(\mathbf{k}_1^2)F_g(\mathbf{k}_2^2)\cdot \\
&\quad \times\big[\mathbf{k}_1^2+\mathbf{k}_2^2\big]\;\Big[C_{//}\; D_{//}^{(BW)}(\omega_1,\omega_2)+C_X\; D_X^{(++)}(\omega_1,\omega_2)\Big] \\
&\Rightarrow +\frac{8g_s^4}{3m_Q^2}\int\!\!\int \frac{d^3k_1 d^3k_2}{(2\pi)^6}\, e^{i(\mathbf{k}_1+\mathbf{k}_2)\cdot\mathbf{r}}\; F_g(\mathbf{k}_1^2)F_g(\mathbf{k}_2^2)\;\big[\mathbf{k}_1^2+\mathbf{k}_2^2\big]\;\cdot \\
&\quad \times\frac{1}{2\omega_1^2\omega_2^2}\Big[\frac{1}{\omega_1}+\frac{1}{\omega_2}-\frac{2}{\omega_1+\omega_2}\Big].
\end{aligned}
\tag{9.11}
$$

The Fourier transformation can be worked out using the identities above, etc. Note that without TMO the repulsion is weaker.

2. **Adiabatic Contributions** $\sigma=+-,-+$ The two-gluon exchange with one negative-energy quark in the intermediate state gives in the adiabatic approximation, since for $\kappa_g=0$ all expressions $\big\{\ldots\big\}\to-(\mathbf{k}_1\cdot\mathbf{k}_2)$,

$$
\begin{aligned}
V_{gg}^{(+-)} &\approx -\frac{g_s^4}{2m_Q^2}\int\!\!\int \frac{d^3k_1 d^3k_2}{(2\pi)^6}\, e^{i(\mathbf{k}_1+\mathbf{k}_2)\cdot\mathbf{r}}\; F_g(\mathbf{k}_1^2)F_g(\mathbf{k}_2^2)\cdot \\
&\quad \times\big[\mathbf{k}_1\cdot\mathbf{k}_2\big]\;\Big[C_{//}\; D_{//}^{(+-)}(\omega_1,\omega_2)+C_X\; D_X^{(+-)}(\omega_1,\omega_2)\Big]
\end{aligned}
\tag{9.12}
$$

In the adiabatic approximation the energy-denominators are

$$
\begin{aligned}
D_{//}^{(+-)} &= \frac{1}{2\omega_1\omega_2}\Bigg\{\frac{1}{\omega_1+\omega_2}\left[\frac{1}{\omega_1\;(\omega_1+2m_Q)}+\frac{1}{\omega_2\;(\omega_2+2m_Q)}\right] \\
&\quad +\frac{1}{\omega_1+\omega_2+2m_Q}\left[\frac{1}{\omega_1\;(\omega_1+2m_Q)}+\frac{1}{\omega_2\;(\omega_2+2m_Q)}\right. \\
&\quad \left.+\frac{1}{(\omega_1+2m_Q)(\omega_2+2m_Q)}+\frac{1}{\omega_1\omega_2}\right]\Bigg\},
\end{aligned}
\tag{9.13}
$$

and

$$
\begin{aligned}
D_X^{(+-)} &= \frac{1}{2\omega_1\omega_2}\Bigg\{\frac{1}{\omega_1+\omega_2}\left[\frac{1}{\omega_1\;(\omega_2+2m_Q)}+\frac{1}{\omega_2\;(\omega_1+2m_Q)}\right] \\
&\quad +\frac{1}{2m_Q}\left[\frac{1}{\omega_1\;(\omega_2+2m_Q)}+\frac{1}{\omega_2\;(\omega_1+2m_Q)}\right. \\
&\quad \left.+\frac{1}{(\omega_1+2m_Q)(\omega_2+2m_Q)}+\frac{1}{\omega_1\omega_2}\right]\Bigg\}.
\end{aligned}
\tag{9.14}
$$

The QQ-amplitude becomes, see [31],

$$
M_{2gluon}^{(+-)} = -\frac{g_s^4}{m_Q^2}\;(\mathbf{k}_1\cdot\mathbf{k}_2)\;\Big[C_{//}D_{//}^{(+-)}+C_X D_X^{(+-)}\Big]. \tag{9.15}
$$

Here, and in the following, a factor of 2 has been included coming from an identical contribution from $\sigma=(-+)$. For all terms in Eq. (9.13-9.14) the separation of the $\mathbf{k}_1$ and $\mathbf{k}_2$ dependence using integral representations has been given in [11, 12], except for $[\omega_1+\omega_2+2m_Q]^{-1}$. For this a rather complicated formula is required. We note that for $m_G\approx m_Q$ we have the bounds $2(m_G+m_Q)\le[\omega_1+\omega_2+2m_Q]<2(\omega_1+\omega_2)$, and we choose to make the approximation $\approx 2(\omega_1+\omega_2)$. Furthermore, using the splitting $[\omega(\omega+2m_Q)]^{-1}=[1/\omega-1/(\omega+2m_Q)]/2m_Q$ we can rewrite the denominator for the parallel graphs as

$$
\begin{aligned}
D_{//}^{(+-)} &= \frac{1}{4\omega_1\omega_2}\frac{1}{\omega_1+\omega_2}\left[\frac{3}{\omega_1(\omega_1+2m_Q)}+\frac{3}{\omega_2(\omega_2+2m_Q)}+\frac{1}{(\omega_1+2m_Q)(\omega_2+2m_Q)}+\frac{1}{\omega_1\omega_2}\right] \\
&= \frac{1}{4\omega_1^2\omega_2^2}\frac{1}{(\omega_1+2m_Q)(\omega_2+2m_Q)}\frac{1}{\omega_1+\omega_2}\left[3(\omega_1^2+\omega_2^2)+2\omega_1\omega_2+8m_Q(\omega_1+\omega_2)+4m_Q^2\right] \\
&= \frac{3}{4a}\frac{1}{\omega_1^2\omega_2^2}\left[1-\frac{\omega_1\omega_2}{(\omega_1+a)(\omega_2+a)}+\frac{a}{3(\omega_1+\omega_2)}\left(1-\frac{5\omega_1\omega_2}{(\omega_1+a)(\omega_2+a)}\right)\right],
\end{aligned}
$$

where $a = 2m_Q$. Then, in configuration space we obtain the the 2-gluon exchange potential

$$V_{//}^{(+-)}(r_1,r_2) = \frac{g_s^4}{4m_Q^2}\, C_{//}\ (\boldsymbol{\nabla}_1\cdot\boldsymbol{\nabla}_2)\Big\{3H_{0,2}(a,r_1,r_2)+3H_{2,0}(a,r_1,r_2) +2H_{1,1}(a,r_1,r_2)+8m_Q\ G_{2,1}(a,r_1)G_{2,1}(a,r_2)+4m_Q^2\ H_{2,2}(a,r_1,r_2)\Big\}, \tag{9.16a}$$

$$= \frac{3g_s^4}{8m_Q^3}\, C_{//}\ (\boldsymbol{\nabla}_1\cdot\boldsymbol{\nabla}_2)\Big\{I_2(m_G,r_1)I_2(m_G,r_2)-G_{1,1}(a,r_1)G_{1,1}(a,r_2) -\frac{a}{3}\big[5H_{2,2}(a,r_1,r_2)-H_{2,2}(a=0,r_1,r_2)\big]\Big\}. \tag{9.16b}$$

The denominator for the crossed graphs can be written as

$$D_X^{(+-)} = \frac{1}{2\omega_1^2\omega_2^2}\Big\{\Big[1+\frac{\omega_1}{\omega_1+2m_Q}+\frac{\omega_2}{\omega_2+2m_Q}+\frac{\omega_1\omega_2}{(\omega_1+2m_Q)(\omega_2+2m_Q)}\Big]\ \frac{1}{2m_Q} +\frac{2}{\omega_1+\omega_2}\,\frac{\omega_1\omega_2+m_Q(\omega_1+\omega_2)}{(\omega_1+2m_Q)(\omega_2+m_Q)}\Big\}. \tag{9.17}$$

Then, the configuration space 2-gluon exchange potential from the crossed graphs is,

$$V_X^{(+-)}(r_1,r_2) = \frac{g_s^4}{2m_Q^2}\ C_X\ \ (\boldsymbol{\nabla}_1\cdot\boldsymbol{\nabla}_2)\Big\{\Big[I_2(m_G,r_1)I_2(m_G,r_2)+I_2(m_G,r_1)G_{1,1}(a,r_2) +G_{1,1}(a,r_1)I_2(m_G,r_2)+H_{1,1}(a,r_1,r_2)\Big]\ \frac{1}{2m_Q}+2H_{1,1}(a,r_1,r_2)+2m_Q\ G_{2,1}(a,r_1)G_{2,1}(a,r_2)\Big\}. \tag{9.18}$$

Then, the total potential is $V_{2-gluon}^{(+-)}(r) = \lim_{r_1,r_2\to r}\Big[V_{//}^{(+-)}(r_1,r_2)+V_X^{(+-)}(r_1,r_2)\Big]$.

Conclusion: the adiabatic two-gluon exchange contribution for $\sigma = +-,-+$ to two colorless baryons interaction is repulsive.

3. **Non-Adiabatic Contributions** The $1/m_Q$-contribution denominators we can copy from [1] since the Kadyshevky denominators for $\sigma = ++$ are the same as those in the Macke-Klein formalism. The non-adiabatic energy denominators are [12]

$$D_{//}^{(1)}(\omega_1,\omega_2) = +\frac{1}{2\omega_1^2\omega_2^2}\left[\frac{1}{\omega_1^2}+\frac{1}{\omega_2^2}\right], \tag{9.19}$$

$$D_X^{(1)}(\omega_1,\omega_2) = -\frac{1}{\omega_1^2\omega_2^2}\left[\frac{1}{\omega_1^2}+\frac{1}{\omega_2^2}\right], \tag{9.20}$$

and the matrix element has a factor $\mathbf{k}_1\cdot\mathbf{k}_2/2M$ w.r.t. the non-adiabatic matrix element, and $D_i^{(0)}\to D_i^{(1)}$ $(i = //, X)$. Then, for the QQ-amplitude we obtain

$$M_{2gluon}^{(4),1} = g_s^4\Big[C_{//}\ D_{//}^{(1)}+C_X\ D_X^{(1)}\Big] \Rightarrow\ -\frac{2}{9}\frac{(\mathbf{k}_1\cdot\mathbf{k}_2)}{2M}\cdot\frac{g_s^4}{2\omega_1^2\omega_2^2}\left[\frac{1}{\omega_1^2}+\frac{1}{\omega_2^2}\right], \tag{9.21}$$

which leads to a potential with a sign opposite to that for scalar-meson exchange. Therefore, *the non-adiabatic two-gluon exchange contribution to two colorless particles interaction is repulsive.*
The QCD coupling $\alpha_s = g_s^2/4\pi \approx 0.33$ at the confinement scale $\mu \approx 200$ MeV. The double fourier transform typically leads to the so-called rationalized coupling, and for the strength we get $\sim 24\alpha_s^2 \sim 2.2$ which is of the same order as used for the pomeron coupling in ESC-models.

The form (9.21) implies the interquark potential

$$V_{QQ}^{(na)}(r) = \frac{2}{9}\frac{g_s^4}{4M}\cdot\lim_{r_1,r_2\to r}(\boldsymbol{\nabla}_1\cdot\boldsymbol{\nabla}_2)\Big[I_4(r_1)\ I_2(r_2)+I_2(r_1)\ I_4(r_2)\Big] = \frac{2}{9}\frac{g_s^4}{2M}\ I_4'(r)\ I_2'(r). \tag{9.22}$$

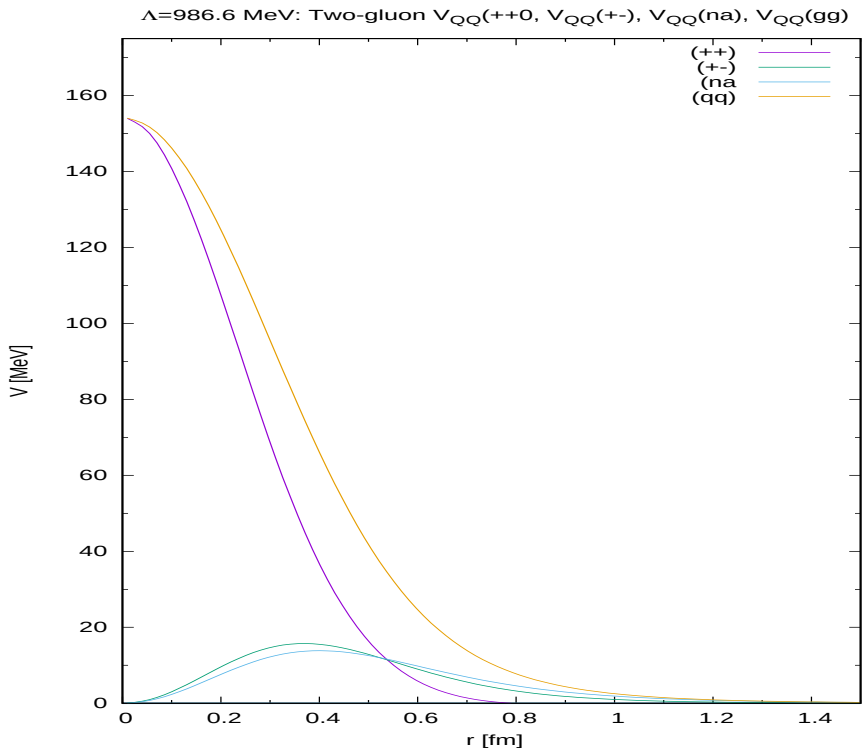

FIG. 3: Two-gluon and Pomeron(ESC16) potentials. $\alpha_s = 0.30$, $\Lambda = 986.6$ MeV, $m_g = 320$ MeV, $m_Q = 315$ MeV, $g_P = 2.72$, $m_P = 212$ MeV.

This form implies that $V_{QQ} \sim r^2$ near the origin. The corresponding $V_{BB} \sim$ *constant* near the origin due to the folding.

For the BB-potential there is an extra factor 9 from the summation over the valence quarks in a baryon.

3. **Numerical Evaluation** In Fig. 3 are plotted the adiabatic $V_{QQ}(++)$, $V_{QQ}(+-)$, the non-adiabatic $V_{QQ}(na)$, and the total 2-gluon-exchange quark-quark potential $V_{QQ}(2g)$. In Fig. 4 are plotted the adiabatic $V_{QQ}(++)$, $V_{QQ}(+-)$, the non-adiabatic $V_{QQ}(na)$, and the total 2-gluon-exchange baryon-baryon potential $V_{BB}(2g)$. In Fig. 4 are plotted $V_{QQ}(2g)$, $V_{Bb}(2g)$, and compared with the Pomeron-exchange potential V_{POM} in ESC08c/ESC16 and V_{POM17} in Ref. [30]. Here, $\alpha_s = 0.30$ and the cut-off $\Lambda = 986.6$ MeV, which gives good agreement with the meson couplings from the ESC16 fit using the QPC-mechanism, see [32] We note that ESC16 has a rather weak pomeron.

4. **Quark-Quark Potential:** In Fig. 3 the $V_{QQ}(++$, $V_{QQ}(+-)$, $V_{QQ}(na)$, and the total QQ-potential $V_{QQ}(tot)$ are shown. This for the parameters used in the quark-pair-creastion (QPC) model in ESC08c for the CQM-computation of the meson-baryon-baryon coupling constants.
5. **Baryon-Baryon Potential:** For making the connection with the baryon-level a folding with the CQM wave functions is necessary. To facilitate this we make a Gaussian fit for the potential functions $V_{BB}(++)$ and $V_{QQ}(+-) + V_{QQ}(na)$ separately. The latter gives a Gaussian $\propto r^2$, as shown in Fig. 3 and Fig. 4. Then, we perform the folding with the quark wave-functions. Denoting the CM positions of the baryons by $\mathbf{R}_1$ and $\mathbf{R}_2$ and the positions of the quarks inside the baryons by $\mathbf{r}_i$ and $\mathbf{r}_j$ respectively, the quark positions are at

$$\mathbf{x}_i = \mathbf{R}_1 + \mathbf{r}_i \ \ , \ \ \mathbf{x}_j = \mathbf{R}_2 + \mathbf{r}_j. \tag{9.23}$$

The fit with Gaussians gives the QQ-potentials, as a function of the distance $\mathbf{x}_{ij} = \mathbf{x}_1 - \mathbf{x}_j$, in the form

$$V_{QQ,ij}(\mathbf{r}_{ij}) \ = \ \sum_k A_{n,k} \ \mathbf{x}_{ij}^n \ \exp\left[-\Lambda_{n,k}^2 \ \mathbf{x}_{ij}^2\right] \ (n = 0, 2). \tag{9.24}$$

TABLE V: Gaussian fit parameters

Λ_k	250	350	450	550	650	750
A_1	-0.009D0	-0006D0	-0.006D0	+0.528D0	+0.259D0	+0.015D0
A_2	+0.019D0	+0.1480	+0.702D0	+1.357D0	+0.763D0	-0.058D0
A_3	+0.038D0	+0.0700	+0.386D0	+0.378D0	-0.058D0	-0.033D0

The BB-potential is obtained by folding the inter-quark potential with the baryonic quark wave functions, i.e.

$$V_{BB}(\mathbf{R}) \;=\; \left\langle \Psi_{2B} \middle| V_{QQ,ij}(\mathbf{x}_i - \mathbf{x}_j) \middle| \Psi_{2B} \right\rangle. \tag{9.25}$$

The overlap integral for the matrix element (9.25) is worked out in Appendix G 1. The folded potential for n=0 becomes

$$n = 0 \;:\; V_{BB}(\mathbf{R}) = \sum_k A_{0,k} \;\left(\frac{U_{0,k}}{\Lambda_{0,k}}\right)^3 \;\exp\Big[-U_{0,k}^2 \mathbf{R}^2)\Big]. \tag{9.26}$$

Here, $U_{n,k} = \Lambda_N \Lambda_{n,k} \sqrt{3/(3\Lambda_N^2 + 4\Lambda_{n,k}^2)}$, where $\Lambda_N = 1/R_B^2$.

The Pomeron-potential depends on the parameters: $(R_B, \alpha_s, m_Q, m_G, \Lambda)$. Here R_B is the (effective) quark radius in a baryon, and $\Lambda = \Lambda_{QQG}$ the quark-gluon form factor cut-off. From the ESC-model [32] with the quark-pair creation constant $\gamma = 2.19$ one has $\alpha_s = 0.30$. Furthermore $R_B = 0.7$ fm and $\Lambda = 986.6$ MeV. Since the constituent quark mass for $M_B/3$ is important for the connection between the baryon and quark-level potentials, we have choosen to vary the gluon mass. The instanton-model gives $m_G \approx 420$ MeV [26]. It appears that for $m_G = 320$ MeV the phenomenological Pomeron-potential in ESC08c/ESC16 is reproduced.

In Table IX A the fit of the two-gluon exchange potentials are perfectly fitted to a set of 6 Gaussians. Separately fitted are (i) $V_{QQ}(++)$, (ii) $V_{QQ}(+-) + V_{QQ}(na)$, and (iii) the sum of these two, called $V_{QQ}(tot)$. The parameters A_1, A_2, A_3 coreespond to the cases (i), (ii), and (iii) respectively.

In Table IX A the two-gluon exchange QQ-potentials are shown, together with the folded BB-potentials. Also is shown the Pomeron-potential from ESC08c/ESC16-model, where the iow-energy gluon mass is adjusted. Compared to the instaton-model value 420 MeV [26] the difference is within the uncertainty of the latter value.

In Fig. 4 the $V_{QQ}(tot)$ potential and the Pomeron potential V_P in ESC08c-model are shown. Below, the folded $V_{QQ}(tot)$ is shown to match rather accurately with the phenomenological V_P in ESC08c.

X. DISCUSSION AND CONCLUSIONS

The advantage of the Kadyshevsky formalism is that it is relatistic and at the same time in its appearance close to the so called old perturbation theory. An important feature is that the particles in the intermediate states are on-mass-shell, which is ideal for the implementation of form factors, in particularly Gaussian ones. In momentum space one can do the calculations taking the full relativistic momentum dependence of the fermions and mesons into account.

In this paper the application of two-gluon exchange to the Pomeron is in the spirit of the Low-Nussinov model [14, 15]. Our goal is to explain the Pomeron-exchange potential as used in the soft-core Nijmegen baryon-baryon potentials. The constituent quark model is essential for this calculation, and is justified because of the instanton structure of the QCD vacuum. The latter implies for low-momentum transfer physics the rather heavy gluon mass m_g, leading to a rather short-range TVE-potential.

It is found that there are three types of repulsive contributions of order $(1/m_Q^2)$: (i) The first from intermediate states with two fermions ($\sigma = ++$) giving a Gaussian-Yukawa type of potential. (ii) The second from intermediate states with a fermoin and an antifermion in the intermediate states ($\sigma = +-, -+$) giving a Gaussian-Yukawa potential with a zero in the origin. (iii) The third contribution from the non-adiabatic terms for $\sigma = ++$, also a Gaussian-Yukawa potential with a zero in the origin.

It is found that the strength of the Pomeron from the Low-Nussinov TVE-mechanism in QCD explains the phenomenological Pomeron as used in the soft-core Nijmegen potential, see Table IX A.

TABLE VI: Input V_{QQ} and output folded V_{BB} potentials. The parameters are $\alpha_s = 0.30$, $R_B = 0.7$ fm, $m_G = 320$ MeV, $m_Q = 345$ MeV, and $\Lambda_{QQG} = 986.6$ MeV.

r[fm]	V_{QQ}(++)	V_{BB}(++)	V_{QQ}(+-;na)	V_{BB}(+-;na)	V_{QQ}(tot)	V_{BB}(tot)	V_P(ESC08c)
0.10	140.798	73.803	5.364	83.444	146.184	157.461	156.105
0.20	107.463	70.892	17.166	81.148	124.674	152.248	150.792
0.30	68.666	66.290	26.880	77.458	95.582	143.947	142.335
0.40	36.756	60.339	29.358	72.569	66.153	133.094	131.287
0.50	16.361	53.457	25.410	66.730	41.827	120.355	118.332
0.60	5.841	46.089	18.763	60.223	24.657	106.460	104.221
0.70	1.414	38.662	12.482	53.340	13.926	92.129	89.698
0.80	-0.065	31.547	7.813	46.367	7.765	78.018	75.438
0.90	-0.394	25.030	4.759	39.559	4.388	64.668	61.996
1.00	-0.369	19.302	2.890	33.126	2.552	52.483	49.787
1.10	-0.274	14.458	1.773	27.231	1.529	41.720	39.069
1.20	-0.188	10.509	1.105	21.978	0.936	32.497	29.959
1.30	-0.124	7.405	0.699	17.420	0.577	24.816	22.449
1.40	-0.079	5.050	0.447	13.564	0.354	18.589	16.438
1.50	-0.049	3.325	0.286	10.380	0.215	13.667	11.762
1.60	-0.030	2.107	0.182	7.810	0.128	9.869	8.223
1.70	-0.017	1.278	0.114	5.781	0.074	7.005	5.619
1.80	-0.010	0.736	0.071	4.212	0.042	4.891	3.751
1.90	-0.005	0.396	0.042	3.023	0.023	3.363	2.447
2.00	-0.003	0.193	0.025	2.139	0.012	2.278	1.560

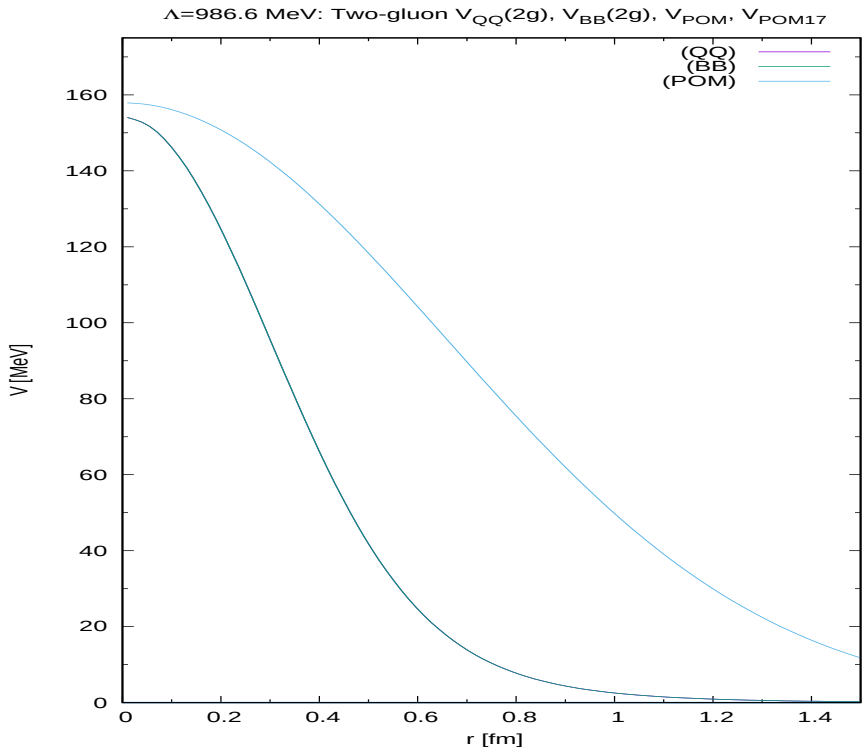

FIG. 4: Two-gluon QQ, BB and Pomeron(ESC08c potentials. $\alpha_s = 0.30$, $\Lambda = 986.6$ MeV, $m_g = 320$ MeV, $m_Q = 315$ MeV, $g_P = 2.72$, $m_P = 212$ MeV.

APPENDIX A: KADYSHEVSKY-RULES IN MOMENTUM-SPACE

In this appendix the rules for the Kadyshevsky-diagrams [3–5] are given. We follow the set up of the appendices B in [29] where the rules for the Feynman-graphs are given. The differences will then come to the surface in a most transparant manner. Starting from the expression of the S-operator, one has

$$\begin{aligned} S &= 1+\sum_{n=1}^{\infty}\left(\frac{i}{\hbar}\right)^n\int_{-\infty}^{+\infty}\dots\int_{-\infty}^{+\infty}\theta(x_n^0-x_{n-1}^0)\theta(x_{n-1}^0-x_{n-2}^0)\dots\theta(x_2^0-x_1^0)\cdot \\ &\qquad \times\mathcal{L}_I(x_n)\ \mathcal{L}_I(x_{n-1})\dots\mathcal{L}_I(x_1)\cdot d^4x_n\dots d^4x_1 \\ &\equiv 1+\sum_{n=1}^{\infty}S_n\ , \end{aligned} \tag{A1}$$

we follow [3] and introduce the time-like vector n^μ with $n^2=n_0^2-\mathbf{n}^2=1, n_0>0$. Then (A1) can be brought into a completely 4-dimensional form by the replacement

$$\theta(x^0)\to\theta(x\cdot n)\quad,\quad n\cdot x=n_0x^0-\mathbf{n}\cdot\mathbf{x}\ . \tag{A2}$$

This gives ($\hbar=1$)

$$\begin{aligned} S_n &= i^n\int_{-\infty}^{+\infty}\dots\int_{-\infty}^{+\infty}\theta[n\cdot(x_n-x_{n-1})]\theta[n\cdot(x_{n-1}-x_{n-2})]\dots\theta[n\cdot(x_2-x_1)]\cdot \\ &\qquad \times\mathcal{L}_I(x_n)\ \mathcal{L}_I(x_{n-1})\dots\mathcal{L}_I(x_1)\cdot d^4x_n\dots d^4x_1\ . \end{aligned} \tag{A3}$$

From the expression (A3) one can work out the rules for the Kadyshevsky graphs in a way which parallels the derivation of the Feynman rules. The differences come from the treatment of the θ-functions. In the case of the Feynman graphs one includes the θ-functions into the propagators by applying the Wick-expansion to the T-products of the field operators. In the case of the Kadyshevsky graphs one employs a four-dimensional form of the θ-functions, exploiting (A2),

$$\theta(n\cdot x)=-\frac{1}{2\pi i}\int_{-\infty}^{+\infty}d\kappa\frac{\exp\left[-i\kappa(n\cdot x)\right]}{\kappa+i\epsilon}\ , \tag{A4}$$

and one applies the Wick-expansion to the ordinary products of the field operators. Then, the propagators are given by

$$\begin{aligned} \langle 0|\phi(x)\phi(y)|0\rangle &= D^{(+)}(x-y)=\int\frac{d^4q}{(2\pi)^3}\theta(q_0)\delta(q^2-\mu^2) \\ \langle 0|A_\mu(x)A_\nu(y)|0\rangle &= D^{(+)}_{\mu\nu}(x-y)=-g_{\mu\nu}\int\frac{d^4q}{(2\pi)^3}\theta(q_0)\delta(q^2) \\ \langle 0|\psi(x)_\beta\bar\psi(y)_\alpha|0\rangle &= S^{(+)}_{\beta\alpha}(x-y)=\int\frac{d^4p}{(2\pi)^3}\theta(p_0)\left(\not p+m\right)_{\beta\alpha}\delta(p^2-m^2)\ . \end{aligned} \tag{A5}$$

In the Kadyshevsky-graph theory the considered Hilbert-space is enlarged by admitting states containing 'quasi-particles'. The latter carry only 4-momentum, and serve to have formally four-momentum conservation at each vertex. The quasi-particles refer to the κ-variables in the Fourier transforms (A4) of the θ-functions appearing in (A3). These quasi-particle states $|\kappa_1,\dots\rangle$ are normalized by

$$\langle\kappa_1'\dots|\kappa_1,\dots\rangle=\delta(\kappa_1'-\kappa_1)\dots \tag{A6}$$

The θ-functions in (A3) connect only internal points of the graphs. In order to handle integral equations, occurring in for example the Bethe-Salpeter- and Schwinger-Dyson-equations, one needs to consider amplitudes with external quasi-particles as well as internal quasi-particles. The external quasi-particle entering a vertex is included only into the four-momentum conservation rule of that vertex, including both the external and the internal quasi-particle 4-momentum.

After these preliminary remarks we now list the momentum-space rules for the computation of the $-M_{\kappa',\kappa}$-amplitudes, defined by

$$S_{\kappa',\kappa}=1_{\kappa',\kappa}-(2\pi)^4i\delta^4(P_f+\kappa' n-P_i-\kappa n)\ M_{\kappa',\kappa}. \tag{A7}$$

The invariant amplitude $-M_{\kappa',\kappa}$ is computed by drawing all connected Feynman graphs for the considered process. The amplitude [5]

$$-(2\pi)^4\delta(\sum_i p_{i,out} + \kappa' n - \sum_i p_{i,in} - \kappa n) M_{\kappa',\kappa}(G) \tag{A8}$$

corresponding to graph G is built up by associating factors with the elements of the graph, which we list below:

I. Those factors, independent of the specific details of the interactions, are given by the following rules:

1. Draw the Feynman graph G. Arbitrarily number its vertices and orient each internal line from the vertex with the larger number to the vertex with the smaller number, assigning to it a 4-momentum p. Then, *without changing the orientation*, change the (single) internal fermion lines to double (antifermion) lines such as to conserve the fermion number in every vertex.

2. Connect with thin lines the first vertex with the second, the second with the third, etc. Orient them in the direction of increasing numbers and assign to them a 4-momentum $\kappa_s n$, where $s = 1, 2, \ldots, n-1$ is the number of the vertex which a given dotted line leaves. Attach to the first vertex an incoming external dotted line with 4-momentum $\kappa_i n$, and to the last vertex n an outgoing external dotted line with 4-momentum $\kappa_f n$.

3. For incoming (outgoing) boson and fermion lines: identical to the rules for Feynman graphs [5, 29], see Table VII.

TABLE VII: Kadyshevski rules internal lines.

Line	Particle	State	Factor in m.e.
$\bullet - - < - - q\ \alpha$	fermion	in	$[(2\pi)^{3/2}/\sqrt{2q_0}]\ u_\alpha(\mathbf{q})$
$\bullet ===<=== q\ \alpha$	antifermion	in	$[(2\pi)^{3/2}/\sqrt{2q_0}]\ \bar{v}_\alpha(\mathbf{q})$
$\bullet - -- < - - -$ k	meson	in	$[(2\pi)^{3/2}/\sqrt{2k_0}]$
$-- < - - \bullet\ p\ \beta$	fermion	out	$[(2\pi)^{3/2}/\sqrt{2p_0}]\ \bar{u}_\beta(\mathbf{p})$
$==<== \bullet\ p\ \beta$	antifermion	out	$[(2\pi)^{3/2}/\sqrt{2p_0}]\ v_\beta(\mathbf{p})$
$\cdots\cdots < \cdots\cdots \bullet$ k	meson	out	$[(2\pi)^{3/2}/\sqrt{2k_0}]$

4. For each internal dotted line with momentum κn a factor

$$G_0(\kappa) = -\frac{1}{\kappa + i\epsilon}\ . \tag{A9}$$

5. For each internal boson line with momentum q a factor

$$\Delta^{(+)}(q) = \theta(q_0)\delta(q^2 - \mu^2)\ . \tag{A10}$$

6. For each internal fermion line with momentum p and *positive energy* a factor

$$S^{(+)}_{\beta\alpha}(p) = (\not{p} + m)_{\beta\alpha}\,\theta(p_0)\delta(p^2 - m^2)\ . \tag{A11}$$

For each internal fermion line with momentum p and *negative energy* a factor

$$S^{(-)}_{\beta\alpha}(p) = (\not{p} - m)_{\beta\alpha}\,\theta(-p_0)\delta(p^2 - m^2), \tag{A12}$$

[5] Notice here the (-)-sign, which is due to the (-)-sign in (A7).

TABLE VIII: Kadyshevski rules internal lines.

Line	Particle	Pairing	Factor in m.e.
$j' \bullet -- < -- \bullet\ j$	fermion	$\psi_\beta(q_{j'}\bar{\psi}_\alpha(p_j); j' < j$	$S^{(+)}_{\beta\alpha}(p_j, M)$
$j' \bullet ===< === \bullet\ j$	antifermion	$\bar{\psi}_\alpha(p_j\psi_\beta(q_{j'}); j' < j$	$S^{(+)}_{\beta\alpha}(q_j, -M)$
$j' \bullet \cdots\cdots < \cdots\cdots \bullet\ j$	meson	$\phi(k_{j'}\phi(k_j); j' < j$	$\Delta^{(+)}(k_j)$

in accordance with Table VIII [5].

7. For each internal photon line, using the Feynman gauge, a factor

$$D^{(+)}(q)_{\mu\nu} = -g_{\mu\nu}\theta(q_0)\delta(q^2)\ . \tag{A13}$$

8a. For each vertex, number s, a factor

$$(2\pi)^4\delta^4\left(\sum_i p_{i,out} + \kappa_{s+1} - \sum_i p_{i,in} - \kappa_s\right)\ , \tag{A14}$$

where $p_{i,out}$ and $p_{i,in}$ are the outgoing respectively the incoming momenta at the vertex with number s.

8b. Integrate over each internal particle line , momentum l: $\int d^4l/(2\pi)^3$.

9. Integrate over each internal quasi-particle (dotted) line with momentum $\kappa_s n$: $\int_{-\infty}^{+\infty} d\kappa_s/(2\pi)$.

10. *Not* a factor -1 for each closed loop.

11. A factor -1 between graphs which differ only by an interchange of two-external fermions. This not only for the interchange of identical fermions in the final state, but also the interchange of e.g. an initial fermion and a similar anti-fermion in the final state.

12. Repeat the operations (1)-(11) for all $n!$ numberings of the vertices of the given Feynman graph and sum.

II. Those factors coming from the structure and type of vertices are, given for each vertex by the matrix element $\langle \ldots | \mathcal{L}_I(0) | \ldots \rangle$. Therefore, they are, apart from a factor $(-i)$, identical to that given in [29], appendices B.

APPENDIX B: ORIENTATION KADYSHEVSKY GRAPHS FOR THE PLANAR AND CROSSED BOX DIAGRAMS

Here, we use the Kadyshevsky prescription [3–5] for the orientation of the internal lines in the 4th order graphs for fermion-fermion scattering. In the figure below we order the vertices for the $4! = 24$ box-graphs, and find that only six configurations have exlusively positive baryons, i.e. correspond to BB-scattering/interaction. There are 12 graphs with one anti-fermion in the intermediate states, and 6 graphs with two anti-fermions in the intermediate states. The latter correspond to the so-called 1Z- and 2Z-graphs, which are important for Quark-quark (QQ) interactions.

In Fig. 5 at the left corners of each graph there are incoming positive-energy nucleon lines, and at the right corners there are outgoing positive energy nucleon lines. If at any vertex the arrows of the nucleon lines are opposisite, the pair-suppression mechanism makes these graphs negligible in the case of BB-scattering. However, for Quark-quark interaction this is not the case.

Inspectation of the graphs in Fig. 5 shows that there are only six graphs that survive in the limit of strong pair-suppression. They are: the first three graphs in row one, the third and fifth graph in row two, and the fyfth graph in the row five.

In the two-fermion scattering processes the incoming lines enter from the right and the outgoing lines leave the graphs on the left. We index the graphs with (r,c) wher r= row number, and c-column number for the internal fermion lines.

1. The $(+,+)$-graphs are: (1,1), (1,2), (1,3), (2,3), (2,5), (3,5).
2. The $(+,-)$-graphs are: (1,4), (1,5), (1,6), (2,4), (2,6), (3,6).
3. The $(-,+)$-graphs are: (2,1), (3,1), (3,2), (4,1), (4,3), (4,5).

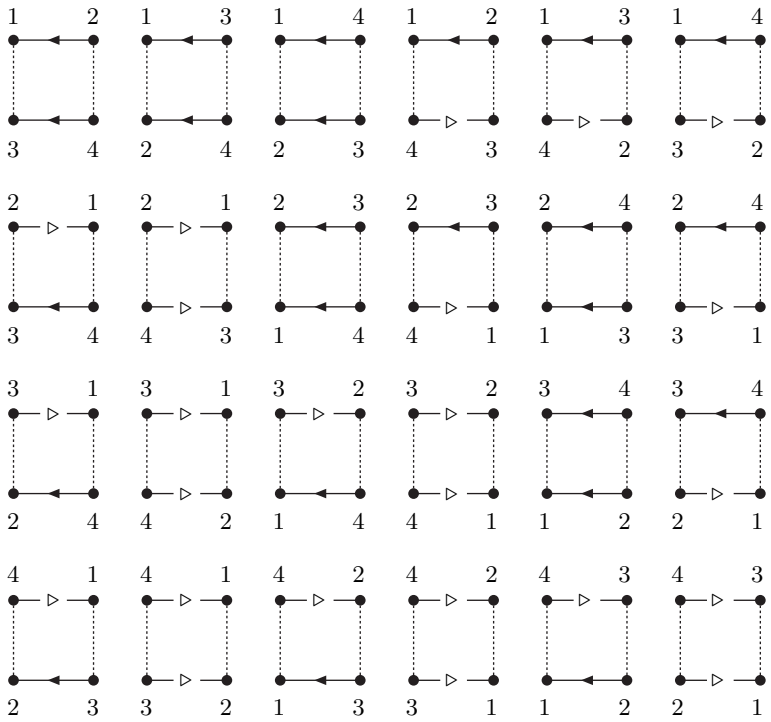

FIG. 5: *Kadyshevsky vertex configurations. The solid filled-arrow lines denote baryons with positive energy, and the solid open-arrow lines denote baryons with negative energy. The dashed lines refers to the mesons.*

4. The $(-,-)$-graphs are: (2,2), (3,2), (3,4), (4,2), (4,4), (4,6).

The crossed graphs are obtained by simply crossing the meson lines in the graphs.

APPENDIX C: FOURTH-ORDER KADYSHEVSKY GRAPHS $\sigma = [++]$

1. The planar-box graphs

Following the rules of Appendix A we have drawn the planar two meson echange graphs in Figs. 6-8. Here, the numbering of the vertices can be readoff by following the quasi-particle lines, beginning with the entering κ-line. The quasi-particle lines κ_i for $i = 1, 2, 3$ are then defined according to Appendix A. Then, again following the rules of Appendix A we list below the resulting amplitudes.

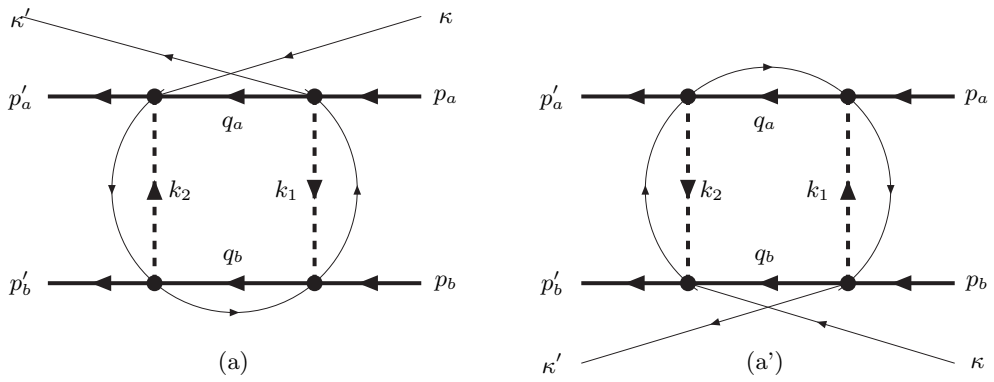

FIG. 6: *Planar Kadyshevsky graphs. The solid lines denote baryons. The dashed lines refers to the mesons.*

Graph (a) in the planar-box Feynman-Kadyshevsky diagrams Fig. 6 gives for the fourth-order kernel [6]

$$
\begin{aligned}
&(2\pi)^4\delta^4\left(p'_a+p'_b+\kappa' n-p_a-p_b-\kappa n\right)\; M^{(//,a)}_{\kappa',\kappa}=\int\frac{d^4q_a}{(2\pi)^3}\int\frac{d^4q_b}{(2\pi)^3}\cdot\\
&\times\int\frac{d^4k_1}{(2\pi)^3}\int\frac{d^4k_2}{(2\pi)^3}\;\delta_+\left[k_1^2-m_1^2\right]\delta_+\left[k_2^2-m_2^2\right]\cdot\widetilde{S}_F^{(+)}(q_a)\;\widetilde{S}_F^{(-)}(q_b)\\
&\times\int_{-\infty}^{\infty}\frac{d\kappa_1}{2\pi}\int_{-\infty}^{\infty}\frac{d\kappa_2}{2\pi}\int_{-\infty}^{\infty}\frac{d\kappa_3}{2\pi}\frac{1}{\kappa_1-i\epsilon}\frac{1}{\kappa_2-i\epsilon}\frac{1}{\kappa_3-i\epsilon}\cdot\\
&\times(2\pi)^4\delta^4\left(\kappa_1 n+p'_a-q_a-k_2-\kappa n\right)(2\pi)^4\delta^4\left(\kappa_3 n+p_a-q_a-k_1-\kappa' n\right)\cdot\\
&\times(2\pi)^4\delta^4\left(\kappa_2 n-\frac{1}{2}(\kappa'+\kappa)n-(q_a+q_b)+\frac{1}{2}(p'_a+p'_b+p_a+p_b)\right).
\end{aligned}
\tag{C1}
$$

With the delta-functions all κ-integrals can be carried out. Also, the integrations over the zero-components can be carried out, thanks to the on-mass-shell δ_+-functions. We will do so in the CM-system, where we can use the specific form of the n^μ-vector. We note that the expression for the amplitude in (C2) for only positive-energy nucleons in the intermediate state is manifest covariant.
similar calculations are carried through for the graphs (a'),(b),(b'),(c), and (c'). In the CM-system this leads to the

[6] In (C1) there are 3 $G_0(\kappa)$-factors giving a factor $(-)^3=-1$. This sign is canceled against the (-)-sign in (A8). The same is the case for all other 4th-order graphs treated in this apaper.

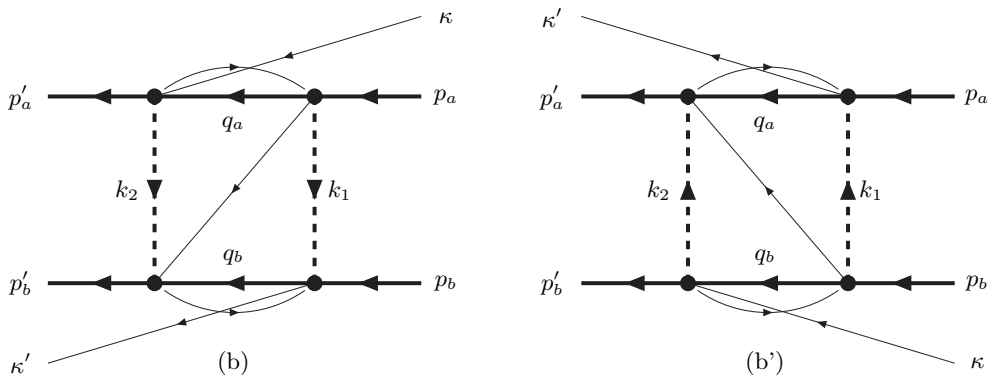

FIG. 7: *Planar Kadyshevsky graphs. The solid lines denote baryons. The dashed lines refers to the mesons. The thin lines denote the quasi-momentum particles.*

denominators ($\sigma = [++]$)

$$D^{(//,a)}_{\sigma;\kappa',\kappa}(\omega_1,\omega_2) = +\frac{1}{\omega_1+\kappa'+[E_a(\mathbf{q})-E_a(\mathbf{p})]+i\epsilon}\cdot\frac{1}{\omega_2+\kappa+[E_a(\mathbf{q})-E_a(\mathbf{p}')]+i\epsilon}\cdot \times\frac{1}{\frac{1}{2}(\kappa'+\kappa)+[E_a(\mathbf{q})+E_b(\mathbf{q})]-\frac{1}{2}[E_b(\mathbf{p}')+E_a(\mathbf{p}')+E_b(\mathbf{p})+E_a(\mathbf{p})]+i\epsilon}, \quad \text{(C2a)}$$

$$D^{(//,a')}_{\sigma;\kappa',\kappa}(\omega_1,\omega_2) = +\frac{1}{\omega_1+\kappa'+[E_b(\mathbf{q})-E_b(\mathbf{p})]+i\epsilon}\cdot\frac{1}{\omega_2+\kappa+[E_b(\mathbf{q})-E_b(\mathbf{p}')]+i\epsilon}\cdot \times\frac{1}{\frac{1}{2}(\kappa'+\kappa)+(E_a(\mathbf{q})+E_b(\mathbf{q})-\frac{1}{2}[E_b(\mathbf{p}')+E_a(\mathbf{p}')+E_b(\mathbf{p})+E_a(\mathbf{p})]+i\epsilon}, \quad \text{(C2b)}$$

$$D^{(//,b)}_{\sigma;\kappa',\kappa}(\omega_1,\omega_2) = +\frac{1}{\omega_1+\kappa'+[E_b(\mathbf{q})-E_b(\mathbf{p})]+i\epsilon}\cdot\frac{1}{\omega_2+\kappa+[E_a(\mathbf{q})-E_a(\mathbf{p}')]+i\epsilon}\cdot \times\frac{1}{\omega_1+\omega_2+\frac{1}{2}(\kappa'+\kappa)+\frac{1}{2}[E_b(\mathbf{p}')-E_a(\mathbf{p}')-E_b(\mathbf{p})+E_a[\mathbf{p}]+i\epsilon}, \quad \text{(C2c)}$$

$$D^{(//,b')}_{\sigma;\kappa',\kappa}(\omega_1,\omega_2) = +\frac{1}{\omega_1+\kappa'+[E_a(\mathbf{q})-E_a(\mathbf{p})]+i\epsilon}\cdot\frac{1}{\omega_2+\kappa+[E_b(\mathbf{q})-E_b(\mathbf{p}')]+i\epsilon}\cdot \times\frac{1}{\omega_1+\omega_2+\frac{1}{2}(\kappa'+\kappa)+\frac{1}{2}[E_a(\mathbf{p}')-E_b(\mathbf{p}')-E_a(\mathbf{p})+E_b[\mathbf{p}]+i\epsilon}, \quad \text{(C2d)}$$

$$D^{(//,c)}_{\sigma;\kappa',\kappa}(\omega_1,\omega_2) = +\frac{1}{\omega_1+\kappa'+[E_b(\mathbf{q})-E_b(\mathbf{p})]+i\epsilon}\cdot\frac{1}{\omega_2+\kappa+[E_a(\mathbf{q})-E_b(\mathbf{p}')]+i\epsilon}\cdot \times\frac{1}{\frac{1}{2}(\kappa'+\kappa)+[E_a(\mathbf{q})+E_b(\mathbf{q})]-\frac{1}{2}[E_b(\mathbf{p}')+E_a(\mathbf{p}')+E_b(\mathbf{p})+E_a[\mathbf{p}]+i\epsilon},$$

$$D^{(//,c')}_{\sigma;\kappa',\kappa}(\omega_1,\omega_2) = +\frac{1}{\omega_1+\kappa'+[E_a(\mathbf{q})-E_a(\mathbf{p})]+i\epsilon}\cdot\frac{1}{\omega_2+\kappa+[E_b(\mathbf{q})-E_b(\mathbf{p}')]+i\epsilon}\cdot \times\frac{1}{\frac{1}{2}(\kappa'+\kappa)+[E_a(\mathbf{q})+E_b(\mathbf{q})]-\frac{1}{2}[E_b(\mathbf{p}')+E_a(\mathbf{p}')+E_b(\mathbf{p})+E_a[\mathbf{p}]+i\epsilon}. \quad \text{(C2e)}$$

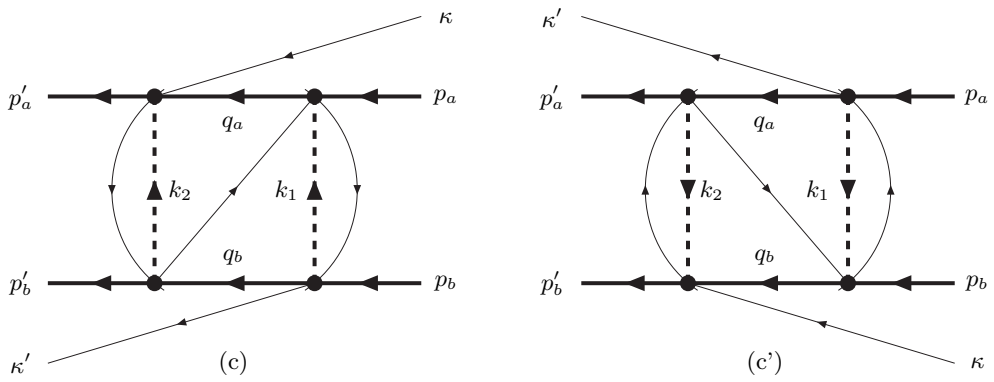

FIG. 8: *Planar Kadyshevsky graphs. The solid lines denote baryons. The dashed lines refers to the pseudo-scalar mesons. The thin lines denote the quasi-momentum particles.*

2. Relation Macke-Klein formalism

To make the connection with the Macke-Klein formalism in [11] we consider elastic scattering, and we rewrite the factors in the denominator $D^{(//,a)}_{\sigma;0,0}(\omega_1,\omega_2)$ in Eq. (C2) as follows:

1. $\omega_1 + E_a(\mathbf{q}) - E_a(\mathbf{p}) = \omega_1 + E_a(\mathbf{q}) + E_b(\mathbf{p}) - [E_a(\mathbf{p}) + E_b(\mathbf{p})] =$
   $\omega_1 + [E_a(\mathbf{q}) + E_b(\mathbf{p})] - W \Rightarrow \omega_1 + A + A'',$

2. $\omega_2 + E_b(\mathbf{q}) - E_b(\mathbf{p}') = \omega_2 + E_b(\mathbf{q}) + E_a(\mathbf{p}') - [E_b(\mathbf{p}') + E_a(\mathbf{p}')] =$
   $\omega_2 + [E_b(\mathbf{q}) + E_a(\mathbf{p}')] - W \Rightarrow \omega_2 + A' + B'',$

3. $\omega_1 + \omega_2 + \frac{1}{2}\left[E_a(\mathbf{p}') - E_b(\mathbf{p}') - E_a(\mathbf{p}) + E_b(\mathbf{p})\right] =$
   $\omega_1 + \omega_2 + \frac{1}{2}\left[2E_a(\mathbf{p}') - (E_a(\mathbf{p}') + E_b(\mathbf{p}')) - (E_a(\mathbf{p}) + E_b(\mathbf{p})] + 2E_b(\mathbf{p})\right] =$
   $\omega_1 + \omega_2 + (E_a(\mathbf{p}') + E_b(\mathbf{p})) - W) \Rightarrow \omega_1 + \omega_2 + A' + A.$

Here $\Rightarrow$ means taking equal masses $M_a = M_b$, and $A = E(\mathbf{p}) - W/2,\ A' = E(\mathbf{p}') - W'/2,\ A'' = E(\mathbf{q}) - W/2,\ B'' = A''$. The expressions for the on-shell denominators become

$$
\begin{aligned}
D^{(//,a)}_{\sigma;0,0}(\omega_1,\omega_2) &\Rightarrow (\omega_1 + A + A'')^{-1}\ (\omega_2 + A' + A'')^{-1}\ [2A'']^{-1}\,,\\
D^{(//,a')}_{\sigma;0,0}(\omega_1,\omega_2) &\Rightarrow (\omega_1 + A + A'')^{-1}\ (\omega_2 + A' + A'')^{-1}\ [2A'']^{-1}\,,\\
D^{(//,b)}_{\sigma;0,0}(\omega_1,\omega_2) &\Rightarrow (\omega_1 + A + A'')^{-1}\ (\omega_2 + A' + A'')^{-1}\ (\omega_1+\omega_2)^{-1}\,,\\
D^{(//,b')}_{\sigma;0,0}(\omega_1,\omega_2) &\Rightarrow (\omega_1 + A + A'')^{-1}\ (\omega_2 + A' + A'')^{-1}\ (\omega_1+\omega_2)^{-1}\,,\\
D^{(//,c)}_{\sigma;0,0}(\omega_1,\omega_2) &\Rightarrow (\omega_1 + A + A'')^{-1}\ (\omega_2 + A' + A'')^{-1}\ [2A'']^{-1}\,,\\
D^{(//,c')}_{\sigma;0,0}(\omega_1,\omega_2) &\Rightarrow (\omega_1 + A + A'')^{-1}\ (\omega_2 + A + A'')^{-1}\ [2A'']^{-1}\,.
\end{aligned}
\tag{C3}
$$

This demonstrates that the Macke-Klein formalism, at least for equal fermion masses, leads to equivalent expressions for the potentials as in [11].

3. The crossed-box graphs

Following the rules of Appendix A we have drawn the crossed two-meson echange graphs in Figs. 9-11. Here, the numbering of the vertices can be read off by following the quasi-particle lines, beginning with the entering κ-line. The quasi-particle lines κ_i for $i = 1, 2, 3$ are then defined according to Appendix A. Then, again following the rules of Appendix A we list below the resulting amplitudes.

Graph (a) in the crossed-box Feynman-Kadyshevsky diagrams Fig. 9 gives for the fourth-order kernel, with only positive energy spinors for the intermediate nucleons,

$$
\begin{aligned}
M^{(X,a)}_{\kappa',\kappa}\left(p'_a, p'_b; p_a, p_b\right) &= \int \frac{d^4q_a}{(2\pi)^3} \int \frac{d^4q_b}{(2\pi)^3} \int \frac{d^4k_1}{(2\pi)^3} \int \frac{d^4k_2}{(2\pi)^3} \cdot \\
&\times \delta_+\left[k_1^2 - m_1^2\right] \delta_+\left[k_2^2 - m_2^2\right] \cdot \delta_+\left[q_a^2 - M_a^2\right] \delta_+\left[q_b^2 - M_b^2\right] \\
&\times \int_{-\infty}^{\infty} \frac{d\kappa_1}{2\pi} \int_{-\infty}^{\infty} \frac{d\kappa_2}{2\pi} \int_{-\infty}^{\infty} \frac{d\kappa_3}{2\pi} \frac{1}{\kappa_1 - i\epsilon} \frac{1}{\kappa_2 - i\epsilon} \frac{1}{\kappa_3 - i\epsilon} \cdot \\
&\times (2\pi)^4 \delta^4\left(\kappa_1 n + p'_a - q_a - k_2 - \kappa n\right) (2\pi)^4 \delta^4\left(\kappa_3 n + p_a - q_a - k_1 - \kappa' n\right) \cdot \\
&\times (2\pi)^4 \delta^4\left(\kappa_2 n - \frac{1}{2}(\kappa' + \kappa) n - (k_1 + k_2) + \frac{1}{2}(p'_b + p'_a + p_b + p_a) - (q_a + q_b)\right) . \qquad \text{(C4)}
\end{aligned}
$$

With the delta-functions all κ-integrals can be carried out. Also, the integrations over the zero-components can be carried out, thanks to the on-mass-shell δ_+-functions.

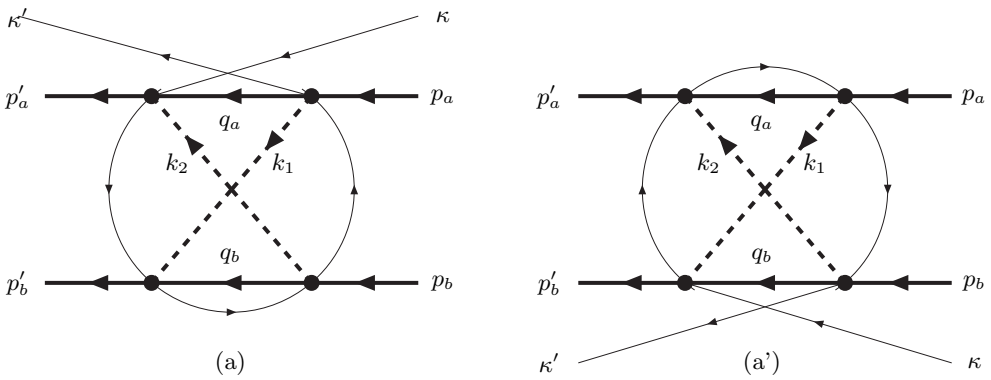

FIG. 9: *Crossed Kadyshevsky graphs. The solid lines denote baryons. The dashed lines refers to the mesons.*

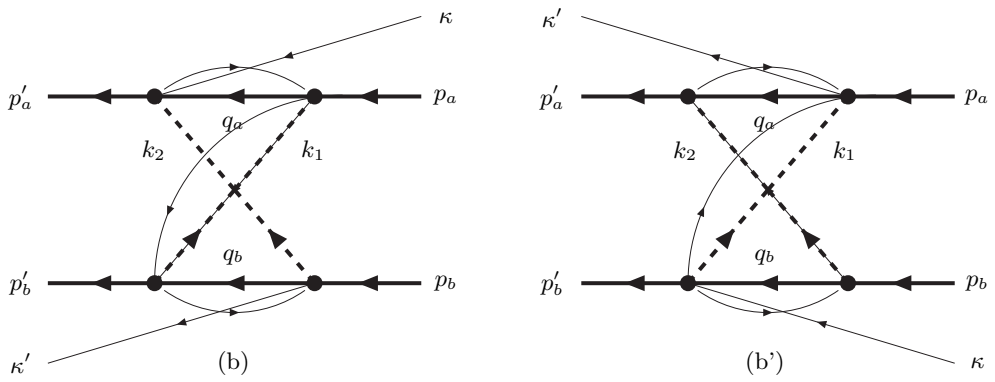

FIG. 10: *Crossed Kadyshevsky graphs. The solid lines denote baryons. The dashed lines refers to the pseudo-scalar mesons. The thin lines denote the quasi-momentum particles.*

Similar calculations are carried through for the graphs (a'),(b),(b'),(c), and (c'). In the CM-system this leads to

$$D^{(X,a)}_{\sigma;\kappa',\kappa}(\omega_1,\omega_2) = +\frac{1}{\omega_1+\kappa'+[E_a(\mathbf{q})-E_a(\mathbf{p})]+i\epsilon}\cdot\frac{1}{\omega_2+\kappa+[E_a(\mathbf{q})-E_a(\mathbf{p}')]+i\epsilon}\cdot \times\frac{1}{\omega_1+\omega_2+\frac{1}{2}(\kappa'+\kappa)+E_a(\mathbf{q})+E_b(\mathbf{q})-\frac{1}{2}\left[E_a(\mathbf{p}')+E_b(\mathbf{p}')+E_b(\mathbf{p})+E_a(\mathbf{p})\right]+i\epsilon}, \quad \text{(C5a)}$$

$$D^{(X,a')}_{\sigma;\kappa',\kappa}(\omega_1,\omega_2) = +\frac{1}{\omega_1+\kappa+[E_b(\mathbf{q})-E_b(\mathbf{p}')]+i\epsilon}\cdot\frac{1}{\omega_2+\kappa'+[E_b(\mathbf{q})-E_b(\mathbf{p})]+i\epsilon}\cdot \times\frac{1}{\frac{1}{2}(\kappa'+\kappa)+\omega_1+\omega_2-\frac{1}{2}\left[E_a(\mathbf{p}')+E_b(\mathbf{p}')+E_a(\mathbf{p})+E_a(\mathbf{p})\right]\left[E_a(\mathbf{q})+E_b(\mathbf{q})\right]+i\epsilon}, \quad \text{(C5b)}$$

$$D^{(X,b)}_{\sigma;\kappa',\kappa}(\omega_1,\omega_2) = +\frac{1}{\omega_2+\kappa+[E_a(\mathbf{q})-E_a(\mathbf{p}')]+i\epsilon}\cdot\frac{1}{\omega_2+\kappa'+[E_b(\mathbf{q})-E_b(\mathbf{p})]+i\epsilon}\cdot \times\frac{1}{\omega_1+\omega_2+\frac{1}{2}(\kappa'+\kappa)+\omega_1+\omega_2+\frac{1}{2}\left[E_b(\mathbf{p}')-E_a(\mathbf{p}')-E_b(\mathbf{p})+E_a(\mathbf{p})\right]+i\epsilon}, \quad \text{(C5c)}$$

$$D^{(X,b')}_{\sigma;\kappa',\kappa}(\omega_1,\omega_2) = +\frac{1}{\omega_1+\kappa+[E_b(\mathbf{q})-_b(\mathbf{p}')]+i\epsilon}\cdot\frac{1}{\omega_1+\kappa'+[E_a(\mathbf{q})-E_a(\mathbf{p})]+i\epsilon}\cdot \times\frac{1}{\omega_1+\omega_2+\frac{1}{2}(\kappa'+\kappa)+\omega_1+\omega_2+\frac{1}{2}\left[E_a(\mathbf{p}')-E_b(\mathbf{p}')-E_a(\mathbf{p})+E_b(\mathbf{p})\right]+i\epsilon}, \quad \text{(C5d)}$$

$$D^{(X,c)}_{\sigma;\kappa',\kappa}(\omega_1,\omega_2) = +\frac{1}{\omega_2+\kappa+[E_a(\mathbf{q})-E_a(\mathbf{p}')]+i\epsilon}\cdot\frac{1}{\omega_2+\kappa'+[E_b(\mathbf{q})-E_b(\mathbf{p})]+i\epsilon}\cdot \times\frac{1}{\frac{1}{2}(\kappa'+\kappa)+(E_a(\mathbf{q})+\omega_1+\omega_2-\frac{1}{2}\left[E_b(\mathbf{p}')+E_a(\mathbf{p}')+E_b(\mathbf{p})+E_a(\mathbf{p})\right]+[E_a(\mathbf{q})+E_b(\mathbf{q})+i\epsilon}, \quad \text{(C5e)}$$

$$D^{(X,c')}_{\sigma;\kappa',\kappa}(\omega_1,\omega_2) = +\frac{1}{\omega_1+\kappa+[E_b(\mathbf{q})-E_b(\mathbf{p}')]+i\epsilon}\cdot\frac{1}{\omega_1+\kappa'+[E_a(\mathbf{q})-E_a(\mathbf{p})]+i\epsilon}\cdot \times\frac{1}{\frac{1}{2}(\kappa'+\kappa)+\omega_1+\omega_2-\frac{1}{2}\left[E_b(\mathbf{p}')+E_a(\mathbf{p}')+E_b(\mathbf{p})+E_a(\mathbf{p})\right]+[E_a(\mathbf{q})+E_b(\mathbf{q})]+i\epsilon}. \quad \text{(C5f)}$$

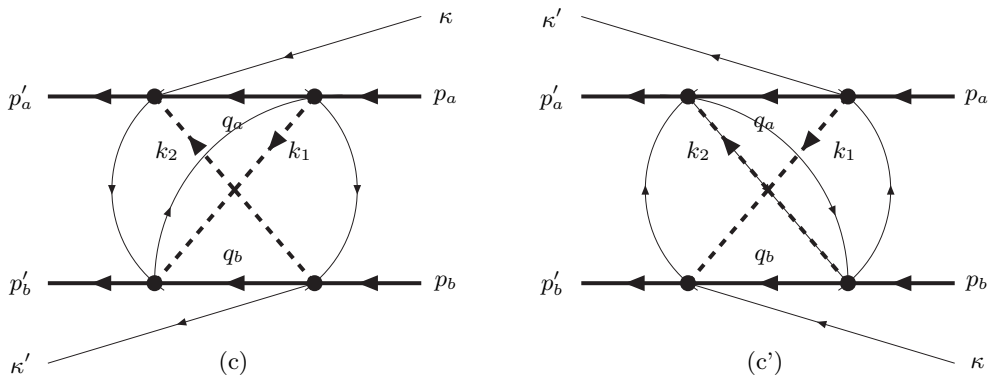

FIG. 11: *Crossed Kadyshevsky graphs. The solid lines denote baryons. The dashed lines refers to the pseudo-scalar mesons. The thin lines denote the quasi-momentum particles.*

4. Relation Macke-Klein formalism

Taking equal masses $M_a = M_b$, and the notation used in [11] $A = E(\mathbf{p}) - W/2,\ A' = E(\mathbf{p}') - W'/2,\ A'' = E(\mathbf{q}) - W/2,\ B'' = A''$, the expressions for the on-shell denominators become

$$\begin{aligned}
D^{(X,a)}_{\sigma;0,0}(\omega_1,\omega_2) &\Rightarrow (\omega_1 + A' + A'')^{-1}\ (\omega_2 + A + A'')^{-1}\ (\omega_1 + \omega_2 + 2A'')^{-1}\,,\\
D^{(X,a')}_{\sigma;0,0}(\omega_1,\omega_2) &\Rightarrow (\omega_1 + A' + A'')^{-1}\ (\omega_2 + A + A'')^{-1}\ (\omega_1 + \omega_2 + 2A'')^{-1}\,,\\
D^{(X,b)}_{\sigma;0,0}(\omega_1,\omega_2) &\Rightarrow (\omega_2 + A' + A'')^{-1}\ (\omega_2 + A + A'')^{-1}\ (\omega_1 + \omega_2)^{-1}\,,\\
D^{(X,b')}_{\sigma;0,0}(\omega_1,\omega_2) &\Rightarrow (\omega_1 + A' + A'')^{-1}\ (\omega_1 + A + A'')^{-1}\ (\omega_1 + \omega_2)^{-1}\,,\\
D^{(X,c)}_{\sigma;0,0}(\omega_1,\omega_2) &\Rightarrow (\omega_2 + A' + A'')^{-1}\ (\omega_2 + A + A'')^{-1}\ (\omega_1 + \omega_2 + 2A'')^{-1}\,,\\
D^{(X,c')}_{\sigma;0,0}(\omega_1,\omega_2) &\Rightarrow (\omega_1 + A' + A'')^{-1}\ (\omega_1 + A + A'')^{-1}\ (\omega_1 + \omega_2 + 2A'')^{-1}\,.
\end{aligned} \tag{C6}$$

5. Adiabatic Approximations

In the adiabatic approximation $A = A' = 0$. The expressions for the denominators become:

Planar-graphs:

$$\begin{aligned}
D^{(//,a)}_{\sigma;0,0}(ad) &= \frac{1}{\omega_1}\ \frac{1}{2A''}\ \frac{1}{\omega_2} \quad , \ D^{(//,a')}_{\sigma;0,0}(ad) = \frac{1}{\omega_1}\ \frac{1}{2A''}\ \frac{1}{\omega_2},\\
D^{(//,b)}_{\sigma;0,0}(ad) &= \frac{1}{\omega_1}\ \frac{1}{\omega_1+\omega_2}\ \frac{1}{\omega_2} \quad , \ D^{(//,b')}_{\sigma;0,0}(ad) = \frac{1}{\omega_1}\ \frac{1}{\omega_1+\omega_2}\ \frac{1}{\omega_2},\\
D^{(//,c)}_{\sigma;0,0}(ad) &= \frac{1}{\omega_1}\ \frac{1}{2A''}\ \frac{1}{\omega_2} \quad , \ D^{(//,c')}_{\sigma;0,0}(ad) = \frac{1}{\omega_1}\ \frac{1}{2A''}\ \frac{1}{\omega_2}.
\end{aligned} \tag{C7}$$

Crossed-graphs:

$$D^{(X,a)}_{\sigma;0,0}(ad) = \frac{1}{\omega_1}\,\frac{1}{\omega_1+\omega_2}\,\frac{1}{\omega_2} \quad , \; D^{(X,a')}_{\sigma;0,0}(ad) = \frac{1}{\omega_1}\,\frac{1}{\omega_1+\omega_2}\,\frac{1}{\omega_2},$$
$$D^{(X,b)}_{\sigma;0,0}(ad) = \frac{1}{\omega_2}\,\frac{1}{\omega_1+\omega_2}\,\frac{1}{\omega_2} \quad , \; D^{(X,b')}_{\sigma;0,0}(ad) = \frac{1}{\omega_1}\,\frac{1}{\omega_1+\omega_2}\,\frac{1}{\omega_1},$$
$$D^{(X,c)}_{\sigma;0,0}(ad) = \frac{1}{\omega_2}\,\frac{1}{\omega_1+\omega_2}\,\frac{1}{\omega_2} \quad , \; D^{(X,c')}_{\sigma;0,0}(ad) = \frac{1}{\omega_1}\,\frac{1}{\omega_1+\omega_2}\,\frac{1}{\omega_1}. \tag{C8}$$

Notice that the spinor-numerator factors for the parallel graphs are the same, and so we have the symmetry $\omega_1 \leftrightarrow \omega_2$ *as can be seen from the expressions above, and similarly for the crossed graphs.*

Defining $D^{(//)}_{\sigma;0,0}(ad) = \sum_{i=a,b,c,a',b',c'} D^{(//,i)}(ad)$. Similarly $D^{(X)}_{\sigma;0,0}(ad)$ for the crossed graphs. We have for the parallel graphs

$$D^{(//)}_{\sigma;0,0}(ad) \;=\; \frac{1}{\omega_1}\,\frac{4}{2A''}\,\frac{1}{\omega_2} + \frac{2}{\omega_1\omega_2}\,\frac{1}{\omega_1+\omega_2}. \tag{C9}$$

and for the crossed graphs

$$D^{(X)}_{\sigma;0,0}(ad) \;=\; \frac{2}{\omega_1\omega_2}\left[1+\frac{\omega_1}{\omega_2}+\frac{\omega_2}{\omega_1}\right]\frac{1}{\omega_1+\omega_2}. \tag{C10}$$

Comparison: The denominators $D^{(//,a)}(ad), D^{(//,a')}(ad)$ correspons to the so-called TMO-graphs. Subtracting the one-meson-exchange iterated graph $D^{(//,a)}(ad), D^{(//,a')}(ad) \Rightarrow 0$. This subtraction avoids *"double counting"*, when used in the integral equations. Taking into account the leading non-adiabatic corrections, see for details [11], one obtains in total

$$D^{(//,a)}_{\sigma;0,0}(ad) + D^{(//,a')}_{\sigma;0,0}(ad) \Rightarrow -\frac{1}{\omega_1\omega_2}\left(\frac{1}{\omega_1}+\frac{1}{\omega_2}\right). \tag{C11}$$

contributions, including the 1/M corrections from the TMO-graphs, for the planar graphs in formulas (8.1)-(9.4)

$$D^{(//)}(ad) \;=\; \frac{1}{\omega_1\omega_2}\left[\frac{1}{\omega_1+\omega_2}-\frac{1}{\omega_1}-\frac{1}{\omega_2}\right],$$

and for the crossed graphs in formulas (8.3)-(8.5)

$$D^{(X)}(ad) \;=\; \frac{1}{\omega_1\omega_2}\left[\frac{1}{\omega_1}+\frac{1}{\omega_2}-\frac{1}{\omega_1+\omega_2}\right] = -D^{(//)}(ad).$$

APPENDIX D: FOURTH-ORDER KADYSHEVSKY GRAPHS $\sigma = (+-)$

1. The planar-box graphs

Following the rules of Appendix A we have drawn the planar two meson echange graphs in Figs. 12-14. Here, the numbering of the vertices can be readoff by following the quasi-particle lines, beginning with the entering κ-line. The quasi-particle lines κ_i for $i = 1, 2, 3$ are then defined according to Appendix A. Then, again following the rules of Appendix A we list below the resulting amplitudes.

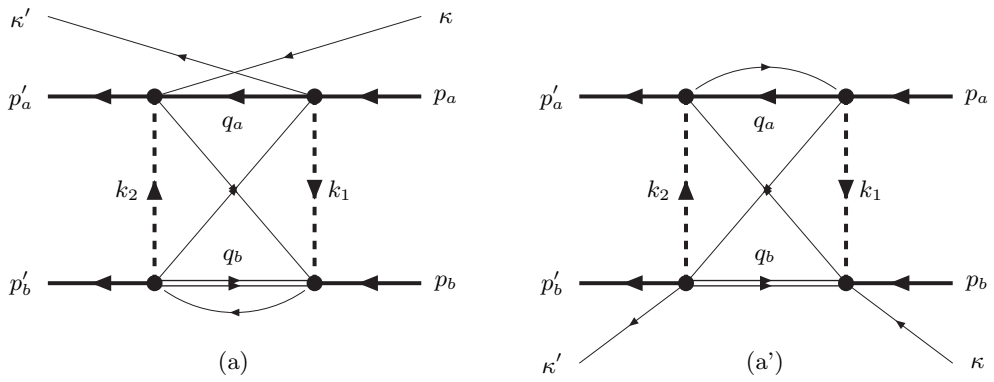

FIG. 12: *Planar Kadyshevsky graphs. The solid line denote the baryon, the thin double-line the antibaryon. The dashed lines refers to the mesons. The thin lines denote the quasi-momentum particles.*

Graph (a) in the planar-box Feynman-Kadyshevsky diagrams Fig. 12 gives for the fourth-order kernel

$$
\begin{aligned}
&(2\pi)^4\delta^4\left(p'_a+p'_b+\kappa' n-p_a-p_b-\kappa n\right)\; M^{(//,a)}_{\kappa',\kappa}=\int\frac{d^4q_a}{(2\pi)^3}\int\frac{d^4q_b}{(2\pi)^3}\cdot\\
&\times\int\frac{d^4k_1}{(2\pi)^3}\int\frac{d^4k_2}{(2\pi)^3}\;\delta_+\left[k_1^2-m_1^2\right]\delta_+\left[k_2^2-m_2^2\right]\cdot\widetilde{S}_F^{(+)}(q_a)\;\widetilde{S}_F^{(-)}(q_b)\\
&\times\int_{-\infty}^{\infty}\frac{d\kappa_1}{2\pi}\int_{-\infty}^{\infty}\frac{d\kappa_2}{2\pi}\int_{-\infty}^{\infty}\frac{d\kappa_3}{2\pi}\frac{1}{\kappa_1-i\epsilon}\frac{1}{\kappa_2-i\epsilon}\frac{1}{\kappa_3-i\epsilon}\cdot\\
&\times(2\pi)^4\delta^4\left(\kappa_1 n+p'_a-q_a-k_2-\kappa n\right)(2\pi)^4\delta^4\left(\kappa_3 n+p_a-q_a-k_1-\kappa' n\right)\cdot\\
&\times(2\pi)^4\delta^4\left(\kappa_2 n-\frac{1}{2}(\kappa'+\kappa)n-(k_1+k_2)+\frac{1}{2}(p'_a-p'_b+p_a-p_b)\right).
\end{aligned}
\tag{D1}
$$

With the delta-functions all κ-integrals can be carried out. Also, the integrations over the zero-components can be carried out, thanks to the on-mass-shell δ_+-functions. We will do so in the CM-system, where we can use the specific form of the n^μ-vector. We note that the expression for the amplitude in (D1) for only positive-energy nucleons in the intermediate state is manifest covariant.
Similar calculations are carried through for the graphs (a'),(b),(b'),(c), and (c').

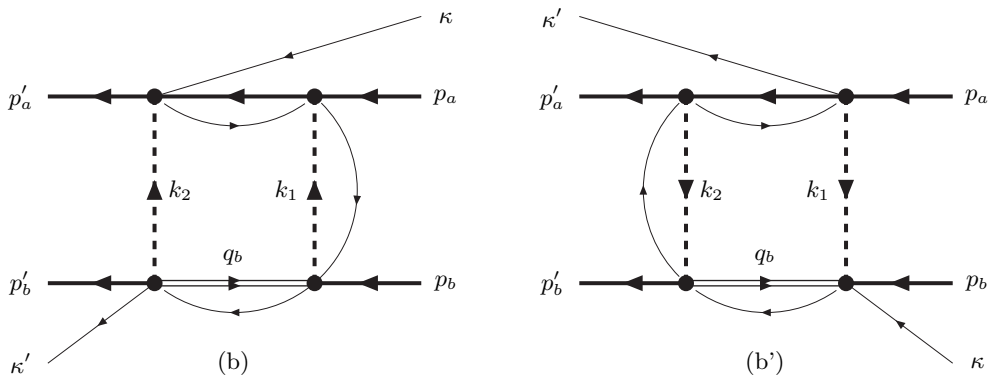

FIG. 13: *Planar Kadyshevsky graphs. The solid lines denote baryons. The dashed lines refers to the mesons. The thin lines denote the quasi-momentum particles.*

In the CM-system this leads to the denominators [$\sigma = (+-)$])

$$D^{(//,a)}_{\sigma;\kappa',\kappa}(\omega_1,\omega_2) = +\frac{1}{\omega_1+\kappa'+[E_a(\mathbf{q})-E_a(\mathbf{p})]+i\epsilon}\cdot\frac{1}{\omega_2+\kappa+[E_a(\mathbf{q})-E_a(\mathbf{p}')]+i\epsilon}\cdot$$
$$\times\frac{1}{\omega_1+\omega_2+\frac{1}{2}(\kappa'+\kappa)+[E_a(\mathbf{q})+E_b(\mathbf{q})]+\frac{1}{2}\left[E_b(\mathbf{p}')-E_a(\mathbf{p}')+E_b(\mathbf{p})-E_a(\mathbf{p})\right]+i\epsilon}, \quad \text{(D2a)}$$

$$D^{(//,a')}_{\sigma;\kappa',\kappa}(\omega_1,\omega_2) = +\frac{1}{\omega_1+\kappa+[E_b(\mathbf{p})+E_b(\mathbf{q})]+i\epsilon}\cdot\frac{1}{\omega_2+\kappa'+[E_b(\mathbf{p}')+E_b(\mathbf{q})]+i\epsilon}\cdot$$
$$\times\frac{1}{\omega_1+\omega_2+\frac{1}{2}(\kappa'+\kappa)+[E_a(\mathbf{q})+E_b(\mathbf{q})]+\frac{1}{2}\left[E_b(\mathbf{p}')-E_a(\mathbf{p}')+E_b(\mathbf{p})-E_a(\mathbf{p})\right]+i\epsilon}, \quad \text{(D2b)}$$

$$D^{(//,b)}_{\sigma;\kappa',\kappa}(\omega_1,\omega_2) = +\frac{1}{\omega_2+\kappa-[E_a(\mathbf{p}')-E_a(\mathbf{q})]+i\epsilon}\cdot\frac{1}{\omega_2+\kappa'+[E_b(\mathbf{p}')+E_b(\mathbf{q})]+i\epsilon}\cdot$$
$$\times\frac{1}{\omega_1+\omega_2+\frac{1}{2}(\kappa'+\kappa)+\frac{1}{2}\left[E_b(\mathbf{p}')-E_a(\mathbf{p}')-E_b(\mathbf{p})+E_a(\mathbf{p}]+i\epsilon\right.}, \quad \text{(D2c)}$$

$$D^{(//,b')}_{\sigma;\kappa',\kappa}(\omega_1,\omega_2) = +\frac{1}{\omega_1+\kappa+[E_b(\mathbf{p})+E_b(\mathbf{q})]+i\epsilon}\cdot\frac{1}{\omega_1+\kappa'-[E_a(\mathbf{p})-E_a(\mathbf{q})]+i\epsilon}\cdot$$
$$\times\frac{1}{\omega_1+\omega_2+\frac{1}{2}(\kappa'+\kappa)+\frac{1}{2}\left[E_a(\mathbf{p}')-E_b(\mathbf{p}')-E_a(\mathbf{p})+E_b(\mathbf{p}]+i\epsilon\right.}, \quad \text{(D2d)}$$

$$D^{(//,c)}_{\sigma;\kappa',\kappa}(\omega_1,\omega_2) = +\frac{1}{\omega_2+\kappa-[E_a(\mathbf{p})-E_a(\mathbf{q})]+i\epsilon}\cdot\frac{1}{\omega_2+\kappa'+[E_b(\mathbf{p}')+E_b(\mathbf{q})]+i\epsilon}\cdot$$
$$\times\frac{1}{\omega_1+\omega_2+\frac{1}{2}(\kappa'+\kappa)+[E_a(\mathbf{q})+E_b(\mathbf{q})]+\frac{1}{2}\left[E_b(\mathbf{p}')-E_a(\mathbf{p}')+E_b(\mathbf{p})-E_a(\mathbf{p}]+i\epsilon\right.}, \quad \text{(D2e)}$$

$$D^{(//,c')}_{\sigma;\kappa',\kappa}(\omega_1,\omega_2) = +\frac{1}{\omega_1+\kappa+[E_b(\mathbf{p})+E_b(\mathbf{q})]+i\epsilon}\cdot\frac{1}{\omega_1+\kappa'-[E_a(\mathbf{p})-E_a(\mathbf{q})]+i\epsilon}\cdot$$
$$\times\frac{1}{\omega_1+\omega_2+\frac{1}{2}(\kappa'+\kappa)+(E_a(\mathbf{q})+E_b(\mathbf{q}))+\frac{1}{2}\left[E_b(\mathbf{p}')-E_a(\mathbf{p}')+E_b(\mathbf{p})-E_a(\mathbf{p}]+i\epsilon\right.}. \quad \text{(D2f)}$$

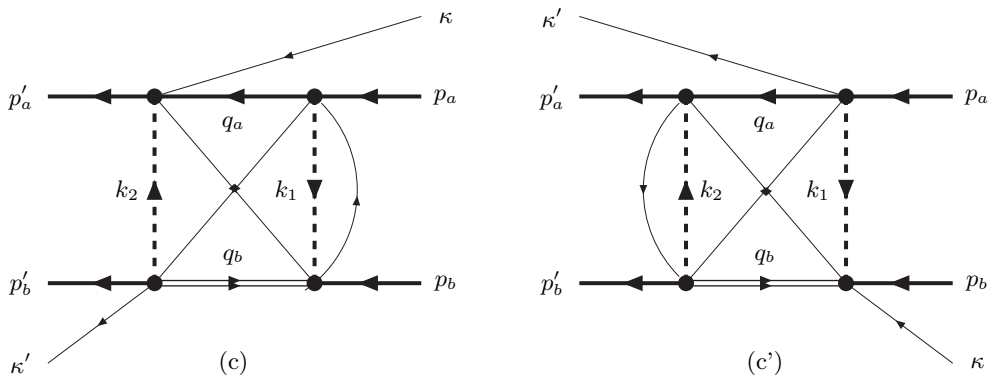

FIG. 14: *Planar Kadyshevsky graphs. The solid lines denote baryons. The dashed lines refers to the mesons. The thin lines denote the quasi-momentum particles.*

2. The crossed-box graphs

Graph (a) in the crossed-box Feynman-Kadyshevsky diagrams Fig. 15 gives for the fourth-order kernel, with only positive energy spinors for the intermediate nucleons,

$$M^{(X,a)}_{\kappa',\kappa}\left(p'_a,p'_b;p_a,p_b\right)=\int\frac{d^4q_a}{(2\pi)^3}\int\frac{d^4q_b}{(2\pi)^3}\int\frac{d^4k_1}{(2\pi)^3}\int\frac{d^4k_2}{(2\pi)^3}\cdot$$

$$\times\delta_+\left[k_1^2-m_1^2\right]\delta_+\left[k_2^2-m_2^2\right]\cdot\delta_+\left[q_a^2-M_a^2\right]\delta_+\left[q_b^2-M_b^2\right]$$

$$\times\int_{-\infty}^{\infty}\frac{d\kappa_1}{2\pi}\int_{-\infty}^{\infty}\frac{d\kappa_2}{2\pi}\int_{-\infty}^{\infty}\frac{d\kappa_3}{2\pi}\frac{1}{\kappa_1-i\epsilon}\frac{1}{\kappa_2-i\epsilon}\frac{1}{\kappa_3-i\epsilon}\cdot$$

$$\times(2\pi)^4\delta^4\left(\kappa_1 n+p'_a-q_a-k_2-\kappa n\right)(2\pi)^4\delta^4\left(\kappa_3 n+p_a-q_a-k_1-\kappa' n\right)\cdot$$

$$\times(2\pi)^4\delta^4\left(\kappa_2 n-\frac{1}{2}(\kappa'+\kappa)n-\frac{1}{2}(p'_b-p'_a+p_b-p_a)-(q_a+q_b)\right). \tag{D3}$$

With the delta-functions all κ-integrals can be carried out. Also, the integrations over the zero-components can be carried out, thanks to the on-mass-shell δ_+-functions.

Similar calculations are carried through for the graphs (a'),(b),(b'),(c), and (c'). In the CM-system this leads to

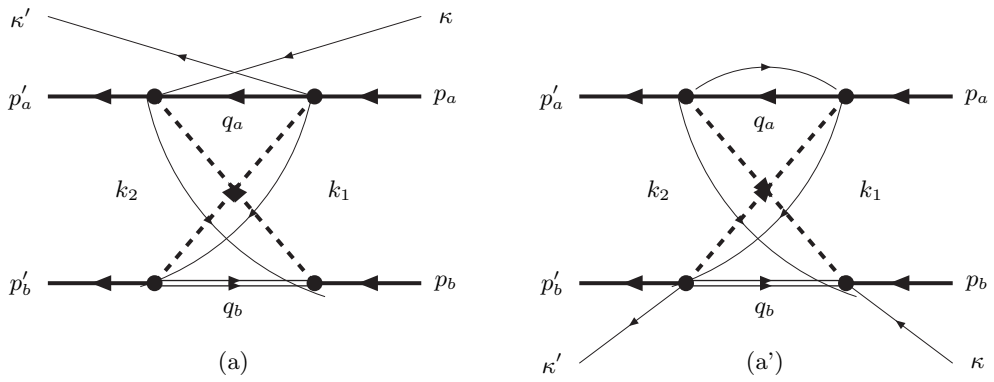

FIG. 15: *Crossed-box Kadyshevsky graphs. The solid lines denote baryons. The dashed lines refers to the mesons. The thin lines denote the quasi-momentum particles.*

the denominators [$\sigma = (+-)$])

$$
\begin{aligned}
D^{(X,a)}_{\sigma;\kappa',\kappa}(\omega_1,\omega_2) &= +\frac{1}{\omega_2+\kappa+[E_a(\mathbf{q})-E_a(\mathbf{p}')]+i\epsilon}\cdot\frac{1}{\omega_1+\kappa'+[E_a(\mathbf{q})-E_a(\mathbf{p})]+i\epsilon}\cdot \\
&\quad\times\frac{1}{\frac{1}{2}(\kappa'+\kappa)+E_a(\mathbf{q})+E_b(\mathbf{q})+\frac{1}{2}\left[E_b(\mathbf{p}')-E_a(\mathbf{p}')+E_b(\mathbf{p})-E_a(\mathbf{p})\right]+i\epsilon}, \qquad \text{(D4a)}\\
D^{(X,a')}_{\sigma;\kappa',\kappa}(\omega_1,\omega_2) &= +\frac{1}{\omega_1+\kappa+[E_b(\mathbf{q})+E_b(\mathbf{p})]+i\epsilon}\cdot\frac{1}{\omega_2+\kappa'+[E_b(\mathbf{q})+E_b(\mathbf{p}')]+i\epsilon}\cdot \\
&\quad\times\frac{1}{\frac{1}{2}(\kappa'+\kappa)+E_a(\mathbf{q})+E_b(\mathbf{q})+\frac{1}{2}\left[E_b(\mathbf{p}')-E_a(\mathbf{p}')+E_b(\mathbf{p})-E_a(\mathbf{p})\right]+i\epsilon}, \qquad \text{(D4b)}\\
D^{(X,b)}_{\sigma;\kappa',\kappa}(\omega_1,\omega_2) &= +\frac{1}{\omega_2+\kappa+[E_a(\mathbf{q})-E_a(\mathbf{p}')]+i\epsilon}\cdot\frac{1}{\omega_1+\kappa'+[E_b(\mathbf{q})+E_b(\mathbf{p}')]+i\epsilon}\cdot \\
&\quad\times\frac{1}{\omega_1+\omega_2+\frac{1}{2}(\kappa'+\kappa)+\frac{1}{2}\left[E_b(\mathbf{p}')-E_a(\mathbf{p}')-E_b(\mathbf{p})+E_a(\mathbf{p})\right]+i\epsilon}, \qquad \text{(D4c)}\\
D^{(X,b')}_{\sigma;\kappa',\kappa}(\omega_1,\omega_2) &= +\frac{1}{\omega_2+\kappa+[E_b(\mathbf{q})+E_b(\mathbf{p})]+i\epsilon}\cdot\frac{1}{\omega_1+\kappa'+[E_a(\mathbf{q})-E_a(\mathbf{p})]+i\epsilon}\cdot \\
&\quad\times\frac{1}{\omega_1+\omega_2+\frac{1}{2}(\kappa'+\kappa)++\frac{1}{2}\left[E_a(\mathbf{p}')-E_b(\mathbf{p}')-E_a(\mathbf{p})+E_b(\mathbf{p})\right]+i\epsilon}, \qquad \text{(D4d)}\\
D^{(X,c)}_{\sigma;\kappa',\kappa}(\omega_1,\omega_2) &= +\frac{1}{\omega_2+\kappa+[E_a(\mathbf{q})-E_a(\mathbf{p}')]+i\epsilon}\cdot\frac{1}{\omega_1+\kappa'+[E_b(\mathbf{q})+E_b(\mathbf{p})]+i\epsilon}\cdot \\
&\quad\times\frac{1}{\frac{1}{2}(\kappa'+\kappa)+(E_a(\mathbf{q})+E_b(\mathbf{q}))+\frac{1}{2}\left[E_b(\mathbf{p}')-E_a(\mathbf{p}')+E_b(\mathbf{p})-E_a(\mathbf{p})\right]+i\epsilon}, \qquad \text{(D4e)}\\
D^{(X,c')}_{\sigma;\kappa',\kappa}(\omega_1,\omega_2) &= +\frac{1}{\omega_2+\kappa+[E_b(\mathbf{q})+E_b(\mathbf{p}')]+i\epsilon}\cdot\frac{1}{\omega_1+\kappa'+[E_a(\mathbf{q})-E_a(\mathbf{p})]+i\epsilon}\cdot \\
&\quad\times\frac{1}{\frac{1}{2}(\kappa'+\kappa)+(E_a(\mathbf{q})+E_b(\mathbf{q}))+\frac{1}{2}\left[E_b(\mathbf{p}')-E_a(\mathbf{p}')+E_b(\mathbf{p})-E_a(\mathbf{p})\right]+i\epsilon}. \qquad \text{(D4f)}
\end{aligned}
$$

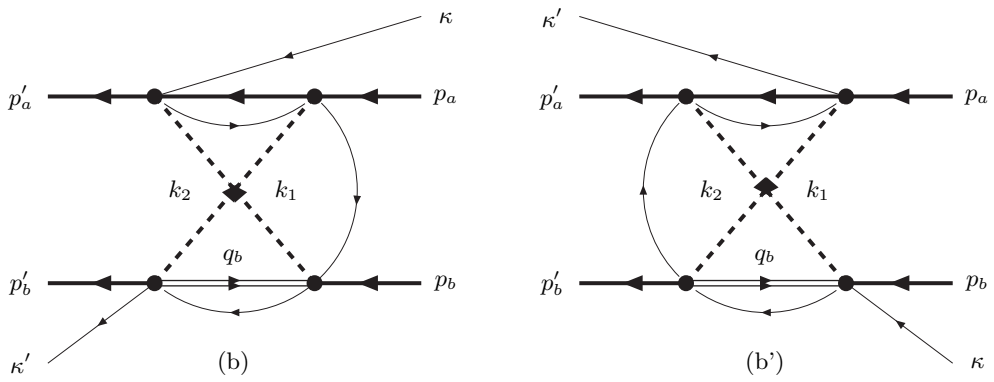

FIG. 16: *Crossed Kadyshevsky graphs. The solid lines denote baryons. The dashed lines refers to the mesons. The thin lines denote the quasi-momentum particles.*

3. Adiabatic Approximations

In the adiabatic approximation $A = A' = A'' = 0, B'' = 2M$. The expressions for the denominators become:

Planar-graphs:

$$\begin{aligned}
D^{(//,a)}_{\sigma;0,0}(ad) &= \frac{1}{\omega_1}\,\frac{1}{\omega_1+\omega_2+2M}\,\frac{1}{\omega_2} \quad , \quad D^{(//,a')}_{\sigma;0,0}(ad) = \frac{1}{\omega_1+2M}\,\frac{1}{\omega_1+\omega_2+2M}\,\frac{1}{\omega_2+2M},\\
D^{(//,b)}_{\sigma;0,0}(ad) &= \frac{1}{\omega_2+2M}\,\frac{1}{\omega_1+\omega_2}\,\frac{1}{\omega_2} \quad , \quad D^{(//,b')}_{\sigma;0,0}(ad) = \frac{1}{\omega_1}\,\frac{1}{\omega_1+\omega_2}\,\frac{1}{\omega_1+2M},\\
D^{(//,c)}_{\sigma;0,0}(ad) &= \frac{1}{\omega_2+2M}\,\frac{1}{\omega_1+\omega_2+2M}\,\frac{1}{\omega_2} \quad , \quad D^{(//,c')}_{\sigma;0,0}(ad) = \frac{1}{\omega_1}\,\frac{1}{\omega_1+\omega_2+2M}\,\frac{1}{\omega_1+2M}.
\end{aligned} \tag{D5}$$

Crossed-graphs:

$$\begin{aligned}
D^{(X,a)}_{\sigma;0,0}(ad) &= \frac{1}{\omega_1}\,\frac{1}{2M}\,\frac{1}{\omega_2} \quad , \quad D^{(X,a')}_{\sigma;0,0}(ad) = \frac{1}{\omega_1+2M}\,\frac{1}{2M}\,\frac{1}{\omega_2+2M},\\
D^{(X,b)}_{\sigma;0,0}(ad) &= \frac{1}{\omega_1+2M}\,\frac{1}{\omega_1+\omega_2}\,\frac{1}{\omega_2} \quad , \quad D^{(X,b')}_{\sigma;0,0}(ad) = \frac{1}{\omega_1}\,\frac{1}{\omega_1+\omega_2}\,\frac{1}{\omega_2+2M},\\
D^{(X,c)}_{\sigma;0,0}(ad) &= \frac{1}{\omega_1+2M}\,\frac{1}{2M}\,\frac{1}{\omega_2} \quad , \quad D^{(X,c')}_{\sigma;0,0}(ad) = \frac{1}{\omega_1}\,\frac{1}{2M}\,\frac{1}{\omega_2+2M}.
\end{aligned} \tag{D6}$$

Notice that the spinor-numerator factors for the parallel graphs are the same, and so we have the symmetry $\omega_1 \leftrightarrow \omega_2$ as can be seen from the expressions above, and similarly for the crossed graphs.

Defining $D^{(//)}_{\sigma;0,0}(ad) = \sum_{i=a,b,c,a',b',c'} D^{(//,i)}(ad)$. Similarly $D^{(X)}_{\sigma;0,0}(ad)$ for the crossed graphs. We have for the parallel grapgs

$$\begin{aligned}
D^{(//)}_{\sigma;0,0}(ad) \;=\; & \left[\frac{1}{\omega_1\omega_2}+\frac{1}{\omega_1(\omega_1+2M)}+\frac{1}{\omega_2(\omega_2+2M)}+\frac{1}{(\omega_1+2M)(\omega_2+2M)}\right]\frac{1}{\omega_1+\omega_2+2M}\\
& +\left[\frac{1}{\omega_1(\omega_1+2M)}+\frac{1}{\omega_2(\omega_2+2M)}\right]\frac{1}{\omega_1+\omega_2},
\end{aligned} \tag{D7}$$

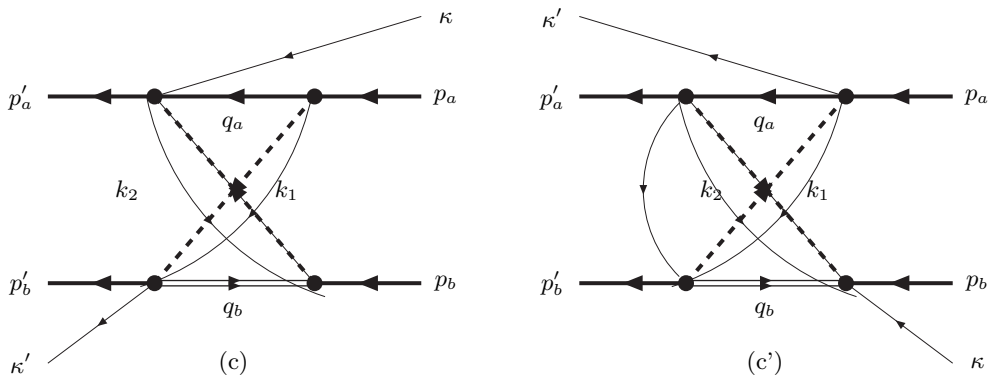

FIG. 17: *Crossed Kadyshevsky graphs. The solid lines denote baryons. The dashed lines refers to the mesons. The thin lines denote the quasi-momentum particles.*

and for the crossed graphs

$$D^{(X)}_{\sigma;0,0}(ad) = \left[\frac{1}{\omega_1\omega_2}+\frac{1}{\omega_1(\omega_2+2M)}+\frac{1}{\omega_2(\omega_1+2M)}+\frac{1}{(\omega_1+2M)(\omega_2+2M)}\right]\frac{1}{2M} + \left[\frac{1}{\omega_1(\omega_2+2M)}+\frac{1}{(\omega_1+2M)\omega_2}\right]\frac{1}{\omega_1+\omega_2}. \tag{D8}$$

For the antifermion in the a-line identical contributions are obtained so that we get a factor 2 in the sum.

APPENDIX E: FOURTH-ORDER KADYSHEVSKY GRAPHA $\sigma = [--]$

1. The planar-box graphs

Following the rules of Appendix A we have drawn the planar two meson echange graphs in Figs. 18-20. Here, the numbering of the vertices can be readoff by following the quasi-particle lines, beginning with the entering κ-line. The quasi-particle lines κ_i for $i = 1, 2, 3$ are then defined according to Appendix A. Then, again following the rules of Appendix A we list below the resulting amplitudes. In these notes we select the graphs with two antinucleons in the intermediate states.

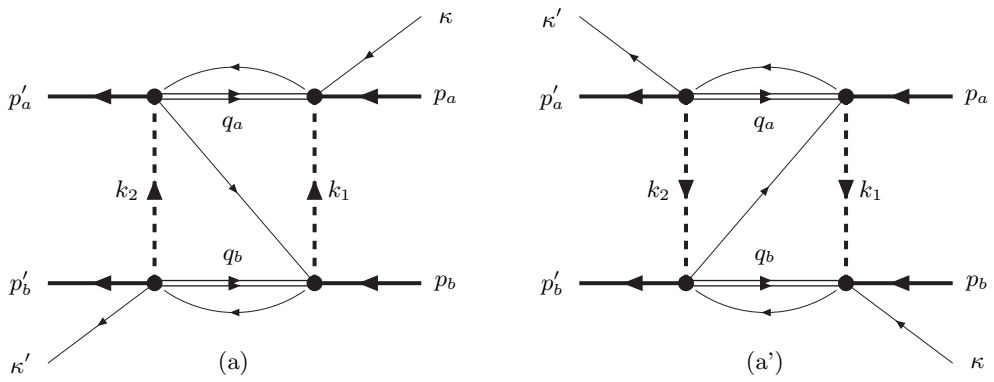

FIG. 18: *Planar Kadyshevsky graphs. The solid line denote the baryon, the thin double-line the antibaryon. The dashed lines refers to the mesons. The single thin lines denote the quasi-momentum particles.*

Graph (a) in the planar-box Feynman-Kadyshevsky diagrams Fig. 18 gives for the fourth-order kernel

$$
\begin{aligned}
M^{(//,a)}_{\sigma;\kappa',\kappa} &= \int \frac{d^4q_a}{(2\pi)^3} \int \frac{d^4q_b}{(2\pi)^3} \cdot \\
&\times \int \frac{d^4k_1}{(2\pi)^3} \int \frac{d^4k_2}{(2\pi)^3}\, \delta_+\left[k_1^2 - m_1^2\right] \delta_+\left[k_2^2 - m_2^2\right] \cdot \widetilde{S}_F^{(+)}(q_a)\; \widetilde{S}_F^{(-)}(q_b) \\
&\times \int_{-\infty}^{\infty} \frac{d\kappa_1}{2\pi} \int_{-\infty}^{\infty} \frac{d\kappa_2}{2\pi} \int_{-\infty}^{\infty} \frac{d\kappa_3}{2\pi} \frac{1}{\kappa_1 - i\epsilon} \frac{1}{\kappa_2 - i\epsilon} \frac{1}{\kappa_3 - i\epsilon} \cdot \\
&\times (2\pi)^4 \delta^4\left(\kappa_1 n - p_a - q_a - k_1 - \kappa n\right) (2\pi)^4 \delta^4\left(\kappa_3 n - p'_b - q_b - k_2 - \kappa' n\right) \cdot \\
&\times (2\pi)^4 \delta^4\left(\kappa_2 n - \frac{1}{2}(\kappa' + \kappa) n - (k_1 + k_2) + \frac{1}{2}(p'_a - p'_b - p_a + p_b)\right) .
\end{aligned}
\tag{E1}
$$

Now, in (E1) there are four delta-functions from which we obtain the overall four-momentum conservation, including κ and κ'. With the delta-functions all κ-integrals can be carried out. Also, the integrations over the zero-components can be carried out, thanks to the on-mass-shell δ_+-functions. We will do so in the CM-system, where we can use the specific form of the n^μ-vector. Similar calculations are carried through for the graphs (a'), (b), (b'), (c), and (c').

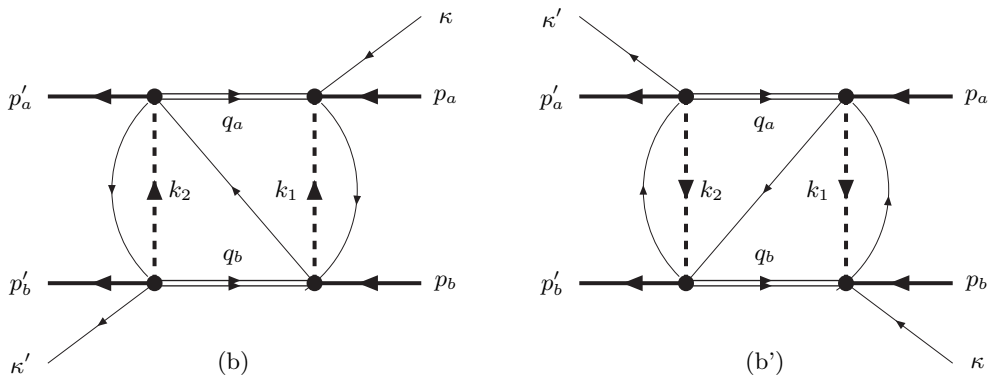

FIG. 19: *Planar Kadyshevsky graphs. The solid lines denote baryons. The dashed lines refers to the mesons. The single thin lines denote the quasi-momentum particles.*

Performing the κ_i-integrals (i=1,2,3) leads to the denominators ($\sigma = [--]$)

$$D^{(//,a)}_{\sigma;\kappa',\kappa}(\omega_1,\omega_2) = +\frac{1}{\omega_1+\kappa+[E_a(\mathbf{p})+E_a(\mathbf{q})]+i\epsilon}\cdot\frac{1}{\omega_2+\kappa'+[E_b(\mathbf{p}')+E_b(\mathbf{q})]+i\epsilon}\cdot \times\frac{1}{\omega_1+\omega_2+\frac{1}{2}(\kappa'+\kappa)+\frac{1}{2}[E_b(\mathbf{p}')-E_a(\mathbf{p}')-E_b(\mathbf{p})+E_a(\mathbf{p})]+i\epsilon}, \quad \text{(E2a)}$$

$$D^{(//,a')}_{\sigma;\kappa',\kappa}(\omega_1,\omega_2) = +\frac{1}{\omega_1+\kappa+[E_b(\mathbf{p})+E_b(\mathbf{q})]+i\epsilon}\cdot\frac{1}{\omega_2+\kappa'+[E_b(\mathbf{q})+E_a(\mathbf{p}')]+i\epsilon}\cdot \times\frac{1}{\omega_1+\omega_2+\frac{1}{2}(\kappa'+\kappa)+\frac{1}{2}[E_a(\mathbf{p}')-E_b(\mathbf{p}')+E_b(\mathbf{p})-E_a(\mathbf{p})]+i\epsilon}, \quad \text{(E2b)}$$

$$D^{(//,b)}_{\sigma;\kappa',\kappa}(\omega_1,\omega_2) = +\frac{1}{\omega_1+\kappa+[E_a(\mathbf{p})+E_a(\mathbf{q})]+i\epsilon}\cdot\frac{1}{\omega_2+\kappa'+[E_b(\mathbf{p}')+E_b(\mathbf{q})]+i\epsilon}\cdot \times\frac{1}{\frac{1}{2}(\kappa'+\kappa)+[E_a(\mathbf{q})+E_b(\mathbf{q})]+\frac{1}{2}[E_b(\mathbf{p}')+E_a(\mathbf{p}')+E_b(\mathbf{p})+E_a(\mathbf{p}]+i\epsilon}, \quad \text{(E2c)}$$

$$D^{(//,b')}_{\sigma;\kappa',\kappa}(\omega_1,\omega_2) = +\frac{1}{\omega_1+\kappa+[E_b(\mathbf{p})+E_b(\mathbf{q})]+i\epsilon}\cdot\frac{1}{\omega_2+\kappa'+[E_a(\mathbf{p}'+E_a(\mathbf{q})]+i\epsilon}\cdot \times\frac{1}{\frac{1}{2}(\kappa'+\kappa)+[E_a(\mathbf{q})+E_b(\mathbf{q})]+\frac{1}{2}[E_a(\mathbf{p}')+E_b(\mathbf{p}')+E_a(\mathbf{p})+E_b(\mathbf{p}]+i\epsilon}, \quad \text{(E2d)}$$

$$D^{(//,c)}_{\sigma;\kappa',\kappa}(\omega_1,\omega_2) = +\frac{1}{\omega_1+\kappa+[E_a(\mathbf{p})+E_a(\mathbf{q})]+i\epsilon}\cdot\frac{1}{\omega_2+\kappa'+[E_a(\mathbf{p}')+E_a(\mathbf{q})]+i\epsilon}\cdot \times\frac{1}{\frac{1}{2}(\kappa'+\kappa)+\frac{1}{2}[E_b(\mathbf{p}')+E_a(\mathbf{p}')+E_b(\mathbf{p})+E_a(\mathbf{p}]+(E_a(\mathbf{q})+E_b(\mathbf{q}))+i\epsilon}, \quad \text{(E2e)}$$

$$D^{(//,c')}_{\sigma;\kappa',\kappa}(\omega_1,\omega_2) = +\frac{1}{\omega_1+\kappa+[E_b(\mathbf{p})+E_b(\mathbf{q})]+i\epsilon}\cdot\frac{1}{\omega_2+\kappa'+[E_b(\mathbf{p}')+E_b(\mathbf{q})]+i\epsilon}\cdot \times\frac{1}{\frac{1}{2}(\kappa'+\kappa)+[E_a(\mathbf{q})+E_b(\mathbf{q})]+\frac{1}{2}[E_b(\mathbf{p}')+E_a(\mathbf{p}')+E_b(\mathbf{p})+E_a(\mathbf{p}]+i\epsilon}. \quad \text{(E2f)}$$

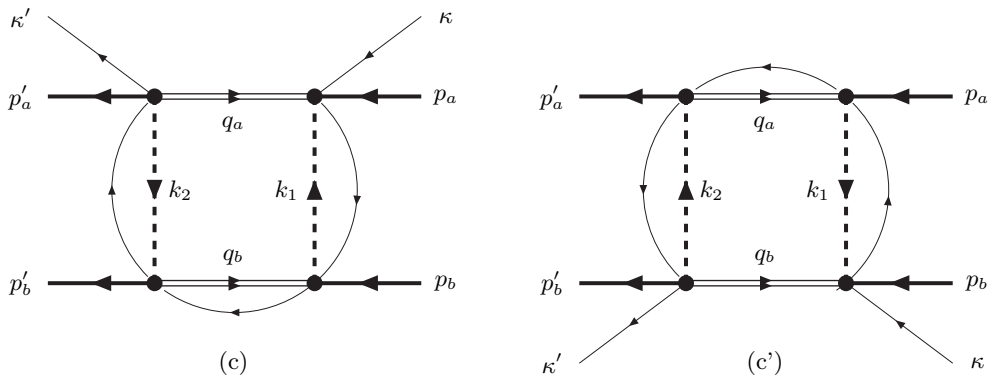

FIG. 20: *Planar Kadyshevsky graphs. The solid lines denote baryons. The dashed lines refers to the mesons. The single thin lines denote the quasi-momentum particles.*

2. The crossed-box graphs

Graph (a) in the crossed-box Kadyshevsky diagrams Fig. 21 gives for the fourth-order kernel, with only positive energy spinors for the intermediate nucleons,

$$M^{(X,a)}_{\sigma;\kappa',\kappa}\left(p'_a,p'_b;p_a,p_b\right)=\int\frac{d^4q_a}{(2\pi)^3}\int\frac{d^4q_b}{(2\pi)^3}\int\frac{d^4k_1}{(2\pi)^3}\int\frac{d^4k_2}{(2\pi)^3}\cdot$$

$$\times\delta_+\left[k_1^2-m_1^2\right]\delta_+\left[k_2^2-m_2^2\right]\cdot\delta_+\left[q_a^2-M_a^2\right]\delta_+\left[q_b^2-M_b^2\right]$$

$$\times\int_{-\infty}^{\infty}\frac{d\kappa_1}{2\pi}\int_{-\infty}^{\infty}\frac{d\kappa_2}{2\pi}\int_{-\infty}^{\infty}\frac{d\kappa_3}{2\pi}\frac{1}{\kappa_1-i\epsilon}\frac{1}{\kappa_2-i\epsilon}\frac{1}{\kappa_3-i\epsilon}\cdot$$

$$\times(2\pi)^4\delta^4\left(\kappa_1 n-p_a-q_a-k_1-\kappa n\right)(2\pi)^4\delta^4\left(\kappa_3 n-p'_b-q_b-k_1-\kappa' n\right)\cdot$$

$$\times(2\pi)^4\delta^4\left(\kappa_2 n-\frac{1}{2}(\kappa'+\kappa)n-(\omega_1+\omega_2)-\frac{1}{2}(p'_b-p'_a+p_b-p_a)\right). \tag{E3}$$

With the delta-functions all κ-integrals can be carried out. Also, the integrations over the zero-components can be carried out, thanks to the on-mass-shell δ_+-functions.

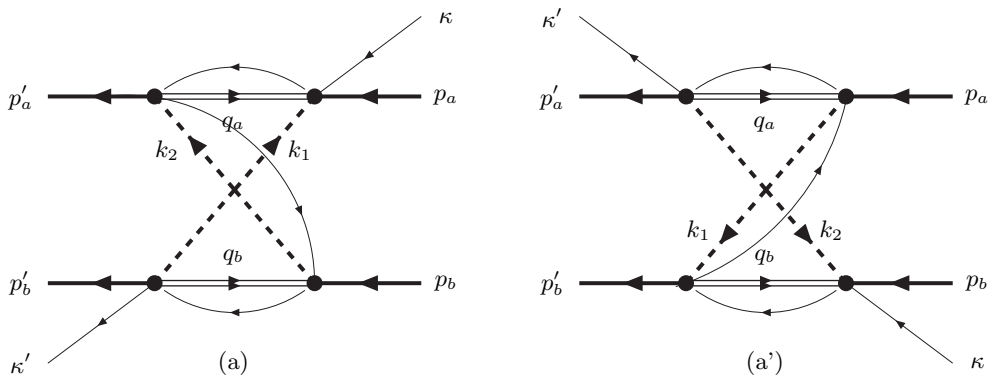

FIG. 21: *Crossed-box Kadyshevsky graphs. The solid lines denote baryons. The dashed lines refers to the mesons. The single thin lines denote the quasi-momentum particles.*

In the CM-system this leads to the denominators

$$D^{(X,a)}_{\sigma;\kappa',\kappa}(\omega_1,\omega_2) = +\frac{1}{\omega_1+\kappa+[E_a(\mathbf{q})+E_a(\mathbf{p})]+i\epsilon}\cdot\frac{1}{\omega_1+\kappa'+[E_b(\mathbf{q})+E_b(\mathbf{p}')]+i\epsilon}\cdot \times\frac{1}{\omega_1+\omega_2+\frac{1}{2}(\kappa'+\kappa)+\frac{1}{2}\left[E_b(\mathbf{p}')-E_a(\mathbf{p}')-E_b(\mathbf{p})+E_a(\mathbf{p})\right]+i\epsilon}, \quad \text{(E4a)}$$

$$D^{(X,a')}_{\sigma;\kappa',\kappa}(\omega_1,\omega_2) = +\frac{1}{\omega_2+\kappa+[E_b(\mathbf{q})+E_b(\mathbf{p})]+i\epsilon}\cdot\frac{1}{\omega_2+\kappa'+[E_a(\mathbf{q})+E_a(\mathbf{p}')]+i\epsilon}\cdot \times\frac{1}{\omega_1+\omega_2+\frac{1}{2}(\kappa'+\kappa)+\frac{1}{2}\left[E_a(\mathbf{p}')-E_b(\mathbf{p}')-E_a(\mathbf{p})+E_b(\mathbf{p})\right]+i\epsilon}, \quad \text{(E4b)}$$

$$D^{(X,b)}_{\sigma;\kappa',\kappa}(\omega_1,\omega_2) = +\frac{1}{\omega_1+\kappa+[E_a(\mathbf{q})+E_a(\mathbf{p})]+i\epsilon}\cdot\frac{1}{\omega_1+\kappa'+[E_b(\mathbf{q})+E_b(\mathbf{p}')]+i\epsilon}\cdot \times\frac{1}{\omega_1+\omega_2+\frac{1}{2}(\kappa'+\kappa)+\frac{1}{2}\left[E_b(\mathbf{p}')+E_a(\mathbf{p}')+E_b(\mathbf{p})+E_a(\mathbf{p})\right]+[E_a(\mathbf{q})+E_b(\mathbf{q})]+i\epsilon}, \quad \text{(E4c)}$$

$$D^{(X,b')}_{\sigma;\kappa',\kappa}(\omega_1,\omega_2) = +\frac{1}{\omega_2+\kappa+[E_b(\mathbf{q})+E_b(\mathbf{p})]+i\epsilon}\cdot\frac{1}{\omega_2+\kappa'+[E_a(\mathbf{q})+E_a(\mathbf{p}')]+i\epsilon}\cdot \times\frac{1}{\omega_1+\omega_2+\frac{1}{2}(\kappa'+\kappa)++\frac{1}{2}\left[E_a(\mathbf{p}')+E_b(\mathbf{p}')+E_a(\mathbf{p})+E_b(\mathbf{p})\right]+[E_a(\mathbf{q})+E_b(\mathbf{q})]+i\epsilon}, \quad \text{(E4d)}$$

$$D^{(X,c)}_{\sigma;\kappa',\kappa}(\omega_1,\omega_2) = +\frac{1}{\omega_1+\kappa+[E_a(\mathbf{q})+E_a(\mathbf{p})]+i\epsilon}\cdot\frac{1}{\omega_2+\kappa'+[E_a(\mathbf{q})+E_a(\mathbf{p}')]+i\epsilon}\cdot \times\frac{1}{\omega_1+\omega_2+\frac{1}{2}(\kappa'+\kappa)+\frac{1}{2}\left[E_b(\mathbf{p}')+E_a(\mathbf{p}')+E_b(\mathbf{p})+E_a(\mathbf{p})\right]+[E_a(\mathbf{q})+E_b(\mathbf{q})]+i\epsilon}, \quad \text{(E4e)}$$

$$D^{(X,c')}_{\sigma;\kappa',\kappa}(\omega_1,\omega_2) = +\frac{1}{\omega_2+\kappa+[E_b(\mathbf{q})+E_b(\mathbf{p})]+i\epsilon}\cdot\frac{1}{\omega_1+\kappa'+[E_b(\mathbf{q})+E_b(\mathbf{p}')]+i\epsilon}\cdot \times\frac{1}{\omega_1+\omega_2+\frac{1}{2}(\kappa'+\kappa)+\frac{1}{2}\left[E_b(\mathbf{p}')+E_a(\mathbf{p}')+E_b(\mathbf{p})+E_a(\mathbf{p})\right]+[E_a(\mathbf{q})+E_b(\mathbf{q})]+i\epsilon}. \quad \text{(E4f)}$$

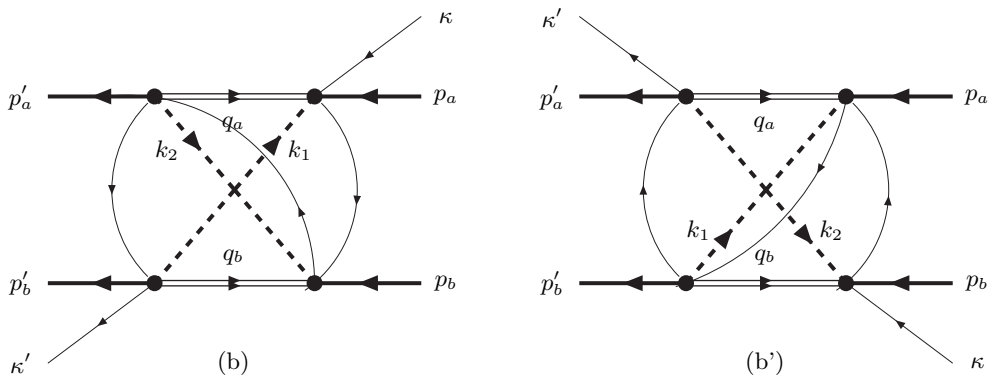

FIG. 22: *Crossed Kadyshevsky graphs. The solid lines denote baryons. The dashed lines refers to the mesons. The single thin lines denote the quasi-momentum particles.*

3. Adiabatic Approximations

In the adiabatic approximation the expressions for the denominators become:

Planar-graphs:

$$\begin{aligned}
D^{(//,a)}_{\sigma;0,0}(ad) &= \frac{1}{\omega_1+2M}\frac{1}{\omega_1+\omega_2}\frac{1}{\omega_2+2M} \quad , \; D^{(//,a')}_{\sigma;0,0}(ad) = \frac{1}{\omega_1+2M}\frac{1}{\omega_1+\omega_2}\frac{1}{\omega_2+2M}, \\
D^{(//,b)}_{\sigma;0,0}(ad) &= \frac{1}{\omega_1+2M}\frac{1}{4M}\frac{1}{\omega_2+2M} \quad , \; D^{(//,b')}_{\sigma;0,0}(ad) = \frac{1}{\omega_1+2M}\frac{1}{4M}\frac{1}{\omega_2+2M}, \\
D^{(//,c)}_{\sigma;0,0}(ad) &= \frac{1}{\omega_1+2M}\frac{1}{4M}\frac{1}{\omega_2+2M} \quad , \; D^{(//,c')}_{\sigma;0,0}(ad) = \frac{1}{\omega_1+2M}\frac{1}{4M}\frac{1}{\omega_2+2M}.
\end{aligned} \tag{E5}$$

Crossed-graphs:

$$\begin{aligned}
D^{(X,a)}_{\sigma;0,0}(ad) &= \frac{1}{\omega_1+2M}\frac{1}{\omega_1+\omega_2}\frac{1}{\omega_1+2M} \quad , \; D^{(X,a')}_{\sigma;0,0}(ad) = \frac{1}{\omega_2+2M}\frac{1}{\omega_1+\omega_2}\frac{1}{\omega_2+2M}, \\
D^{(X,b)}_{\sigma;0,0}(ad) &= \frac{1}{\omega_1+2M}\frac{1}{\omega_1+\omega_2+4M}\frac{1}{\omega_1+2M} \quad , \; D^{(X,b')}_{\sigma;0,0}(ad) = \frac{1}{\omega_2+2M}\frac{1}{\omega_1+\omega_2+4M}\frac{1}{\omega_2+2M}, \\
D^{(X,c)}_{\sigma;0,0}(ad) &= \frac{1}{\omega_1+2M}\frac{1}{\omega_1+\omega_2+4M}\frac{1}{\omega_2+2M} \quad , \; D^{(X,c')}_{\sigma;0,0}(ad) = \frac{1}{\omega_2+2M}\frac{1}{\omega_1+\omega_2+4M}\frac{1}{\omega_1+2M}.
\end{aligned} \tag{E6}$$

Notice that the spinor-numerator factors for the parallel graphs are the same, and so we have the symmetry $\omega_1 \leftrightarrow \omega_2$ as can be seen from the expressions above, and similarly for the crossed graphs.

Defining $D^{(//)}_{\sigma;0,0}(ad) = \sum_{i=a,b,c,a',b',c'} D^{(//,i)}(ad)$. Similarly $D^{(X)}_{\sigma;0,0}(ad)$ for the crossed graphs. We have for the parallel grapgs

$$D^{(//)}_{\sigma;0,0}(ad) \;=\; \frac{1}{(\omega_1+2M)(\omega_2+2M)}\left[\frac{2}{\omega_1+\omega_2}+\frac{4}{4M}\right]. \tag{E7}$$

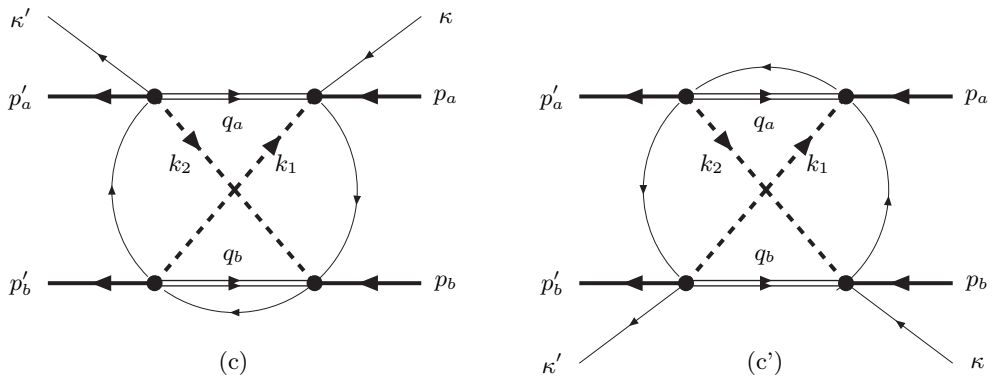

FIG. 23: *Crossed Kadyshevsky graphs. The solid lines denote baryons. The dashed lines refers to the mesons. The single thin lines denote the quasi-momentum particles.*

and for the crossed graphs

$$D^{(X)}_{\sigma;0,0}(ad) = \left[\left(\frac{1}{\omega_1+2M}\right)^2+\left(\frac{1}{\omega_2+2M}\right)^2\right]\frac{1}{\omega_1+\omega_2} + \left[\frac{1}{\omega_1+2M}+\frac{1}{\omega_2+2M}\right]^2\frac{1}{\omega_1+\omega_2+2M}. \tag{E8}$$

APPENDIX F: EXACT REDUCTION DIRAC-SPINORS TO PAULI-SPINORS

The transition from Dirac spinors to Pauli spinors is given here, without approximations. We use the notations $\mathcal{E}=E+M$ and $\mathcal{E}'=E'+M'$, where $E=E(p,M)$ and $E'=E(p',M')$. Also, we omit, on the right-hand side in the expressions below, the final and initial Pauli spinors $\chi'^{\dagger}$ and χ respectively, which are self-evident. The expressions below are derived using the Dirac spinors [29]

$$u(\mathbf{p})=\sqrt{\frac{E+M}{2M}}\begin{pmatrix}\chi\\ \frac{\boldsymbol{\sigma}\cdot\mathbf{p}}{E+M}\,\chi\end{pmatrix},\quad v(\mathbf{p})=\sqrt{\frac{E+M}{2M}}\begin{pmatrix}\frac{\boldsymbol{\sigma}\cdot\mathbf{p}}{E+M}\,\chi\\ \chi\end{pmatrix}. \tag{F1}$$

With these Dirac spinors we have

$$\bar{u}(\mathbf{p}')u(\mathbf{p}) = +\sqrt{\frac{\mathcal{E}'\mathcal{E}}{4M'M}}\left[\left(1-\frac{\mathbf{p}'\cdot\mathbf{p}}{\mathcal{E}'\mathcal{E}}\right)-i\frac{\mathbf{p}'\times\mathbf{p}\cdot\boldsymbol{\sigma}}{\mathcal{E}'\mathcal{E}}\right], \tag{F2a}$$

$$\bar{u}(\mathbf{p}')\gamma_5 u(\mathbf{p}) = -\sqrt{\frac{\mathcal{E}'\mathcal{E}}{4M'M}}\left[\frac{\boldsymbol{\sigma}\cdot\mathbf{p}'}{\mathcal{E}'}-\frac{\boldsymbol{\sigma}\cdot\mathbf{p}}{\mathcal{E}}\right], \tag{F2b}$$

$$\bar{u}(\mathbf{p}')\gamma^0 u(\mathbf{p}) = +\sqrt{\frac{\mathcal{E}'\mathcal{E}}{4M'M}}\left[\left(1+\frac{\mathbf{p}'\cdot\mathbf{p}}{\mathcal{E}'\mathcal{E}}\right)+i\frac{\mathbf{p}'\times\mathbf{p}\cdot\boldsymbol{\sigma}}{\mathcal{E}'\mathcal{E}}\right], \tag{F2c}$$

$$\bar{u}(\mathbf{p}')\boldsymbol{\gamma}\ u(\mathbf{p}) = +\sqrt{\frac{\mathcal{E}'\mathcal{E}}{4M'M}}\left[\left(\frac{\mathbf{p}'}{\mathcal{E}'}+\frac{\mathbf{p}}{\mathcal{E}}\right)+i\left(\frac{\boldsymbol{\sigma}\times\mathbf{p}'}{\mathcal{E}'}-\frac{\boldsymbol{\sigma}\times\mathbf{p}}{\mathcal{E}}\right)\right], \tag{F2d}$$

$$\bar{u}(\mathbf{p}')\gamma_5\gamma^0 u(\mathbf{p}) = -\sqrt{\frac{\mathcal{E}'\mathcal{E}}{4M'M}}\left[\frac{\boldsymbol{\sigma}\cdot\mathbf{p}'}{\mathcal{E}'}+\frac{\boldsymbol{\sigma}\cdot\mathbf{p}}{\mathcal{E}}\right], \tag{F2e}$$

$$\begin{aligned}\bar{u}(\mathbf{p}')\gamma_5\boldsymbol{\gamma}\ u(\mathbf{p}) &= -\sqrt{\frac{\mathcal{E}'\mathcal{E}}{4M'M}}\left[\boldsymbol{\sigma}+\frac{(\boldsymbol{\sigma}\cdot\mathbf{p}')\ \boldsymbol{\sigma}\ (\boldsymbol{\sigma}\cdot\mathbf{p})}{\mathcal{E}'\mathcal{E}}\right]\\ &= -\sqrt{\frac{\mathcal{E}'\mathcal{E}}{4M'M}}\left[\left(1-\frac{\mathbf{p}'\cdot\mathbf{p}}{\mathcal{E}'\mathcal{E}}\right)\boldsymbol{\sigma}-i\frac{\mathbf{p}'\times\mathbf{p}}{\mathcal{E}'\mathcal{E}}\right.\\ &\quad\left.+\frac{1}{\mathcal{E}'\mathcal{E}}\left(\boldsymbol{\sigma}\cdot\mathbf{p}\ \mathbf{p}'+\boldsymbol{\sigma}\cdot\mathbf{p}'\ \mathbf{p}\right)\right]\approx-\boldsymbol{\sigma},,\end{aligned} \tag{F2f}$$

where we defined $\mathbf{k}=\mathbf{p}'-\mathbf{p}$, $\mathbf{q}=(\mathbf{p}'+\mathbf{p})/2$, and $\kappa_V=f_V/g_V$.

The Gordon decompositions used in this paper read

$$i\ \bar{u}(p')\ \sigma^{\mu\nu}(p'-p)_\nu u(p)=\bar{u}(p')\left\{(M'+M)\gamma^\mu-(p'+p)^\mu\right\}\ u(p), \tag{F3a}$$

$$i\ \bar{v}(p')\ \sigma^{\mu\nu}(-p'-p)_\nu u(p)=\bar{v}(p')\left\{(M'+M)\gamma^\mu+(p'-p)^\mu\right\}\ u(p). \tag{F3b}$$

For (++)-vertices the complete vector-vertex is

$$\begin{aligned}\bar{u}(p')\Gamma_V^\mu u(p) &\equiv \bar{u}(p')\left[\gamma^\mu+\frac{i}{2\mathcal{M}}\kappa_V\sigma^{\mu\nu}(p'-p)_\nu\right]u(p)\\ &= \bar{u}(p')\left[\left(1+\frac{M'+M}{2\mathcal{M}}\kappa_V\right)\gamma^\mu-\frac{\kappa_V}{2\mathcal{M}}(p'+p)_\mu\right]u(p)\Longrightarrow\end{aligned}$$

$$\begin{aligned}\mu=0\ :\ &+\sqrt{\frac{\mathcal{E}'\mathcal{E}}{4M'M}}\left[\left(1+\frac{M'+M}{2\mathcal{M}}\kappa_V\right)\left(1+\frac{\boldsymbol{\sigma}\cdot\mathbf{p}'\ \boldsymbol{\sigma}\cdot\mathbf{p}}{\mathcal{E}'\mathcal{E}}\right)\right.\\ &\left.-\frac{\kappa_V}{2\mathcal{M}}(E'+E)\left(1-\frac{\boldsymbol{\sigma}\cdot\mathbf{p}'\ \boldsymbol{\sigma}\cdot\mathbf{p}}{\mathcal{E}'\mathcal{E}}\right)\right],\end{aligned} \tag{F4a}$$

$$\begin{aligned}\mu=i\ :\ &+\sqrt{\frac{\mathcal{E}'\mathcal{E}}{4M'M}}\left[\left(1+\frac{M'+M}{2\mathcal{M}}\kappa_V\right)\left\{\left(\frac{\mathbf{p}'}{\mathcal{E}'}+\frac{\mathbf{p}}{\mathcal{E}}\right)+i\left(\frac{\boldsymbol{\sigma}\times\mathbf{p}'}{\mathcal{E}'}-\frac{\boldsymbol{\sigma}\times\mathbf{p}}{\mathcal{E}}\right)\right\}\right.\\ &\left.-\frac{\kappa_V}{2\mathcal{M}}(\mathbf{p}'+\mathbf{p})\left(1-\frac{\boldsymbol{\sigma}\cdot\mathbf{p}'\ \boldsymbol{\sigma}\cdot\mathbf{p}}{\mathcal{E}'\mathcal{E}}\right)\right].\end{aligned} \tag{F4b}$$

$$\bar{v}(\mathbf{p}')u(\mathbf{p}) = +\sqrt{\frac{\mathcal{E}'\mathcal{E}}{4M'M}}\left[\frac{\boldsymbol{\sigma}\cdot\mathbf{p}'}{\mathcal{E}'} - \frac{\boldsymbol{\sigma}\cdot\mathbf{p}}{\mathcal{E}}\right], \tag{F5a}$$

$$\bar{v}(\mathbf{p}')\gamma_5 u(\mathbf{p}) = -\sqrt{\frac{\mathcal{E}'\mathcal{E}}{4M'M}}\left[\left(1 - \frac{\mathbf{p}'\cdot\mathbf{p}}{\mathcal{E}'\mathcal{E}}\right) - i\frac{\mathbf{p}'\times\mathbf{p}\cdot\boldsymbol{\sigma}}{\mathcal{E}'\mathcal{E}}\right], \tag{F5b}$$

$$\bar{v}(\mathbf{p}')\gamma^0 u(\mathbf{p}) = +\sqrt{\frac{\mathcal{E}'\mathcal{E}}{4M'M}}\left[\frac{\boldsymbol{\sigma}\cdot\mathbf{p}'}{\mathcal{E}'} + \frac{\boldsymbol{\sigma}\cdot\mathbf{p}}{\mathcal{E}}\right], \tag{F5c}$$

$$\begin{aligned}\bar{v}(\mathbf{p}')\boldsymbol{\gamma}\, u(\mathbf{p}) &= +\sqrt{\frac{\mathcal{E}'\mathcal{E}}{4M'M}}\left[\boldsymbol{\sigma} + \frac{(\boldsymbol{\sigma}\cdot\mathbf{p}')\ \boldsymbol{\sigma}\ (\boldsymbol{\sigma}\cdot\mathbf{p})}{\mathcal{E}'\mathcal{E}}\right] \\ &= +\sqrt{\frac{\mathcal{E}'\mathcal{E}}{4M'M}}\left[\left(1 - \frac{\mathbf{p}'\cdot\mathbf{p}}{\mathcal{E}'\mathcal{E}}\right)\boldsymbol{\sigma} - i\frac{\mathbf{p}'\times\mathbf{p}}{\mathcal{E}'\mathcal{E}}\right. \\ &\quad \left. + \frac{1}{\mathcal{E}'\mathcal{E}}\left(\boldsymbol{\sigma}\cdot\mathbf{p}\ \mathbf{p}' + \boldsymbol{\sigma}\cdot\mathbf{p}'\ \mathbf{p}\right)\right] \approx +\boldsymbol{\sigma},\end{aligned} \tag{F5d}$$

$$\bar{v}(\mathbf{p}')\gamma_5\gamma^0 u(\mathbf{p}) = +\sqrt{\frac{\mathcal{E}'\mathcal{E}}{4M'M}}\left[\left(1 + \frac{\mathbf{p}'\cdot\mathbf{p}}{\mathcal{E}'\mathcal{E}}\right) + i\frac{\mathbf{p}'\times\mathbf{p}\cdot\boldsymbol{\sigma}}{\mathcal{E}'\mathcal{E}}\right], \tag{F5e}$$

$$\bar{v}(\mathbf{p}')\gamma_5\boldsymbol{\gamma}\, u(\mathbf{p}) = +\sqrt{\frac{\mathcal{E}'\mathcal{E}}{4M'M}}\left[\left(\frac{\mathbf{p}'}{\mathcal{E}'} + \frac{\mathbf{p}}{\mathcal{E}}\right) + i\left(\frac{\boldsymbol{\sigma}\times\mathbf{p}'}{\mathcal{E}'} - \frac{\boldsymbol{\sigma}\times\mathbf{p}}{\mathcal{E}}\right)\right], \tag{F5f}$$

and for the $\bar{u}\Gamma v$ one can use the identity $\bar{u}(\mathbf{p}')\Gamma\ v(\mathbf{p}) = \bar{v}(\mathbf{p})\ [\gamma_0\Gamma^\dagger\ \gamma_0]\ u(\mathbf{p}')$ [7].

For (+-)-vertices the complete vector-vertex is

$$\begin{aligned}\bar{v}(p')\Gamma_V^\mu u(p) &\equiv \bar{v}(p')\left[\gamma^\mu + \frac{i}{2\mathcal{M}}\kappa_V\sigma^{\mu\nu}(-p'-p)_\nu\right]u(p) \\ &= \bar{v}(p')\left[\left(1 + \frac{M'+M}{2\mathcal{M}}\kappa_V\right)\gamma^\mu + \frac{\kappa_V}{2\mathcal{M}}(p'-p)_\mu\right]u(p) \Longrightarrow\end{aligned}$$

$$\begin{aligned}\mu = 0\ :\ &+\sqrt{\frac{\mathcal{E}'\mathcal{E}}{4M'M}}\left[\left(1 + \frac{M'+M}{2\mathcal{M}}\kappa_V\right)\left(\frac{\boldsymbol{\sigma}\cdot\mathbf{p}'}{\mathcal{E}'} + \frac{\boldsymbol{\sigma}\cdot\mathbf{p}}{\mathcal{E}}\right)\right. \\ &\left. + \frac{\kappa_V}{2\mathcal{M}}(E'-E)\left(\frac{\boldsymbol{\sigma}\cdot\mathbf{p}'}{\mathcal{E}'} - \frac{\boldsymbol{\sigma}\cdot\mathbf{p}}{\mathcal{E}}\right)\right],\end{aligned} \tag{F6a}$$

$$\begin{aligned}\mu = i\ :\ &+\sqrt{\frac{\mathcal{E}'\mathcal{E}}{4M'M}}\left[\left(1 + \frac{M'+M}{2\mathcal{M}}\kappa_V\right)\left\{\boldsymbol{\sigma} + \frac{(\boldsymbol{\sigma}\cdot\mathbf{p}')\ \boldsymbol{\sigma}\ (\boldsymbol{\sigma}\cdot\mathbf{p})}{\mathcal{E}'\mathcal{E}}\right\}\right. \\ &\left. + \frac{\kappa_V}{2\mathcal{M}}(\mathbf{p}'-\mathbf{p})\left(\frac{\boldsymbol{\sigma}\cdot\mathbf{p}'}{\mathcal{E}'} - \frac{\boldsymbol{\sigma}\cdot\mathbf{p}}{\mathcal{E}}\right)\right].\end{aligned} \tag{F6b}$$

APPENDIX G: FOLDING AND THE BARYON-BARYON POTENTIAL

We consider a nuclon having a momentum P and label the 3 quarks by a, b, c. The quark momenta are denoted by p_a, p_b, p_c. The spatial part of the composite nucleon wave funtion is taken to be [33]

$$\widetilde{\psi}(p_a, p_b, p_c) = \widetilde{\psi}(p_1, p_2, p_3) = \left(\frac{\sqrt{3}R^2}{\pi}\right)^{3/2}\ \exp\left[-\frac{R^2}{6}\sum_{i<j}(\mathbf{p}_i - \mathbf{p}_j)^2\right]. \tag{G1}$$

[7] Note the relations $v(\mathbf{p}) = \gamma_5\ u(\mathbf{p})$ and $\bar{v}(\mathbf{p}) = -\bar{u}(\mathbf{p})\gamma_5$, which explains the connections between the (F2f) and (F5f) expressions.

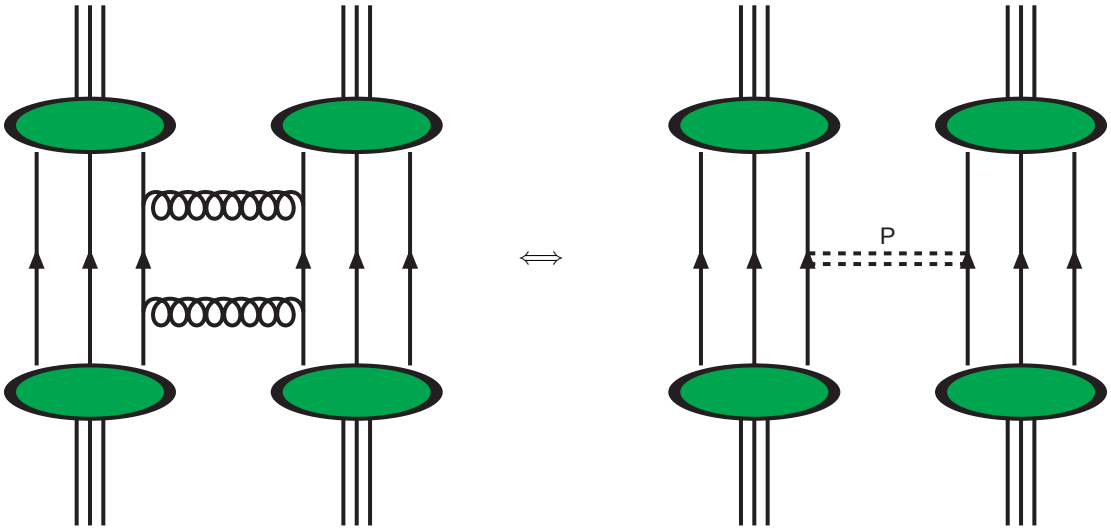

FIG. 24: *Two-gluon exchange in NN-scattering. The bubbles at the corners are the nucleon wave functions. Graphs with exchange of two gluons between the same quarks (a) correspond to the Pomeron (b). Experiment finds that to a good approximation in each nucleon only one quark couple to the gluons, i.e. dominance of the graphs of type (a).*

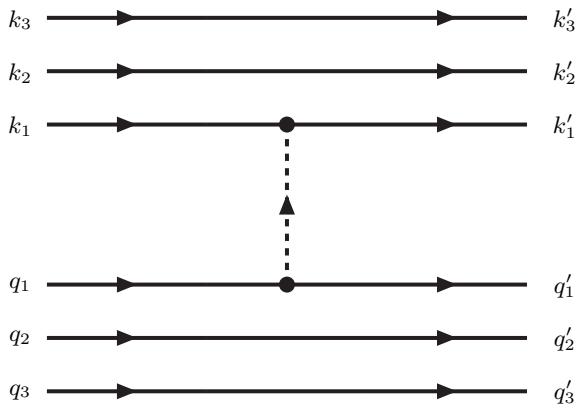

FIG. 25: External and internal momenta for pomeron-exchange

1. Overlap Integrals, Vertex functions

We consider the spin 1/2 baryon-baryon graph for pomeron-exchange between the constituent quarks of the two nucleons. In the following we will use, instead of indices a,b,c, the indices i=1,2,3.

In Fig. 25 we have given the momenta for the initial and final nucleons, and the assigned momenta of the quarks. From momentum conservation we have

$$p_1 = k_1 + k_2 + k_3 \quad , \quad p_2 = q_1 + q_2 + q_3 \ ,$$

$$p'_1 = k'_1 + k'_2 + k'_3 \quad , \quad p'_2 = q'_1 + q'_2 + q'_3 \ , \tag{G2}$$

For meson-exchange with $p_1 - p_1' = p_2' - p_2 \equiv k$, we have for the matrix-element of the potential

$$\begin{aligned}
\langle p_1' p_2' | V | p_1 p_2 \rangle \;=\; & \int \prod_{i=1,3} d^3k_i \;\delta\left(\mathbf{p}_1 - \sum_i \mathbf{k}_i\right) \cdot \int \prod_{j=1,3} d^3k_j' \;\delta\left(\mathbf{p'}_1 - \sum_j \mathbf{k'}_j\right) \cdot \\
\times & \int \prod_{i=1,3} d^3q_i \;\delta\left(\mathbf{p}_2 - \sum_i \mathbf{q}_i\right) \cdot \int \prod_{j=1,3} d^3q_j' \;\delta\left(\mathbf{p'}_2 - \sum_j \mathbf{q'}_j\right) \cdot \\
\times & \;\tilde{\psi}^*_{p_1'}\left(\mathbf{k'}_1, \mathbf{k'}_2, \mathbf{k'}_3\right) \;\tilde{\psi}^*_{p_2'}\left(\mathbf{q'}_1, \mathbf{q'}_2, \mathbf{q'}_3\right) \cdot \tilde{\psi}_{p_1}\left(\mathbf{k}_1, \mathbf{k}_2, \mathbf{k}_3\right) \;\tilde{\psi}_{p_2}\left(\mathbf{q}_1, \mathbf{q}_2, \mathbf{q}_3\right) \;\cdot \\
\times & \;\delta^3\left(\mathbf{k'}_2 - \mathbf{k}_2\right) \;\delta^3\left(\mathbf{k'}_3 - \mathbf{k}_3\right) \;\delta^3\left(\mathbf{q'}_2 - \mathbf{q}_2\right) \;\delta^3\left(\mathbf{q'}_3 - \mathbf{q}_3\right) \;\cdot \\
\times & \;\frac{\gamma\left(k; k_1', k_1\right) \;\gamma\left(k; q_1', q_1\right)}{\mathbf{k}^2 + m_M^2} \cdot \delta^3\left(\mathbf{k} - \mathbf{k}_1' + \mathbf{k}_1\right) \;\delta^3\left(\mathbf{k} + \mathbf{q}_1' - \mathbf{q}_1\right) \;. \qquad \text{(G3)}
\end{aligned}$$

In (G3) the γ's denote the vertex functions. For pomeron-exchange $(\mathbf{k}^+ m^2) \to \mathcal{M}^2$. Using the gaussian wave function of equation (G1), we find for the exponent, denoted by f_N, taking into account that the momenta of the 'spectator quarks 2 and 3 do not change, the expression

$$\begin{aligned}
f_N \;=\; \exp\Bigg[-\frac{R_N^2}{6}\Big\{ & \left(k_1 - k_2\right)^2 + \left(k_1 - k_3\right)^2 + \left(k_2 - k_3\right)^2 \\
& + \left(q_1 - q_2\right)^2 + \left(q_1 - q_3\right)^2 + \left(q_2 - q_3\right)^2 \\
& + \left(k_1' - k_2\right)^2 + \left(k_1' - k_3\right)^2 + \left(k_2 - k_3\right)^2 \\
& + \left(q_1' - q_2\right)^2 + \left(q_1' - q_3\right)^2 + \left(q_2 - q_3\right)^2 \Big\}\Bigg] \qquad \text{(G4)}
\end{aligned}$$

In (G4) $k_1 \equiv \mathbf{k}_1$ etc. Introducing the 3-momenta

$$\begin{aligned}
P_{23} = k_2 + k_3 \quad &, \quad R_{23} = q_2 + q_3 \;, \\
K_{23} = k_2 - k_3 \quad &, \quad Q_{23} = q_2 - q_3 \;, \qquad \text{(G5)}
\end{aligned}$$

for the 'spectator quarks', and the 3-momenta for the 'active' quarks the momenta $\mathbf{Q}$ and $\mathbf{S}$ defined as

$$\begin{aligned}
\mathbf{k} = \mathbf{k}_1' - \mathbf{k}_1 \quad &, \quad \mathbf{k}_1 = \frac{1}{2}\left(\mathbf{Q} - \mathbf{k}\right) \\
\mathbf{Q} = \mathbf{k}_1 + \mathbf{k}_1' \quad &, \quad \mathbf{k}_1' = \frac{1}{2}\left(\mathbf{Q} + \mathbf{k}\right) \\
\mathbf{k} = \mathbf{q}_1 - \mathbf{q}_1' \quad &, \quad \mathbf{q}_1 = \frac{1}{2}\left(\mathbf{S} + \mathbf{k}\right) \\
\mathbf{S} = \mathbf{q}_1 + \mathbf{q}_1' \quad &, \quad \mathbf{q}_1' = \frac{1}{2}\left(\mathbf{S} - \mathbf{k}\right). \qquad \text{(G6)}
\end{aligned}$$

Expressed using these momenta, f_N becomes

$$\begin{aligned}
f_N \;=\; \exp\Bigg[-\frac{R_N^2}{6}\Big\{ & \left(\mathbf{Q}^2 + \mathbf{k}^2\right) - 2\mathbf{P}_{23} \cdot \mathbf{Q} + \left(\mathbf{P}_{23}^2 + \mathbf{K}_{23}^2\right) + 2\mathbf{K}_{23}^2 \\
& + \left(\mathbf{S}^2 + \mathbf{k}^2\right) - 2\mathbf{R}_{23} \cdot \mathbf{S} + \left(\mathbf{R}_{23}^2 + \mathbf{Q}_{23}^2\right) + 2\mathbf{Q}_{23}^2 \Big\}\Bigg]. \qquad \text{(G7)}
\end{aligned}$$

In terms of the new variables defined in (G5) and (G6) the integration over the quark-momenta becomes

$$\begin{aligned}
\left(\frac{1}{8}\right)^4 \int & d^3Q \; d^3S \; d^3P_{23} \; d^3K_{23} \; d^3R_{23} \; d^3Q_{23} \cdot \\
& \times \delta^{(3)}\left(p_1 + \frac{1}{2}\left(k - Q\right) - P_{23}\right) \;\delta^{(3)}\left(p_2 - \frac{1}{2}\left(k + S\right) - R_{23}\right) \cdot \\
& \times \delta^{(3)}\left(p_1' - \frac{1}{2}\left(k + Q\right) - P_{23}\right) \;\delta\left(p_2' + \frac{1}{2}\left(k - S\right) - R_{23}\right) \qquad \text{(G8)}
\end{aligned}$$

From these δ-function constraints one immediately gets

$$\begin{aligned}&\delta^{(3)}\left(p_1' - p_1 - k\right)\ \delta^{(3)}\left(p_2' - p_2 + k\right) = \\ &\delta^{(3)}\left(p_1' - p_1 - k\right)\ \delta^{(3)}\left(p_1' + p_2' - p_1 - p_2\right)\end{aligned} \tag{G9}$$

i.e. overall 3-momentum conservation and the fixing of $\mathbf{k}$ in terms of the external momenta.
Next we go over to the CM-variables. We have

$$\begin{aligned}\mathbf{p}_1 &= -\mathbf{p}_2 = \mathbf{p}\ \ ,\ \ \mathbf{k} = \mathbf{p}' - \mathbf{p}\ \ ,\ \ \mathbf{p} = \mathbf{q} - \frac{1}{2}\mathbf{k}\ \ , \\ \mathbf{p}_1' &= -\mathbf{p}_2' = \mathbf{p}'\ \ ,\ \ \mathbf{q} = \frac{1}{2}(\mathbf{p} + \mathbf{p}')\ \ ,\ \ \mathbf{p}' = \mathbf{q} + \frac{1}{2}\mathbf{k}\ .\end{aligned} \tag{G10}$$

Then using (G5), we find for the expression between the curly brackets in (G6) the following expression

$$\Big\{\ldots\Big\} = \Big\{2\left(\mathbf{q}^2 + \mathbf{k}^2\right) + \frac{9}{4}\left(\mathbf{Q}^2 + \mathbf{S}^2\right) - 3\mathbf{q}\cdot(\mathbf{Q} - \mathbf{S}) + 3\left(\mathbf{K}_{23}^2 + \mathbf{Q}_{23}^2\right)\Big\} \tag{G11}$$

Now since the potential matrix elements will not depend on K_{23} and Q_{23}, apart from the appearance of these momenta in the exponential, we can integrate these variables out,with the result:

$$\int d^3K_{23}\ d^3Q_{23}\ \exp\left[-\frac{R_N^2}{2}\left(\mathbf{K}_{23}^2 + \mathbf{Q}_{23}^2\right)\right] \Rightarrow \left(\frac{2\pi}{R_N^2}\right)^3. \tag{G12}$$

Collecting all results of the section, we find

$$\begin{aligned}\langle p_1'p_2'|V|p_1p_2\rangle &= \left(\frac{1}{8}\right)^4\left(\frac{2\pi}{R_N^2}\right)^3\ \mathcal{N}^4\int d^3Q\ d^3S\cdot\exp\left[-\frac{R_N^2}{3}\left(\mathbf{q}^2 + \mathbf{k}^2\right)\right]\cdot \\ &\quad\times\exp\left[-\frac{R_N^2}{6}\left\{\frac{9}{4}\left(\mathbf{Q}^2 + \mathbf{S}^2\right) - 3\mathbf{q}\cdot(\mathbf{Q} - \mathbf{S})\right\}\right]\cdot \\ &\quad\times\widetilde{V}_{QQ}(\mathbf{Q},\mathbf{S};\mathbf{q},\mathbf{k})\ \delta^{(3)}\left(\mathbf{p}_1' + \mathbf{p}_2' - \mathbf{p}_1 - \mathbf{p}_2\right)\end{aligned} \tag{G13}$$

where $V_{QQ}(\mathbf{Q},\mathbf{S};\mathbf{q},\mathbf{k})$ denotes the QQ-potential which contains the MQQ-vertices and the Pomeron "propagator". For central two-gluon exchange potential $V_{QQ} = V_{QQ}(\mathbf{k})$, and therefore the $d^3Q\ d^3S$-integrals can be carried out

$$J_0 = \int d^3Q\ d^3S\ \exp\Big[-\alpha\Big\{\frac{9}{4}\left(\mathbf{Q}^2 + \mathbf{S}^2\right) - 3\mathbf{q}\cdot(\mathbf{Q} - \mathbf{S})\Big\}\Big] = \left(\frac{4\pi}{9\alpha}\right)^3 e^{-2\alpha\mathbf{q}^2}.$$

This gives

$$\begin{aligned}\langle p_1'p_2'|V|p_1p_2\rangle &= \left(\frac{1}{8}\right)^4\left(\frac{2\pi}{R_N^2}\right)^3\ \left(\frac{8\pi}{3R_N^2}\right)^3\ \mathcal{N}^4\ \exp\left[-\frac{R_N^2}{3}\ \mathbf{k}^2\right]\ \widetilde{V}_{QQ}(\mathbf{k})\ \delta^{(3)}\left(\mathbf{p}_1' + \mathbf{p}_2' - \mathbf{p}_1 - \mathbf{p}_2\right) \\ &= \exp\left[-\frac{R_N^2}{3}\ \mathbf{k}^2\right]\ \widetilde{V}_{QQ}(\mathbf{k})\ \delta^{(3)}\left(\mathbf{p}_1' + \mathbf{p}_2' - \mathbf{p}_1 - \mathbf{p}_2\right)\end{aligned} \tag{G14}$$

This is what is expected, because of the normalization for $\mathbf{k}^2 \to 0$ *the result must be* $\widetilde{V}_{QQ}(0)$.

---

2. Application QQ-potential

From the fit in terms of Gaussians in configuration space

$$V_{QQ,ij}(\mathbf{x}_i - \mathbf{x}_j) = \sum_{n,k} A_{n,k}\ (\mathbf{x}_i - \mathbf{x}_j)^n \exp\Big[-\Lambda_k^2\ (\mathbf{x}_i - \mathbf{x}_j)^2\Big], \tag{G15}$$

where n=0,2. Since this is a local potential it depends ony on $\mathbf{k}'_1 - \mathbf{k}_1 = \mathbf{q}_1 - \mathbf{q}' = \mathbf{k}$.
Therefore, in momentum space

$$\widetilde{V}_{QQ,ij}(\mathbf{k}) = \sum_{n,k} A_{n,k} \ \left(-\frac{d}{d\Lambda_k^2}\right)^{n/2} \ \left\{\left(\frac{\pi}{\Lambda_{k,n}^2}\right)^{3/2} \ \exp\left[-\mathbf{k}^2/(4\Lambda_k^2)\right]\right\}. \tag{G16}$$

Omitting the overall δ-function the overlap results is

$$n=0 \ : \ \langle p'_1 p'_2|V|p_1 p_2\rangle = \sum_k A_{0,k} \ \left(\frac{\pi}{\Lambda_{k,n}^2}\right)^{3/2} \ \exp\left[-\mathbf{k}^2/(4U_{0,k}^2)\right], \tag{G17a}$$

$$n=2 \ : \ \langle p'_1 p'_2|V|p_1 p_2\rangle = \sum_k A_{2,k} \ \left(\frac{\pi}{\Lambda_{k,n}^2}\right)^{3/2} \cdot$$
$$\times \frac{3}{2\Lambda_{2,k}^2}\left[1 - \frac{\mathbf{k}^2}{6\Lambda_{2,k}^2}\right] \ \exp\left[-\mathbf{k}^2/(4U_{2,k}^2)\right]. \tag{G17b}$$

with $U_{n,k} = \Lambda_N \Lambda_{n,k} \ \sqrt{3/(3\Lambda_N^2 + 4\Lambda_{n,k}^2)}$, where $\Lambda_N = 1/R_N^2$. In configuration space

$$n=0 \ : \ V(\mathbf{R}) = \sum_k A_{0,k} \ \left(\frac{U_{0,k}}{\Lambda_{0,k}}\right)^3 \ \exp\left[-U_{0,k}^2\mathbf{R}^2)\right], \tag{G18a}$$

$$n=2 \ : \ V(\mathbf{R}) = \sum_k A_{2,k} \ \left(\frac{U_{2,k}}{\Lambda_{2,k}}\right)^3 \ \exp\left[-U_{2,k}^2\mathbf{R}^2)\right] \cdot$$
$$\times \left(\frac{3}{2\Lambda_{2,k}^2}\right)\left[1 - \left(\frac{U_{2,k}}{\Lambda_{2,k}}\right)^2\left(1 - \frac{2}{3}(U_{2,k}\mathbf{R})^2\right)\right]. \tag{G18b}$$

For $V_{QQ}(+-)$ and $V_{QQ}(na)$, which have a zero at the origin, the form of $V(\mathbf{R})$ for n=2 in (G18) shows that the folding eliminates for BB the zero at the origin from the QQ-potential.

---

[1] Th. A. Rijken, Phys. Rev. **C 73** (2006) 044008.
[2] Th. A. Rijken, M.M. Nagels, and Y. Yamamoto, Progress of Theoretical Physics, Suppl. No. **185**, 14 (2010).
[3] V. G. Kadyshevsky, Sov. Phys. JETP, **19** (1964) 443.
[4] V. G. Kadyshevsky, Nucl. Phys. **B6** 125 (1967);
[5] V. G. Kadyshevsky and N. D. Mattev, Nuov. Cim. **55A**, 275 (1968).
[6] C. Itzykson, V. G. Kadyshevsky, I. T. Todorov, Phys. Rev. **D1**, 2823 (1970).
[7] R.P. Feynman, Phys. Rev. **76**, 769 (1949).
[8] J. Schwinger, Proc. Nat. Acad. of Sciences (USA) **37**, 452 (1951).
[9] E. Salpeter and H.A. Bethe, Phys. Rev. **84**, 1232 (1951).
[10] R.H. Thompson, Phys. Rev. **D1**, 110 (1970).
[11] Th. A. Rijken, Ann. Phys. (N.Y.) **208**, 253 (1991).
[12] Th. A. Rijken and V.G.J. Stoks, Phys. Rev. **C 54** (1996) 2851.
[13] Th. A. Rijken and V.G.J. Stoks, Phys. Rev. **C 54** (1996) 2869.
[14] F.E. Low, Phys. Rev. **D 12** (1975) 163.
[15] S. Nussinov, Phys. Rev. Lett. **34** (1975) 1286.
[16] A. Manohar and H. Georgi, Nucl. Phys. **B 234** (1984) 189.
[17] S. Weinberg, Phys. Rev. **D11** (1975) 3583.
[18] G. 't Hooft, Phys. Rev. **D14** (1976) 3432.
[19] A.A. Belavin, A.M. Polyakov, A.S. Schwarz, and Yu.S. Tyupkin, Phys. Lett. **59B** (1975) 85.
[20] D.I. Diakonov and V.Yu. Petrov, Phys. Lett. **147B** (1984) 351.
[21] D.I. Diakonov and V.Yu. Petrov, Nucl. Phys. **B245** (1984) 259-292.
[22] D.I. Diakonov and V.Yu. Petrov, Nucl. Phys. **B272** (1986) 457-489.

[23] E.V. Shuryak, Phys. Rep. **C115** (1984) 152.
[24] E.V. Shuryak, Nucl. Phys. **B203** (1982) 93-115.
[25] M.A. Shiffman, A.I. Vainshtein, and V.I. Zakharov, Nucl. Phys. **B147** (1979) 385, 448.
[26] M. Hutter, "Instantons in QCD, Theory and Application of the Instanton Liquid Model", Ph.D.-thesis, University of Munich, 1995.
[27] Th.A. Rijken, *Nucleon-Nucleon Interactions*, talk at KITPC workshop on Present status Nuclear Interaction Theory, Beijin August 2014.
[28] P. A. Verhoeven, 'Off-Shell Baryon-Baryon Scattering', Ph.D. University of Nijmegen, 1976; A. Gersten, P.A. Verhoeven, and J.J. de Swart, Nuovo Cimento, Vol. **26 A**, 385 (1975).
[29] We follow the conventions of J.D. Bjorken and S.D. Drell, *Relativistic Quantum Mechanics* and *Relativistic Quantum Fields* (McGraw-Hill Inc., New York; 1965).
[30] M.M. Nagels, T.A. Rijken, and J.J. de Swart, Phys. Rev. D**17**, 768 (1978).
[31] Th.A. Rijken, *Pomeron Couplings and Universal Repulsion in Baryon-Baryon Scattering*, preprint THEF-17d (2017), Nijmegen (unpublished).
[32] M.M. Nagels, Th.A. Rijken, and Y. Yamamoto, *Extended-soft-core Baryon-Baryon Model ESC16 I. Nucleon-Nucleon Scattering; Extended-soft-core Baryon-Baryon Model ESC16 II. Hyperon-Nucleon Interactions*, Open-access website, NN-Online: *http://nn-online.org*
[33] A. Le Yaouanc, L. Oliver, O. Péne, and J.-C. Raynal, Phys. Rev. **D 8**, 2322 (1973); **9**, 1415 (1974).